



Payame Noor University



Control and Optimization in Applied Mathematics (COAM)

Vol. 6, No. 2, Summer-Autumn 2021 (1-21), ©2016 Payame Noor University, Iran

DOI: [10.30473/coam.2022.59941.1169](https://doi.org/10.30473/coam.2022.59941.1169) (Cited this article)

Research Article

## Chaotic Dynamics in a Fractional-Order Hopfield Neural Network and its Stabilization via an Adaptive Model-Free Control Method

Majid Roohi<sup>1,\*</sup> , Mohammad Pourmahmood Aghababa<sup>2</sup>, Javid Ziaei<sup>3</sup>,  
Chongqi Zhang<sup>4,\*</sup>

<sup>1,4</sup>School of Economics and Statistics, Guangzhou University, P.O. Box. 510006, Guangzhou, China.

<sup>2</sup>Electrical and Computer Engineering Department, University of Windsor, Windsor, ON, Canada.

<sup>3</sup>Department of Automation, Biomechanics and Mechatronics, Lods University of Technology, Poland.

**Received:** July 14, 2021; **Accepted:** May 17, 2022.

**Abstract.** The present study introduces a kind of fractional-order Hopfield neural network (FOHNN), and its complex dynamic behavior is investigated through chaos analyses. With the use of phase space analysis and bifurcation diagrams and maximal Lyapunov exponent (MLE) it is demonstrated that for the values of  $0.87 < \alpha < 1$ , as the fractional-order (FO), the dynamical behavior of the mentioned FOHNN is chaotic. Then, the bounded trait of chaotic systems is utilized to derive an adaptive model-free control technique to suppress of complex dynamics of the FOHNN. Furthermore, according to the matrix analysis theorem of non-integer-order systems and the adaptive model-free control methodology, analytical consequences of the designed controller are evidenced. Eventually, two examples are reported to illustrate the applicability of the mentioned model-free control method.

**Keywords.** Fractional-order systems, Hopfield neural network, Bifurcation, Adaptive model-free controller, Stabilization.

**MSC.** 26A33; 92B20; 34H10.

---

\* Corresponding author

majid.roohi67@gmail.com, m.p.aghababa@gmail.com, javid.ziaei@gmail.com, cqzhang@gzhu.edu.cn.  
<http://mathco.journals.pnu.ac.ir>

## 1 Introduction

Recently, one of the essential challenges of sciences and engineering is the trustable modeling of natural phenomena by the lightest possible equations. In this regard, fractional differential equations provide new constructions to this field. In reality, fractional differential equations are a mix of arbitrary order differentiation and integration. The so-called “memory effect” is a distinguishing feature of a positive real-order derivative [46]. However, it is evident that many natural occurrences have long memory qualities. As a result, fractional order (FO) differential equations provide an effective tool for modeling such processes with certain unique qualities, such as extended memory and hereditary traits. [36, 38, 46]. There has recently been significant reporting in the literature on the application of the fractional calculus in a variety of sectors of science and engineering, including financial models [10], energy systems [2], optimization [15, 18], medical sciences [3, 12] and secure communications [8, 43].

Neural networks, introduced at the beginning of the twentieth century, have been used in many scientific fields and applications such as computer science [45], medical science [31], aerospace [22], optimization [14, 20], security [26] and so on. Hopfield neural networks (HNNs) [23, 48] abstracted from brain dynamics are some of the most important neural networks and are able of storing certain memories or patterns in a manner rather similar to the human brain. Owing to the wide applicability in pattern recognition [52, 53], medical science [7] and associative memories [6], there is nowadays much motivation on the study of Hopfield neural networks. Recent two decades have witnessed increasing attention to chaotic systems. High sensitivity to initial values, fractal properties of the motion in the phase space and broad Fourier transform spectra are some substantial properties of a chaotic system. Due to these significant features, chaos theory has been utilized in many practical research issues which include secure communications [54], information processing [39], and neural networks [47, 50]. Furthermore, chaotic and hyper-chaotic behaviors have been reported in many artificial neural networks. In [24], new classes of chaotic Hopfield neural networks have also been offered.

Based on this controversy, in the present study, a new type of three-dimensional fractional-order Hopfield neural network (FOHNN) is provided and its dynamical behaviors are investigated. To this end, we apply the bifurcation analysis and maximal Lyapunov exponent (MLE) criterion. The bifurcation diagram can identify different responses of the system under different situations derived by the change of some effective parameters on dynamics. To be sure that a dynamical system can show chaotic behavior, the positive value of the MLE criterion is sufficient.

It should be noted that the chaotic response is not always desirable. So, the control of FO chaotic systems has become an interesting subject for research. And, recently some control methods have been applied to control/stabilize chaotic treatment of FO dynamical systems [21]. Therefore, diverse approaches for stabilization of FO chaotic systems are applicable. In [29], to  $H_\infty$  synchronize uncertain FO complex systems, by using fuzzy logic, an adaptive controller has been suggested. But, as demonstrated in [1], the authors supposed that the procedure of non-integer differentials were the same as integer ones, hence the main results of their method were not correct. In [19, 41], the problem of stabilization of FO non-autonomous systems using active control methods was investigated. The authors of [5, 40] have introduced switching adaptive control methods to stabilize unknown FO complex systems. Recently, some sliding mode controller approaches have been designed in [42, 49, 51, 55] for the stabilization of FO chaotic systems. In [34], according to Laplace transformation, a robust control method is designed for chaos synchronization in a new fractional hybrid system. In [33], an adaptive sliding terminal is designed to synchronize FO quadratic complex flows. The authors of [25], to synchronize and stabilize the FO complex systems, have suggested an adaptive fuzzy type-2 control method by using a projection algorithm. In [30], using the FO version of Lyapunov-stability-theory, an FO adaptive SMC method is presented to synchronization FO neural networks.  $H_\infty$  performance analysis and stabilization for FO complex neural networks is reported in [35] with a non-fragile robust finite-time controller. In [16], based on a neural estimator, an adaptive FO SMC scheme is designed to control a class of complex systems with nonlinearities.

Although virtually all of the methods presented in the literature have a common weakness, almost all of them share a common weak point: they all employ all of the words associated with the FO systems in the control input. In contrast, there is no specific information regarding the linear and non-linear dynamic aspects of the FO-systems in real-world scenarios. As a result, the development of control mechanisms for the stabilization of FO chaotic systems with model-free structures is a critical subject in both theoretical and experimental studies. Nonetheless, as one knows, the model-free control approach has received little attention in the literature, and the control purpose of this study is to examine this topic further. An adaptive model-free control mechanism is presented in this study, which is intended to suppress the complicated behavior of the suggested FOHNN. The bounded property of the chaotic systems is used for introducing an efficient adaptive model-free control method, in which the linear-or-nonlinear elements in relations of the introduced FOHNN are not utilized. Two numerical simulations are provided to ensure the application and efficacy of the designed adaptive model-free stability strategy. For the purpose of developing an effective adaptive model-free control approach, the bounded property in chaotic systems is

used, and the linear and nonlinear components of the dynamics of the newly presented FOHNN are not utilized. The applicability and effectiveness of the proposed adaptive model-free control approach are demonstrated by a number of simulations, which are also included.

The following is the structure of this work. It is discussed in Section 2 how to formulate preliminary thoughts concerning fractional differential equations. In Section 3, some essential details about bifurcation analysis and maximal Lyapunov exponent are given. Section 4 is devoted to introducing the fractional-order Hopfield neural network. Then, using the MLE criterion and bifurcation analysis, it is shown that the nonlinear behavior of the FOHNN is chaotic. In Section 5, according to the bounded property of the chaotic systems, an adaptive model-free control approach is designed and the theoretical results are proved. Two illustrated examples are presented in Section 6. Finally, a summery of the results of this work are presented in Section 7.

## 2 Preliminary Concepts

In this section, fundamental definitions and concepts about fractional calculus and an essential theorem for stability analysis of FO equations are presented.

**Definition 1.** [37] The Fractional integral is called Riemann-Liouville FO integral for a fractional of FO  $\alpha$  of a continuous function  $\Psi$  is introduced by

$${}_{t_0}I_t = \frac{1}{\Gamma(\alpha)} \int_{t_0}^t \Psi(\theta)(t-\theta)^{\alpha-1} d\theta, \quad (1)$$

where  $t_0$  shows the initial amount of time and  $\Gamma(\cdot)$  shows the Gamma function

$$\Gamma(z) = \int_{t_0}^{\infty} t^{z-1} e^{-t} dt. \quad (2)$$

**Definition 2.** [37] Let  $\alpha \in (r-1, r)$  and  $r \in N$ , then the Caputo FO derivative of order  $\alpha$  for a function  $\Psi : R^+ \rightarrow R$  is given as follows

$${}_{t_0}D_t^\alpha \Psi(t) = \frac{1}{\Gamma(r-\alpha)} \int_{t_0}^t \Psi^{(r)}(\theta)(t-\theta)^{r-\alpha-1} d\theta. \quad (3)$$

In the rest of the article,  $D^\alpha$  demonstrates the Caputo derivative.

**Lemma 1.** [28] Let we have the following FO system:

$$D^\alpha X = G(X), \quad (4)$$

where  $X(t) = [x_1(t), x_2(t), \dots, x_n(t)]^T \in R^n$  and  $\alpha \in (0, 1)$ , then equilibrium point in the FO system (4) reaches to asymptotical stability if there is a positive-definite symmetric, real matrix  $\Omega$  such that the equation

$$\Delta = X^T \Omega D^\alpha X < 0.$$

### 3 Bifurcation Analysis and Maximal Lyapunov Exponent

In nonlinear dynamical systems, the variation of some parameters may cause structural deviations. If a dynamical system has instability in its nature, then the system can exhibit unexpected qualitative changes by enforcing it through an arbitrarily small variation in some parameter. Bifurcation theory is the nonlinear dynamic analysis of sudden changes in the qualitative behavior of a given nonlinear system. Bifurcation analysis can be applied for the study of continuous and discrete systems and can provide the possible long-term evolution of a system as a function of a bifurcation parameter [56, 13, 11].

The exponential divergence of initially nearby trajectories with time is known as sensitivity to initial conditions. This feature is a common property of chaotic systems. The Lyapunov exponent is a criterion for the identification of chaos through the quantification of the sensitivity on initial conditions. An  $m$ -dimensional dynamical system has  $m$  Lyapunov exponents defined as

$$\lambda_i = \lim_{n \rightarrow \infty} \frac{1}{t} \ln \left\| \frac{d_i(t)}{d_i(0)} \right\|, \quad (5)$$

where  $d_i(0)$  and  $d_i(t)$  represent distance between two trajectories at times 0 and  $t$  in the  $i$ th direction, respectively and  $\|\cdot\|$  denotes the vector norm. However, just one positive Lyapunov exponent is sufficient for a nonlinear system to be chaotic. So, in many practical situations, the maximal Lyapunov exponent is computed. In the present study, the algorithm of Rosenstein [44] is applied to calculate the MLE of the system.

### 4 Model Description and Complex Dynamics

Here, a fractional-order description of the Hopfield neural network (HNN) in [23] is presented. Then, using maximal Lyapunov exponent and bifurcation analysis, the complex dynamics of the introduced fractional-order Hopfield neural network (FOHNN) are examined.

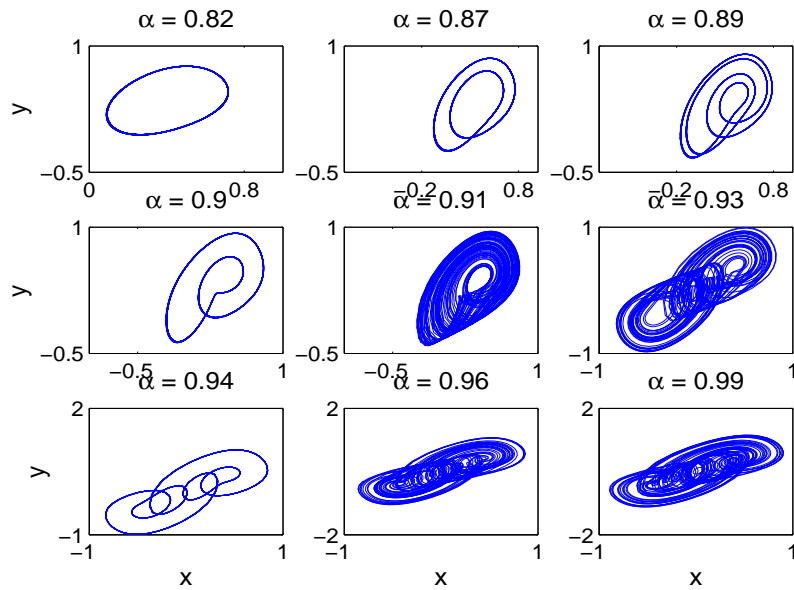


**Figure 1:** Phase space plot of FOHNN (9), for random values of the fractional order  $\alpha$ .

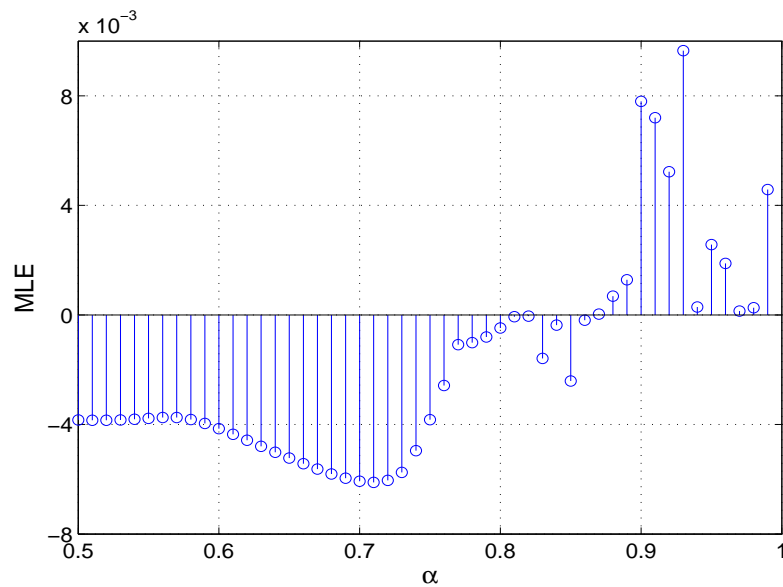


**Figure 2:** The MLEs of FOHNN (9) for different values of the fractional order  $\alpha$  increasing from 0.5 to 1.

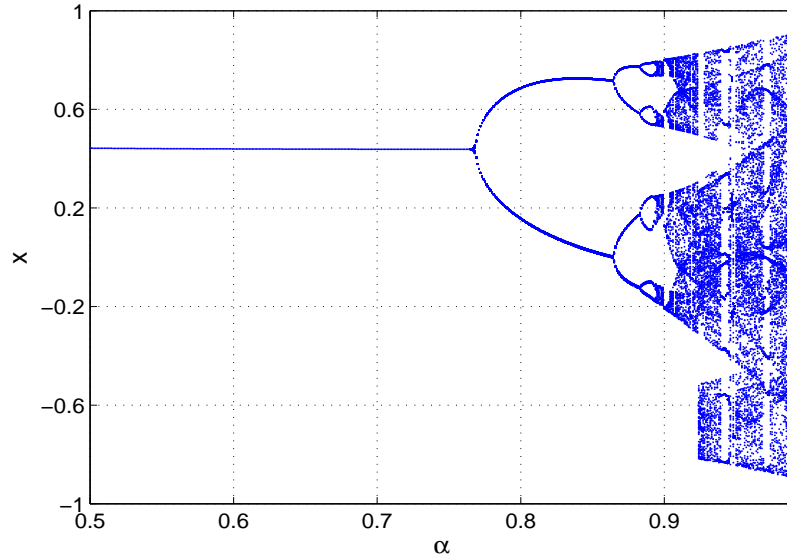


**Figure 3:** Bifurcation diagram of FOHNN (9) with control parameter  $\alpha$  increasing from 0.5 to 1.

#### 4.1 Fractional-order model of Hopfield neural network

An integer-order HNN has been given in [23] as

$$\dot{X} = -CX + Wf(X), \quad (6)$$

where  $X = [x_1, x_2, \dots, x_n]^t \in R^n$  is a vector of dynamical variables,  $C$  is the vector of constant parameters. The weight-matrix  $W$ , is an  $n \times n$  matrix and connects neurons, and  $f(X)$  is a bounded differentiable function defined by  $f(X) = \tan(X)$ .

In the three-dimensional case, the HNN (6) can be represented as

$$\dot{x}_i = -c_i x_i + \sum_{j=1}^3 w_{ij} f(x_j), \quad i = 1, 2, 3, \quad (7)$$

where  $x_i \in R, i = 1, 2, 3$  is the variable of the neural network,  $c_i$  is a constant parameter,  $w_{ij}$  are the elements of  $W$  and  $f(x_i) = \tanh(x_i)$ .

A new chaotic Hopfield neural network has been suggested in [27], which is presented as follows:

$$\begin{cases} \dot{x}_1 = -x_1 + 2 \tanh(x_1) - \tanh(x_2), \\ \dot{x}_2 = -x_2 + 1.7 \tanh(x_1) + 1.71 \tanh(x_2) + 1.1 \tanh(x_3), \\ \dot{x}_3 = -2x_3 - 2.5 \tanh(x_1) - 2.9 \tanh(x_2) + (0.56 + p) \tanh(x_3). \end{cases} \quad (8)$$

The HNN (8) exhibits a chaotic and unpredictable behavior for  $p = 0$ . For more details, the Ref. [27] can be read.

Here, according to the definition of a fractional differential equation and using Equation (8), the following fractional order Hopfield neural network model is proposed.

$$\begin{cases} D^\alpha x_1 &= -x_1 + 2 \tanh(x_1) - \tanh(x_2), \\ D^\alpha x_2 &= -x_2 + 1.7 \tanh(x_1) + 1.71 \tanh(x_2) + 1.1 \tanh(x_3), \\ D^\alpha x_3 &= -2x_3 - 2.5 \tanh(x_1) - 2.9 \tanh(x_2) + (0.56 + p) \tanh(x_3), \end{cases} \quad (9)$$

where  $\alpha \in (0,1)$  is the fractional order of the FOHNN.

**Remark 1.** In (9), in the case of  $p \neq 0$  have been considered in [43] a synchronization problem of a vast class of FO neural networks. It is demonstrated that considering  $p = 0$  does not have any fundamental effect on the framework and behavior of the system.

**Remark 2.** There are different definitions of the dynamics of the Hopfield neural network. For instance, recently, a new class of the 3-dimensional FO Hopfield neural networks has been taken into account in [32]. Moreover, for chaos suppression of the system an adaptive SMC approach is generated and then the attractors are synchronized in a finite time.

## 4.2 Complex dynamical behavior

Now, it is illustrated that the proposed FOHNN can show the wide range of dynamical behaviors like stable behaviors, limit cycles and chaotic motions. These diverse behaviors can be seen in Figure 1, where the  $2-d$  phase orbit of the system have been demonstrated for  $\alpha = 0.82$  (period-2 orbit),  $\alpha = 0.87$  (period-4 orbit),  $\alpha = 0.89$  (period-8 orbit),  $\alpha = 0.9$  (period-4 orbit),  $\alpha = 0.91$  (single-scroll chaotic orbit),  $\alpha = 0.93$  (double-scroll chaotic orbit),  $\alpha = 0.94$  (period-10 orbit),  $\alpha = 0.96$  (double-scroll chaotic orbit) and  $\alpha = 0.99$  (double-scroll chaotic orbit).

As it is shown using maximal Lyapunov exponent criterion, dynamical behaviors of FOHNN (9) are chaotic. The MLE diagrams of FOHNN (9) for distinct values of the FO  $\alpha \in [0.5,0.99]$  are plotted in Figure 2. One can see that for the values of  $0.87 \leq \alpha \leq 0.99$ , the FOHNN (9) has positive value MLE, therefore it has chaotic dynamics in phase space.

Furthermore, the bifurcation diagram shown in Figure 3 aids us for having a pervasive view of the dynamics of the FOHNN. Clearly, the variation of  $\alpha$  has divided dynamics of the system into three regions. The first region contains a single stable fixed point, i.e., system does not oscillate and the dynamics of system terminate in



a single fixed point. This means that different trajectories in accordance with different values of  $\alpha$  have the same qualitative structure and the small perturbation to the system due to the variation of  $\alpha$  does not affect the long-time dynamic of system.

The second region contains consecutive period-doublings. The first period-doubling is the starting point of this region. The creation of new two stable fixed points and the fluctuation of system dynamics between them are distinctive points of the second region in comparison with the first region. Roughly speaking, the phase space of system is a periodic closed orbit. With the increase of  $\alpha$  the generated fixed points are separated from one another. The creation of new fixed points and their divergence continues until the consecutive periods-doubling terminates in chaos where the dynamics possesses infinitely many equilibria and fixed points. The third region defines the chaotic zone, where the system fluctuates in an unsystematic way independent of the value of  $\alpha$ .

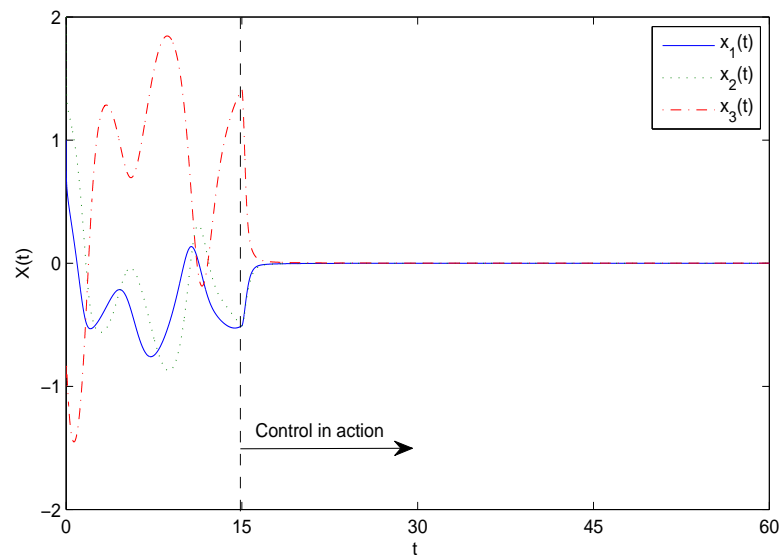


**Figure 4:** State trajectories of the controlled FOHNN system (10) in Example 1 (8).

**Remark 3.** Actually, the adaptive control approaches (15) and (16) are called model-free because the nonlinear/linear dynamical terms of the system have not been used in the design of the controller. This means that the formulation of the controller is only based on the states of the systems.

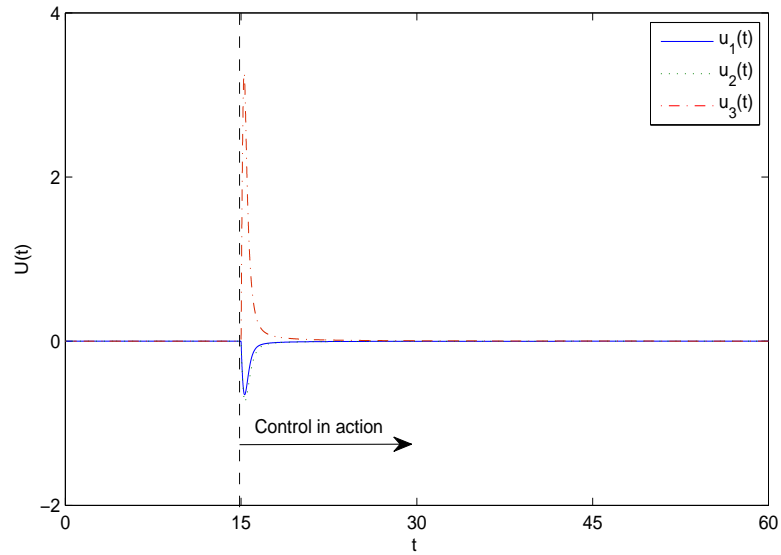


**Figure 5:** Time history of adaptive controller (15), applied on Example 1.

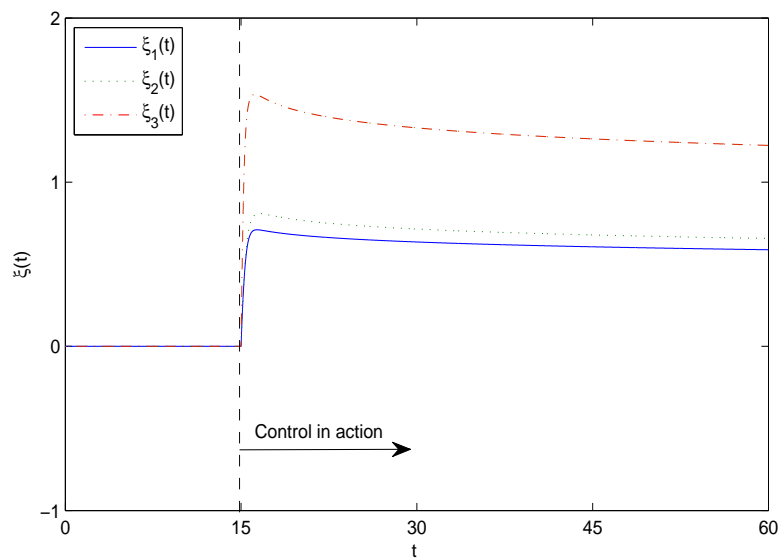


**Figure 6:** Time response of the updating laws (16), in Example 1.

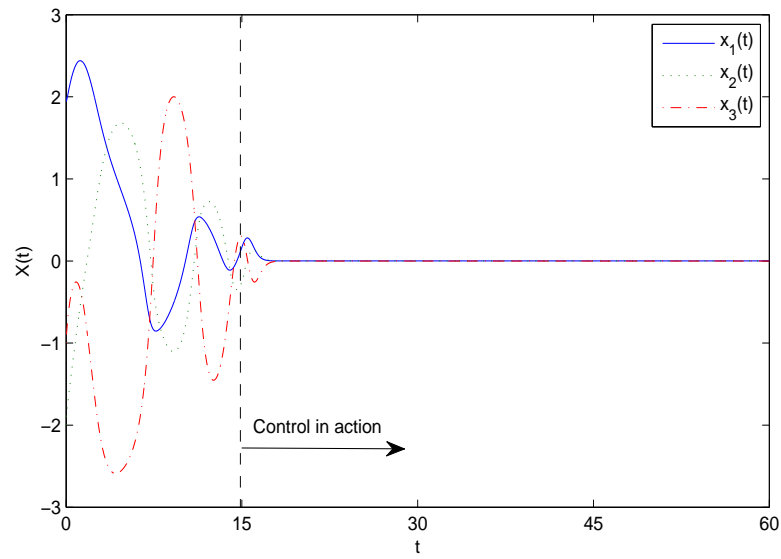


**Figure 7:** State trajectories of the controlled FOHNN system (10) in Example 2.

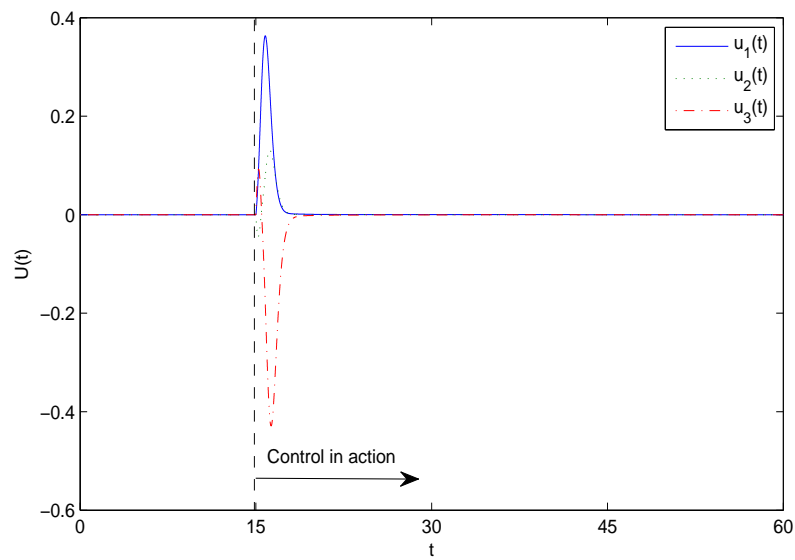


**Figure 8:** Time history of adaptive controller (15), applied on Example 2.

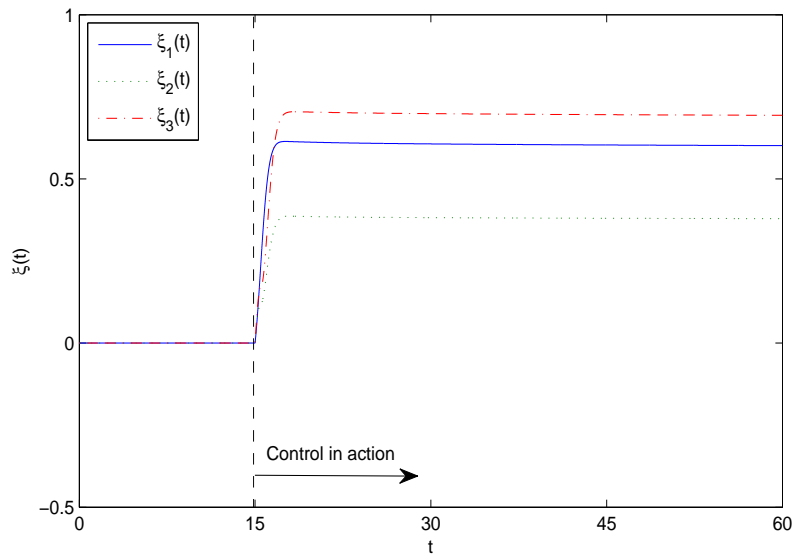


Figure 9: Time response of the updating laws (16), in example 2.

## 5 Control of the Proposed FOHNN

Here, we concern the chaos control problem in system (9) with the adaptive scheme. To suppress the chaotic behavior of system (9), we should add control signals to the system. Consider the following chaotic FOHNN with control input  $u_i$ ,  $i = 1, 2, 3$ :

$$\begin{cases} D^\alpha x_1 = -x_1 + 2 \tanh(x_1) - \tanh(x_2) - u_1, \\ D^\alpha x_2 = -x_2 + 1.7 \tanh(x_1) + 1.71 \tanh(x_2) + 1.1 \tanh(x_3) - u_2, \\ D^\alpha x_3 = -2x_3 - 2.5 \tanh(x_1) - 2.9 \tanh(x_2) + 0.56 \tanh(x_3) - u_3. \end{cases} \quad (10)$$

By converting Equation (10) to a matrix-form, one obtains

$$\begin{bmatrix} D^\alpha x_1 \\ D^\alpha x_2 \\ D^\alpha x_3 \end{bmatrix} = \underbrace{\begin{bmatrix} -1 & 0 & 0 \\ 0 & -1 & 0 \\ 0 & 0 & -2 \end{bmatrix}}_A \underbrace{\begin{bmatrix} x_1 \\ x_2 \\ x_3 \end{bmatrix}}_X + \underbrace{\begin{bmatrix} 2 & -1 & 0 \\ 1.7 & 1.71 & 1.1 \\ -2.5 & -2.9 & 0.56 \end{bmatrix}}_B \underbrace{\begin{bmatrix} \tanh(x_1) \\ \tanh(x_2) \\ \tanh(x_3) \end{bmatrix}}_Y - \underbrace{\begin{bmatrix} u_1 \\ u_2 \\ u_3 \end{bmatrix}}_U, \quad (11)$$

which is equivalent to

$$D^\alpha X = AX + BY - U. \quad (12)$$

If the rows of the matrices  $A$  and  $B$  are called  $a_i$  and  $b_i$  ( $i = 1, 2, 3$ ) respectively, then the Equation (12) is equivalent to

$$\begin{cases} D^\alpha x_1 = g_1(X, Y) - u_1, \\ D^\alpha x_2 = g_2(X, Y) - u_2, \\ D^\alpha x_3 = g_3(X, Y) - u_3, \end{cases} \quad (13)$$

in which  $g_i(X, Y) = a_i X + b_i Y$ ,  $i = 1, 2, 3$ .

**Assumption:** On the basis of phase space, it has been proved that the state trajectories of chaotic systems have a global constraint in their state space [9, 17]. Actually, this is made by irregular attractors of the chaotic systems. As it turns out, this is a byproduct of chaotic systems' irregular attractors. It is therefore necessary to confine the right-hand portion of a complicated system. Because of this, there are finite-valued positive constants  $\rho_i$ ,  $i = 1, 2, 3$  for the nonlinear components of the FOHNN (13),  $g_i(X, Y) = a_i X + b_i Y$ ,  $i = 1, 2, 3$  such that

$$|g_i(X, Y)| < \rho_i < \infty, \quad i = 1, 2, 3. \quad (14)$$

One of the well-known methods with too many desirable features is the adaptive control method. Here, an adaptive model-free controller is proposed to suppress the chaotic behaviors of the FOHNN (10). The controller is designed so that it does not require any information about dynamical terms of FOHNN (10). Thus on the basis of bounded feature in a chaotic system, the adaptive model-free controller is designed as

$$u_i(t) = \xi_i(t) \left( k_i \Upsilon(x_i) + c_i \bar{\Upsilon}(x_i) \right), \quad i = 1, 2, 3, \quad (15)$$

$$D^\alpha \xi_i(t) = \lambda_i |x_i|, \quad \xi_i(0) = \xi_{i0}, \quad i = 1, 2, 3, \quad (16)$$

where

$$\Upsilon(x) = \begin{cases} \text{sign}(x), & \text{if } x > 0, \\ 0, & \text{if } x \leq 0, \end{cases}$$

and

$$\bar{\Upsilon}(x) = \begin{cases} 0, & \text{if } x > 0, \\ -\tanh(x), & \text{if } x \leq 0, \end{cases}$$

where,  $k_i > 1$ ,  $c_i < -1$  and  $\lambda_i > 0$  are constant values and  $\xi_{i0} > 0$  shows the initial condition of the adaptive parameter  $\xi_i(t)$ .

It should be noted that, to avoid undesirable chattering phenomenon the  $\Upsilon$  and the  $\bar{\Upsilon}$  functions are joined in the control approach.

**Theorem 1.** Consider the fractional-order neural network (10) with control inputs. The trajectories of the neural network (10) will asymptotically converge to zero under the control scheme (15) and updating law (16).

*Proof.* Suppose that  $W$  is given by  $W(t) = [X(t), \gamma(t)]^T$ , where

$$X(t) = [x_1(t), x_2(t), x_3(t)]^T \quad \text{and} \quad \gamma(t) = [\gamma_1(t), \gamma_2(t), \gamma_3(t)]^T.$$

Thus,

$$D^\alpha W(t) = [D^\alpha x_1(t), D^\alpha x_2(t), D^\alpha x_3(t), D^\alpha \gamma_1(t), D^\alpha \gamma_2(t), D^\alpha \gamma_3(t)]^T,$$

where

$$\gamma_i = (\rho_i - \xi_i) \quad i = 1, 2, 3.$$

Then,

$$D^\alpha \gamma_i = -D^\alpha \xi_i = -\lambda_i |x_i|, \quad i = 1, 2, 3.$$

Based on Theorem 1, the matrix  $P$  must be chosen in a way that the following relation holds.

$$\Delta = W^T P D^\alpha W < 0.$$

By selecting  $P$  as

$$P = \text{diag}(1, 1, 1, \frac{1}{\lambda_1}, \frac{1}{\lambda_2}, \frac{1}{\lambda_3}),$$

one has

$$\Delta = \sum_{i=1}^3 x_i D^\alpha x_i + \sum_{i=1}^3 \lambda_i^{-1} \gamma_i D^\alpha \gamma_i. \quad (17)$$

Inserting  $D^\alpha x_i$  from Equation (13) into the above equation, one obtains

$$\begin{aligned} \Delta &= \sum_{i=1}^3 x_i (g_i(X, Y) - u_i) + \sum_{i=1}^3 \lambda_i^{-1} \gamma_i \underbrace{(-\lambda_i |x_i|)}_{D^\alpha \gamma_i} \\ &= \sum_{i=1}^3 x_i (g_i(X, Y) - u_i) - \sum_{i=1}^3 \underbrace{(\rho_i - \xi_i)}_{\gamma_i} |x_i|. \end{aligned}$$

According to the relation (14) and the design of  $u_i(t)$  in relation (15), one gets

$$\begin{aligned} \Delta &< \sum_{i=1}^3 \left[ \rho_i |x_i| - \xi_i(t) \left( \xi(t) (k_i \Upsilon(x_i) + c_i \bar{\Upsilon}(x_i)) \right) \right] - \sum_{i=1}^3 (\rho_i - \xi_i) |x_i| \\ &< \sum_{i=1}^3 x_i \left[ \rho_i - \xi_i(t) (k_i \Upsilon(x_i) + c_i \bar{\Upsilon}(x_i)) \right] - \sum_{i=1}^3 (\rho_i - \xi_i) |x_i| \\ &= \sum_{i=1}^3 \left[ \rho_i x_i - x_i \xi_i (k_i \Upsilon(x_i) + c_i \bar{\Upsilon}(x_i)) \right] - \sum_{i=1}^3 \left[ \rho_i |x_i| - \xi_i(t) |x_i| \right] \\ &\leq \sum_{i=1}^3 \left[ \rho_i |x_i| - k_i x_i \xi_i \Upsilon(x_i) - c_i x_i \xi_i \bar{\Upsilon}(x_i) - \rho_i |x_i| + \xi_i(t) |x_i| \right]. \end{aligned}$$

Therefore,

$$\Delta < \sum_{i=1}^3 \left[ \xi_i(t) |x_i| - k_i x_i \xi_i \Upsilon(x_i) - c_i x_i \xi_i \bar{\Upsilon}(x_i) \right]. \quad (18)$$

- Case 1. If  $x_i > 0$ , in (18) we have

$$\begin{aligned}\Delta &< \sum_{i=1}^3 \left[ \xi_i(t)|x_i| - k_i x_i \xi_i \operatorname{sign}(x_i) \right] \\ &= \sum_{i=1}^3 \left( \xi_i(t)|x_i| - k_i \xi_i |x_i| \right) \\ &= \sum_{i=1}^3 \left[ \xi_i(t)|x_i|(1 - k_i) \right].\end{aligned}\quad (19)$$

Since  $k_i > 1$  and the adaptive condition  $\xi_i(t) > 0$  are ensured, we obtain

$$\Delta < \sum_{i=1}^3 \left[ \xi_i(t)|x_i|(1 - k_i) \right] < 0. \quad (20)$$

- Case 2. If  $x_i \leq 0$ , in (18) one has

$$\Delta < \sum_{i=1}^3 \left[ \xi_i(t)|x_i| + c_i x_i \xi_i \tanh(x_i) \right]. \quad (21)$$

Since  $x_i \tanh(x_i) \leq |x_i|$  is true for any  $x_i \in R$ , one obtains

$$\begin{aligned}\Delta &< \sum_{i=1}^3 \left( \xi_i(t)|x_i| + c_i \xi_i |x_i| \right) \\ &= \sum_{i=1}^3 \left[ \xi_i(t)|x_i|(1 + c_i) \right].\end{aligned}\quad (22)$$

Since  $c_i < -1$  and the adaptive condition  $\xi_i(t) > 0$  are ensured,

$$\Delta < \sum_{i=1}^3 \left[ \xi_i(t)|x_i|(1 + c_i) \right] < 0. \quad (23)$$

Thus, the stability condition in Lemma 1 is satisfied by relations (20) and (23). Therefore, the procedure of the proof is done.  $\square$

**Remark 4.** The parameters  $\lambda_i$ ,  $k_i$ ,  $c_i$  and  $\xi_i$  in (15) and (16) mean the switching control gain, which should be adjusted to some special values such that  $\lambda_i > 0$ ,  $k_i > 0$ ,  $\xi_i > 0$  and  $c_i < -1$  for  $i = 1, 2, 3$ , in order to assure the stability of system equilibrium point. According to the controller, it can be shown that the values of these parameters have an effect on the amount of control effort required in the suggested method. To put it another way, high values of the parameters result in a significant control energy.

## 6 Illustrative Examples

To validate the efficiency and applicability of the proposed adaptive control method (15) in suppressing the complex dynamics of the FOHNN in a given time interval, two illustrative examples are provided for different values of  $\alpha$ . It should be indicated that a numerical algorithm, which is presented in [4], is utilized and the controller begins to operate after  $t = 15$  sec.

### 6.1 Example 1

In this example we fix  $\alpha$ , the order of derivative of the FOHNN (10), at 0.91 where the chaotic behavior of the complex network (10) is ensured. Moreover, the initial conditions of the FOHNN (10) are selected as  $x_1(0) = 1$ ,  $x_2(0) = 2$  and  $x_3(0) = -1$ . Subsequently, the parameters of the controller (15) and updating law (16) are chosen as  $k_1 = k_2 = k_3 = 4.5$ ,  $\lambda_1 = \lambda_2 = \lambda_3 = 3$  and  $c_1 = c_2 = c_3 = -1.5$  respectively.

The state trajectories of the controlled FOHNN system (10) and the time history of adaptive controller (15) are plotted in Figures 4 and 5. It is obvious that the strange attractors of the chaotic FOHNN system are stabilized quickly. Furthermore, it is seen that the control input (15) converges to an equilibrium point. The time response of the updating law (16) is depicted in Figure 6. Obviously, all of the parameters of updating law (16) approach to some fixed value. This means that the designed adaptive controller can effectively suppress the chaotic behaviors of fractional-order HNN system and the controller is feasible in the real world.

### 6.2 Example 2

Here, we assume that the fractional order of the FOHNN (10) is equal to 0.99. With this choice, the behavior of (10) will be unstable and chaotic, surely. To overcome this instability, the parameters of the control law (15) and updating law (16) are selected as  $k_1 = k_2 = k_3 = 4$ ,  $\lambda_1 = \lambda_2 = \lambda_3 = 2$  and  $c_1 = c_2 = c_3 = -1$ , respectively. Moreover, the initial values of the FOHNN (10) are chosen as  $x_1(0) = 2$ ,  $x_2(0) = -1$  and  $x_3(0) = 1$ . Figures 7-9 show the state trajectories of the FOHNN (10), the time response of the adaptive controller (15) and the time history of the updating law (16), respectively. It can be seen that the state trajectories and control signals converge to the equilibrium point. Furthermore, all of the parameters of the updating law (16),



approach to the bounded values. This means that the proposed adaptive controller can effectively stabilize the chaotic behavior of the introduced FOHNN.

## 7 Conclusions

In this paper, a new fractional-order Hopfield neural network (FOHNN) was introduced and the existence of chaos was examined. Using the maximal Lyapunov exponent criterion and bifurcation analysis, it was ensured that the FOHNN exhibits chaotic behavior. In this regard, an adaptive control scheme was designed for control and stabilization of the FOHNN. The designed control method was independent of the linear/nonlinear terms of the complex system states. By applying the adaptive control method and the stability analysis theorem of the fractional-order systems, the analytical terms of this controller were proved. Simulation results showed that the introduced FOHNN exhibited chaotic attractors and the proposed adaptive controller could simply undertake the observed chaotic behaviors.

## References

- [1] Aghababa M.P. (2012). "Comments on  $H_\infty$  synchronization of uncertain fractional-order chaotic systems: Adaptive fuzzy approach [ISA Trans 50 (2011) 548-556]", ISA Transactions, 51, 11-12.
- [2] Aghababa M.P. (2015). "Fractional modeling and control of a complex nonlinear energy supply-demand system", Complexity, 20, 74-86.
- [3] Aghababa M.P., Borjkhani M. (2014). "Chaotic fractional-order model for muscular blood vessel and its control via fractional control scheme", Complexity, 20 (2), 37-46.
- [4] Asl M.S., Javidi M. (2017). "An improved PC scheme for nonlinear fractional differential equations: Error and stability analysis", Journal of Computational and Applied Mathematics, 324, 101-117.
- [5] Aghababa M.P., Haghghi A.R., Roohi M. (2015). "Stabilization of unknown fractional-order chaotic systems: an adaptive switching control strategy with application to power systems", IET Generation, Transmission & Distribution, 9, 1883-1893.
- [6] Asakawa S., Kyoya I. (2013). "Hopfield neural network model for explaining double dissociation in semantic memory impairment", BMC Neuroscience, 14, 233.
- [7] Banerjee S., Majumdar D. (2000). "Shape matching in multimodal medical images using point landmarks with Hopfield net", Neurocomputing, 30, 103-116.

- 
- [8] Chen Y., Tang C., Roohi M. (2021). "Design of a model-free adaptive sliding mode control to synchronize chaotic fractional-order systems with input saturation: An application in secure communications", *Journal of the Franklin Institute*, 8109-8137.
- [9] Curran P.F., Chua L.O. (1997). "Absolute stability theory and the synchronization problem", *International Journal of Bifurcation and Chaos*, 7, 1375-1382.
- [10] Danca M.F., Garrappa R., Tang K.S., Chen G. (2013). "Sustaining stable dynamics of a fractional-order chaotic financial system by parameter switching", *Computers & Mathematics with Applications*, 66, 702-716.
- [11] Diks C., Wagener F.O.O. (2008). "A bifurcation theory for a class of discrete time Markovian stochastic systems", *Physica D: Nonlinear Phenomena*, 237, 3297-3306.
- [12] Ding Y., Wang Z., Ye H. (2012). "Optimal control of a fractional-order HIV-immune system with memory", *IEEE Transactions on Control Systems Technology*, 20, 763-769.
- [13] Du J., Sheng Z., Mei Q., Huang H. (2009). "Study on output dynamic competition model and its global bifurcation", *International Journal of Nonlinear Sciences and Numerical Simulation*, 10, 129-136.
- [14] Effati S., Moghaddas M. (2016). "A novel neural network based on NCP function for solving constrained nonconvex optimization problems", *Complexity*, 21, 130-141.
- [15] Esfahani Z., Roohi M., Gheisarnejad M., Dragicević T., Khooban M.H. (2019). "Optimal non-integer sliding mode control for frequency regulation in stand-alone modern power grids", *Applied Sciences*, 9, 3411.
- [16] Fei J., Lu C. (2018). "Adaptive fractional-order sliding mode controller with neural estimator", *Journal of the Franklin Institute*, 355, 2369-2391.
- [17] Fradkov A.L., Evans R. (2005). "Control of chaos: Methods and applications in engineering", *Annual Reviews in Control*, 29, 33-56.
- [18] Gomaa Haroun A., Yin-Ya L. (2019). "A novel optimized fractional-order hybrid fuzzy intelligent PID controller for interconnected realistic power systems", *Transactions of the Institute of Measurement and Control*, 41, 3065-3080.
- [19] Haghghi A., Aghababa M.P., Asghary N., Roohi M. (2020). "A nonlinear control scheme for stabilization of fractional-order dynamical chaotic systems", *Journal of Advanced Mathematical Modeling*, 10, 19-38.
- [20] Hamza M.F., Yap H.J., Choudhury I.A. (2017). "Recent advances on the use of meta-heuristic optimization algorithms to optimize the type-2 fuzzy logic systems in intelligent control", *Neural Computing and Applications*, 28, 979-999.
- [21] He S., Sun K., Wang H. (2016). "Solution and dynamics analysis of a fractional-order hyperchaotic system", *Mathematical Methods in the Applied Sciences*, 39, 2965-2973.
- [22] Hong C.H., Choi K.C., Kim B.S. (2009). "Applications of adaptive neural network control to an unmanned airship", *International Journal of Control, Automation and Systems*, 7, 911.

- [23] Hopfield J.J. (1984). "Neurons with graded response have collective computational properties like those of two-state neurons", *Proceedings of the national academy of sciences*, 81, 3088-3092.
- [24] Huang W.Z., Huang Y. (2008). "Chaos of a new class of Hopfield neural networks", 206, 1-11.
- [25] Jafari P., Teshnehlab M., Tavakoli-Kakhki M. (2018). "Adaptive type-2 fuzzy system for synchronization and stabilization of chaotic non-linear fractional order systems", *IET Control Theory & Applications*, 12, 183-193.
- [26] Javan D.S., Mashhadi H.R., Rouhani M. (2013). "A fast static security assessment method based on radial basis function neural networks using enhanced clustering", *International Journal of Electrical Power and Energy Systems*, 44, 988-996.
- [27] Li J., Liu F., Guan Z., Li T. (2013). "A new chaotic Hopfield neural network and its synthesis via parameter switchings", *Neurocomputing*, 117, 33-39.
- [28] Li C., Tong Y. (2013). "Adaptive control and synchronization of a fractional-order chaotic system", *Pramana*, 80, 583-592.
- [29] Lin T.C., Kuo C.H. (2011). " $H_\infty$  synchronization of uncertain fractional-order chaotic systems: Adaptive fuzzy approach", *ISA Transactions*, 50, 548-556.
- [30] Liu H., Pan Y., Li S., Chen Y. (2018). "Synchronization for fractional-order neural networks with full/under-actuation using fractional-order sliding mode control", *International Journal of Machine Learning and Cybernetics*, 9, 1219-1232.
- [31] Liu H., Wen Y., Luan F., Gao Y. (2009). "Application of experimental design and radial basis function neural network to the separation and determination of active components in traditional Chinese medicines by capillary electrophoresis", *Analytica Chimica Acta*, 88-93.
- [32] Mahmoud E.E., Jahanzib L.S., Trikha P., Almaghrabi O.A. (2021). "Analysis and control of the fractional chaotic Hopfield neural network. *Advances in Difference Equations*", *Advances in Difference Equations*, 126.
- [33] Mofid O., Mobayen S. (2018). "Adaptive synchronization of fractional-order quadratic chaotic flows with nonhyperbolic equilibrium", *Journal of Vibration and Control*, 24, 4971-4987.
- [34] Ouannas A., Azar A.T., Vaidyanathan S. (2017). "A robust method for new fractional hybrid chaos synchronization", *Mathematical Methods in the Applied Sciences*, 40, 1804-1812.
- [35] Peng X., Wu H. (2020). "Non-fragile robust finite-time stabilization and  $H_\infty$  performance analysis for fractional-order delayed neural networks with discontinuous activations under the asynchronous switching", *Neural Computing and Applications*, 32, 4045-4071.
- [36] Petrás I. (2011). "An effective numerical method and its utilization to solution of fractional models used in bioengineering applications", *Advances in Difference Equations*, 652789.

- [37] Podlubny I. (1998). "Fractional differential equations: An introduction to fractional derivatives, fractional differential equations, to methods of their solution and some of their applications", Elsevier Science.
- [38] Podlubny I. (2002). "Geometric and physical interpretation of fractional integration and fractional differentiation", *Fractional Calculus and Applied Analysis*, 5, 367-386.
- [39] Ramezani A., Safarinejadian B., Zarei J. (2019). "Fractional-order chaotic cryptography in colored noise environment by using fractional order interpolatory cubature Kalman filter", *Transactions of the Institute of Measurement and Control*, 41, 3206-3222.
- [40] Roohi M., Aghababa M.P., Haghghi A.R. (2015). "Switching adaptive controllers to control fractional-order complex systems with unknown structure and input nonlinearities", *Complexity*, 21, 211-223.
- [41] Roohi M., Hadian H., Aghababa M.P., Amiri S.M.M. (2017). "Design of an active control method for complete stabilization of unknown fractional-order non-autonomous systems", *International Workshop on Mathematics and Decision Science: Fuzzy Information and Engineering and Decision*, 646, 131-142.
- [42] Roohi M., Khooban M.H., Esfahani Z., Aghababa M.P., Dragicevic T. (2019). "A switching sliding mode control technique for chaos suppression of fractional-order complex systems", *Transactions of the Institute of Measurement and Control*, 41, 2932-2946.
- [43] Roohi M., Zhang C., Chen Y. (2020). "Adaptive model-free synchronization of different fractional-order neural networks with an application in cryptography", *Nonlinear Dynamics*, 2020, 3979-4001.
- [44] Rosenstein M.T., Collins J.J., De Luca C.J. (1993). "A practical method for calculating largest Lyapunov exponents from small data sets", *Physica D: Nonlinear Phenomena*, 65, 117-134.
- [45] Shrivastava Y., Singh B. (2019). "Stable cutting zone prediction in computer numerical control turning based on empirical mode decomposition and artificial neural network approach", *Transactions of the Institute of Measurement and Control*, 41, 193-209.
- [46] Sun H., Zhang Y., Baleanu D., Chen W., Chen Y.Q. (2018). "A new collection of real-world applications of fractional calculus in science and engineering", *Communications in Nonlinear Science and Numerical Simulation*, 64, 213-231.
- [47] Suykens J.A., Vandewalle J. (2005). "Cellular neural networks, multi-scroll chaos and synchronization", *World Scientific Series on Nonlinear Science Series A*, 50, 248.
- [48] Tank D., Hopfield J.J. (1986). "Simple neural optimization networks: An A/D converter, signal decision circuit, and a linear programming circuit", *IEEE Transactions on Circuits and Systems*, 33, 533-541.
- [49] Wang B., Liu Y. J., Yu F., Wang J., Yang J. (2017). "Robust finite-time control of fractional-order nonlinear systems via frequency distributed model", *Nonlinear Dynamics*, 85, 2133-2142.

- [50] Wang L., Li S., Tian F., Fu X. (2004). "A noisy chaotic neural network for solving combinatorial optimization problems: Stochastic chaotic simulated annealing", *IEEE Transactions on Systems, Man, and Cybernetics, Part B*, 34, 2119-2125.
- [51] Wang, R, Liu, Y.J, Yu, F.S, Wang, J.Y, Yang, J.L. (2017). "Adaptive variable universe of discourse fuzzy control for a class of nonlinear systems with unknown dead zones", *International Journal of Adaptive Control and Signal Processing*, 31 (12), 1934-1951.
- [52] Wang X.Y., Li Z.M. (2019). "A color image encryption algorithm based on Hopfield chaotic neural network. *Optics and Lasers in Engineering*", *Optics and Lasers in Engineering*, 115, 107-118.
- [53] Wei J.D., Cheng H.J., Chang C.W. (2019). "Hopfield network-based approach to detect seam-carved images and identify tampered regions", *Neural Computing and Applications*, 31, 6479-6492.
- [54] Xu G., Xu J., Liu F., Zang F. (2017). "Secure communication based on the synchronous control of hysteretic chaotic neuron", *Neurocomputing*, 227, 108-112.
- [55] Yin C., Dadras S., Zhong S.M. (2012). "Design an adaptive sliding mode controller for drive-response synchronization of two different uncertain fractional-order chaotic systems with fully unknown parameters", *Journal of the Franklin Institute*, 349, 3078-3101.
- [56] Yu J., Pan W.Z., Ng T.W. (2008). "Bifurcation and chaos in the generalized Korteweg-de Vries equation under a harmonic excitation", *International Journal of Nonlinear Sciences and Numerical Simulation*, 9, 37-40.

#### How to Cite this Article:

Roohi, M., Pourmahmood Aghababa, M., Ziaei, J., Zhang, C. (2022). "Chaotic dynamics in a fractional-order Hopfield neural network and its stabilization via an adaptive model-free control method", *Control and Optimization in Applied Mathematics*, 6(2): 1-21. doi: 10.30473/coam.2022.59941.1169



#### COPYRIGHTS

© 2021 by the authors. Licensee PNU, Tehran, Iran. This article is an open access article distributed under the terms and conditions of the Creative Commons Attribution 4.0 International (CC BY4.0) (<http://creativecommons.org/licenses/by/4.0>)






Payame Noor University



Control and Optimization in Applied Mathematics (COAM)  
Vol. 6, No. 2, Summer-Autumn 2021 (23-35), ©2016 Payame Noor University, Iran

DOI. [10.30473/coam.2021.60747.1176](https://doi.org/10.30473/coam.2021.60747.1176) (Cited this article) 

## Research Article

# Guignard Qualifications and Stationary Conditions for Mathematical Programming with Nonsmooth Switching Constraints

Fatemeh Gorgini Shabankareh<sup>1</sup>, Nader Kanzi<sup>2</sup>, Javad Izadi<sup>3\*</sup>, Kamal Fallahi<sup>4</sup>

<sup>1,2,3,4</sup>Department of Mathematics, Payame Noor University (PNU),  
P.O. Box. 19395-4697, Tehran, Iran.

**Received:** September 09, 2021; **Accepted:** January 24, 2022.

**Abstract.** In this paper, some constraint qualifications of the Guignard type are defined for optimization problems with continuously differentiable objective functions and locally Lipschitz switching constraints. Then, a new type of stationary condition, named as parametric stationary condition, is presented for the problem, and it is shown that all the stationarity conditions in various papers can be deduced from it. This paper can be considered as an extension of a recent article (see Kanzow, et al.) to the nonsmooth case. Finally, the article ends with two important examples. The results of the article are formulated according to Clark subdifferential and using nonsmooth analysis methods.

**Keywords.** Constraint qualification, Stationary conditions, Optimality conditions, Switching constraints.

**MSC.** 90C34, 90C40, 49J52.

---

\* Corresponding author

f.gorgini2016@gmail.com, nad.kanzi@gmail.com, j.izadi@pnu.ac.ir, fallahi1361@gmail.com  
<http://mathco.journals.pnu.ac.ir>

## 1 Introduction

This paper focuses on the following “mathematical programming with switching constraints” (MPSC, in brief):

$$(P) \quad \begin{aligned} \min \quad & f(x) \\ \text{s.t.} \quad & G_i(x)H_i(x) = 0, \quad i = 1, \dots, m, \\ & x \in \mathbb{R}^n \end{aligned}$$

where,  $f : \mathbb{R}^n \rightarrow \mathbb{R}$  is continuously differentiable, and  $H_i, G_i : \mathbb{R}^n \rightarrow \mathbb{R}$  are locally Lipschitz for all  $i \in I := \{1, \dots, m\}$ .

Recently, MPSCs have been introduced by Mehlitz [9] as a new type of optimization problem. Mehlitz showed that some of the well-known constraint qualifications such as Mangasarian-Fromovitz and linear independent constraint qualifications (CQ) do not hold at each feasible point of MPSCs, and he introduced Abadie and Guignard type CQs for these problems. Then, he presented some different optimality conditions, named stationary conditions, for MPSCs under these CQs. Due to the wide applications of MPSC in control theory, physics, topological optimization, etc., research on it was considered by many researchers. The exact penalty method, the relaxation schemes, and the topological approach for solving MPSCs are studied in [8], [5] and [12], respectively.

In the previous works that referenced earlier, all functions which define MPSC are continuously differentiable. To the best of our knowledge, the current article is the first that studies the stationary conditions for MPSCs where their constraints are non-smooth, meaning that they are not necessarily differentiable. In this paper, we assume that the objective function is differentiable.

The structure of subsequent sections of this paper is as follows. Section 2 contains the elementary definitions, notations, theorems, and relations that are required in the sequel. In Section 3, we will introduce some Guignard type CQs for problem (P). Also, different kinds of stationary conditions at optimal solutions of (P) are presented in this section.

## 2 Notations and Preliminaries

In this section, we recall some definitions and theorems in non-smooth analysis, which are widely used in the sequel, from [3, 4].

Given a nonempty set  $B \subseteq \mathbb{R}^n$ , we denote by  $\overline{B}$  and  $\text{cone}(B)$ , the closure of  $B$  and the convex cone of  $B$ , respectively; i.e.,  $\text{cone}(B) = \text{conv}(\bigcup_{\beta \geq 0} \beta B)$  where  $\text{conv}(A)$  denotes the convex hull of  $A$ . The polar cone of  $B$  is defined by

$$B^0 := \{x \in \mathbb{R}^n \mid \langle x, b \rangle \leq 0, \quad \forall b \in B\},$$

where  $\langle x, b \rangle$  refers to the standard inner product of  $x$  and  $b$  in  $\mathbb{R}^n$ . Also, the orthogonal cone to  $B$  is denoted by  $B^\perp$ ,



$$B^\perp := B^0 \cap (-B)^0 = \{x \in \mathbb{R}^n \mid \langle x, b \rangle = 0, \quad \forall b \in B\}.$$

Let  $\emptyset^0 = \emptyset^\perp := \mathbb{R}^n$ . The bipolar theorem [4] states that

$$B^{00} := (B^0)^0 = \overline{\text{cone}(B)} := \overline{\text{cone}(B)}. \quad (1)$$

Clearly, the following relations hold,

$$B^0 = (\text{cone}(B))^0 = (\overline{\text{cone}(B)})^0, \quad (2)$$

$$B_1 \subseteq B_2 \implies B_2^0 \subseteq B_1^0. \quad (3)$$

Suppose that  $B_1, \dots, B_p$  are convex subsets of  $\mathbb{R}^n$ , and  $\mathcal{B} := \bigcup_{\ell=1}^p B_\ell$ . Then, it is easy to see that [4]

$$\text{cone}(\mathcal{B}) = \left\{ \sum_{\ell=1}^p \beta_\ell b_\ell \mid b_\ell \in B_\ell, \beta_\ell \geq 0 \right\}. \quad (4)$$

The Buligand tangent cone (or contingent cone) and the Frechet normal cone of a nonempty set  $B \subseteq \mathbb{R}^n$  at  $x_0 \in B$  are respectively denoted by  $\Gamma(B, x_0)$  and  $N(B, x_0)$ , defined as

$$\Gamma(B, x_0) := \left\{ v \in \mathbb{R}^n \mid \exists t_\ell \downarrow 0, \exists v_\ell \rightarrow v \text{ such that } x_0 + t_\ell v_\ell \in B \quad \forall \ell \in \mathbb{N} \right\},$$

$$N(B, x_0) := (\Gamma(B, x_0))^0.$$

**Theorem 1.** [4] Let  $x_0 \in B \subseteq \mathbb{R}^n$  be a minimizer of a continuously differentiable function  $\varphi : \mathbb{R}^n \rightarrow \mathbb{R}$  on  $B$ . Then,

$$0_n \in \{\nabla\varphi(x_0)\} + N(B, x_0),$$

in which  $0_n := \overbrace{(0, \dots, 0)}^{n \text{ times}}$  is the zero vector of  $\mathbb{R}^n$ , and  $\nabla\varphi(x_0)$  denotes the classic gradient of  $\varphi$  at  $x_0$ .

A real-valued function  $\psi : \mathbb{R}^n \rightarrow \mathbb{R}$  is said to be Lipschitz near  $x_0 \in \mathbb{R}^n$  if there exist a neighborhood  $U_0$  for  $x_0$  and a positive number  $L_0 > 0$  such that

$$|\psi(x) - \psi(x_0)| \leq L_0 \|x - x_0\|, \quad \text{for all } x \in U_0.$$

$\psi$  is said to be locally Lipschitz when it is Lipschitz near all  $x_0 \in \mathbb{R}^n$ . For a given locally Lipschitz function  $\psi : \mathbb{R}^n \rightarrow \mathbb{R}$ , the Clarke directional derivative of  $\psi$  at  $x_0$  in the direction  $v \in \mathbb{R}^n$ , and the Clarke subdifferential of  $\psi$  at  $x_0$  are respectively defined by [3]

$$\psi^0(x_0; v) := \limsup_{y \rightarrow x_0, t \downarrow 0} \frac{\psi(y + tv) - \psi(y)}{t},$$

$$\partial_c \psi(x_0) := \left\{ \xi \in \mathbb{R}^n \mid \langle \xi, v \rangle \leq \psi^0(x_0; v) \quad \text{for all } v \in \mathbb{R}^n \right\}.$$

The Clarke subdifferential is a generalization of the classical derivative; i.e., if  $\psi$  is continuously differentiable at  $x_0$ , we have  $\partial_c \psi(x_0) = \{\nabla \psi(x_0)\}$ . Also, the Clarke subdifferential of each locally Lipschitz function at all points in its domain is always nonempty, convex, and compact.

As the last point of this section, we recall ([4]) that if  $\varphi$  and  $\psi_t$ , for  $t = 1, \dots, p$ , are locally Lipschitz functions from  $\mathbb{R}^n$  to  $\mathbb{R}$ , we say that the optimization problem

$$\min \varphi(x) \text{ s.t. } x \in \Pi := \left\{ x \in \mathbb{R}^n \mid \psi_t(x) \leq 0, \quad t = 1, 2, \dots, p \right\},$$

satisfies the Guignard constraint qualification at  $x_0 \in \Pi$  if

$$\left( \bigcup_{t \in T_0} \partial_c \psi_t(x_0) \right)^\circ \subseteq \overline{\text{cone}}(\Gamma(\Pi, x_0)),$$

where  $T_0 := \{t \mid \psi_t(x_0) = 0\}$ .

### 3 The Main Results

Throughout this article, we suppose that the feasible set of  $(P)$ , named  $S$ , is nonempty, i.e.,

$$S := \{x \in \mathbb{R}^n \mid G_i(x)H_i(x) = 0, \quad i \in I\} \neq \emptyset.$$

Let  $\hat{x} \in S$  be a feasible point that will be fixed throughout this section. We divide the index set  $I$  into the following three index sets:

$$\begin{aligned} I_G &:= \{i \in I \mid H_i(\hat{x}) \neq 0, G_i(\hat{x}) = 0\}, \\ I_H &:= \{i \in I \mid H_i(\hat{x}) = 0, G_i(\hat{x}) \neq 0\}, \\ I_{GH} &:= \{i \in I \mid H_i(\hat{x}) = 0, G_i(\hat{x}) = 0\}. \end{aligned}$$

Notice that,  $I = I_G \cup I_H \cup I_{GH}$ . As shown in [9], the problem

$$\begin{aligned} (P^*) \quad & \min && f(x) \\ & \text{s.t.} && G_i(x) = 0, && i \in I_G, \\ & && H_i(x) = 0, && i \in I_H, \end{aligned}$$

is locally equivalent to  $(P)$  when  $I_{GH} = \emptyset$ . In order to add the constraints related to index  $I_{GH}$  to  $(P^*)$ , we consider two index sets  $I_1 \subseteq I_{GH}$  and  $I_2 \subseteq I_{GH}$  in such a way that  $I_1 \cup I_2 = I_{GH}$ , then, we add the constraints corresponding to  $I_1$  and  $I_2$  to the first and second lines of the constraints of problem  $(P^*)$ , respectively. So, we obtain the following parametric problem which is defined in terms of parameters  $I_1$  and  $I_2$ :

$$\begin{aligned} (P_{I_2}^{I_1}) \quad & \min && f(x) \\ & \text{s.t.} && G_i(x) = 0, && i \in I_G \cup I_1, \\ & && H_i(x) = 0, && i \in I_H \cup I_2. \end{aligned}$$

**Remark 1.** The index sets  $I_1$  and  $I_2$  can be such that  $I_1 \cap I_2 \neq \emptyset$ , and they do not need to be separate. Also, one of the index sets  $I_1$  and  $I_2$  may be equal to empty (in this case, the other is necessarily equal to  $I_{GH}$ ).

For the sake of simplicity, motivated by [6, 7], for all  $J_1 \subseteq I$  and  $J_2 \subseteq I$ , put

$$\mathcal{G}^{J_1} := \bigcup_{i \in J_1} \partial_c G_i(\hat{x}), \quad \mathcal{H}^{J_2} := \bigcup_{i \in J_2} \partial_c H_i(\hat{x}),$$

$$\mathcal{Z}_{J_2}^{J_1} := \mathcal{G}^{J_1} \cup (-\mathcal{G}^{J_1}) \cup \mathcal{H}^{J_2} \cup (-\mathcal{H}^{J_2}).$$

Note that, corresponding to  $(P^*)$  and  $(P_{I_2}^{I_1})$ , we obtain the linearized cones  $(\mathcal{G}^{I_G})^\perp \cap (\mathcal{H}^{I_H})^\perp$  and  $(\mathcal{G}^{I_G \cup I_1})^\perp \cap (\mathcal{H}^{I_H \cup I_2})^\perp$ , respectively. Since, the equalities

$$(\mathcal{G}^{I_G})^\perp \cap (\mathcal{H}^{I_H})^\perp = (\mathcal{Z}_{I_H}^{I_G})^0, \quad \text{and} \quad (\mathcal{G}^{I_G \cup I_1})^\perp \cap (\mathcal{H}^{I_H \cup I_2})^\perp = (\mathcal{Z}_{I_H \cup I_2}^{I_G \cup I_1})^0,$$

are clearly true, we are guided by the following definition.

**Definition 1.** We say that  $(P)$  satisfies the

(i): generalized Guignard constraint qualification, denoted by GGCQ, at  $\hat{x}$ , if

$$(\mathcal{Z}_{I_H}^{I_G})^0 \subseteq \overline{\text{cone}}(\Gamma(S, \hat{x})).$$

(ii):  $(I_1, I_2)$ -parametric Guignard constraint qualification, denoted by PGCQ $_{I_2}^{I_1}$ , at  $\hat{x}$ , if

$$(\mathcal{Z}_{I_H \cup I_2}^{I_G \cup I_1})^0 \subseteq \overline{\text{cone}}(\Gamma(S, \hat{x})).$$

**Remark 2.** Since the feasible set of  $(P^*)$  contains  $S$  and the feasible set of  $(P_{I_2}^{I_1})$  is contained in  $S$ , the following statements are true.

- Each optimal solution of  $(P)$  which is feasible for  $(P_{I_2}^{I_1})$  is also an optimal solution for  $(P_{I_2}^{I_1})$ .
- PGCQ $_{I_2}^{I_1}$  (resp. GGCQ) is not equivalent to Guignard CQ for  $(P_{I_2}^{I_1})$  (resp.  $(P^*)$ ).

Before stating the necessary optimality conditions for  $(P)$ , we need to prove the following lemma.

**Lemma 1.** If  $J_1$  and  $J_2$  are two subsets of  $I$ , then

$$\text{cone}(\mathcal{Z}_{J_2}^{J_1}) = \bigcup_{(\mu_r) \in \mathbb{R}^{|J_1|}} \bigcup_{(\eta_s) \in \mathbb{R}^{|J_2|}} \left( \sum_{r \in J_1} \mu_r \partial_c G_r(\hat{x}) + \sum_{s \in J_2} \eta_s \partial_c H_s(\hat{x}) \right).$$

*Proof.* Since the Clarke subdifferential of each locally Lipschitz function is convex, the definition of  $\mathcal{Z}_{J_2}^{I_1}$  and (4) conclude that

$$\text{cone}(\mathcal{Z}_{J_2}^{I_1}) = \left\{ \sum_{r \in J_1} \alpha_r \hat{g}_r + \sum_{r \in J_1} \beta_r \tilde{g}_r + \sum_{s \in J_2} \gamma_s \hat{h}_s + \sum_{s \in J_2} \omega_s \tilde{h}_s \mid \alpha_r, \beta_r, \gamma_s, \omega_s \geq 0, \right. \\ \left. \hat{g}_r \in \partial_c G_r(\hat{x}), \tilde{g}_r \in \partial_c (-G_r)(\hat{x}), \hat{h}_s \in \partial_c H_s(\hat{x}), \tilde{h}_s \in \partial_c (-H_s)(\hat{x}) \right\}.$$

Owing to  $\partial_c (-G_r)(\hat{x}) = -\partial_c G_r(\hat{x})$  as  $r \in J_1$ , for each  $\tilde{g}_r \in \partial_c (-G_r)(\hat{x})$ , there exists a  $\hat{g}_r \in \partial_c G_r(\hat{x})$  such that  $\tilde{g}_r = -\hat{g}_r$ . Similarly, for each  $\tilde{h}_s \in \partial_c (-H_s)(\hat{x})$ , there exists a  $\hat{h}_s \in \partial_c H_s(\hat{x})$  such that  $\tilde{h}_s = -\hat{h}_s$  as  $s \in J_2$ . Thus,

$$\text{cone}(\mathcal{Z}_{J_2}^{I_1}) = \left\{ \sum_{r \in J_1} (\alpha_r - \beta_r) \hat{g}_r + \sum_{s \in J_2} (\gamma_s - \omega_s) \hat{h}_s \mid \alpha_r, \beta_r, \gamma_s, \omega_s \geq 0, \right. \\ \left. \hat{g}_r \in \partial_c G_r(\hat{x}), \hat{h}_s \in \partial_c H_s(\hat{x}) \right\}.$$

Taking  $\mu_r := \alpha_r - \beta_r \in \mathbb{R}$  and  $\eta_s := \gamma_s - \omega_s \in \mathbb{R}$  as  $r \in J_1$  and  $s \in J_2$ , the latter equality implies that

$$\text{cone}(\mathcal{Z}_{J_2}^{I_1}) = \left\{ \sum_{r \in J_1} \mu_r \hat{g}_r + \sum_{s \in J_2} \eta_s \hat{h}_s \mid \mu_r, \eta_s \in \mathbb{R}, \hat{g}_r \in \partial_c G_r(\hat{x}), \hat{h}_s \in \partial_c H_s(\hat{x}) \right\} \\ = \bigcup_{(\mu_r) \in \mathbb{R}^{|J_1|}} \bigcup_{(\eta_s) \in \mathbb{R}^{|J_2|}} \left( \sum_{r \in J_1} \mu_r \partial_c G_r(\hat{x}) + \sum_{s \in J_2} \eta_s \partial_c H_s(\hat{x}) \right).$$

□

Now, we state the nonsmooth version of strongly stationary (S-stationary, in short) condition presented in [9].

**Theorem 2. (S-Stationary Condition):** Suppose that  $\hat{x}$  is an optimal solution of (P) and the GGCQ holds at  $\hat{x}$ . If  $\overline{\text{cone}}(\mathcal{Z}_{I_H}^{I_G}) = \text{cone}(\mathcal{Z}_{I_H}^{I_G})$  (equivalently,  $\text{cone}(\mathcal{Z}_{I_H}^{I_G})$  is closed), then there exist some multipliers  $\lambda_i^G, \lambda_i^H \in \mathbb{R}$  as  $i \in I$ , such that

$$-\nabla f(\hat{x}) \in \sum_{i \in I} \left( \lambda_i^G \partial_c G_i(\hat{x}) + \lambda_i^H \partial_c H_i(\hat{x}) \right), \quad (5)$$

$$\lambda_i^G = 0, \quad i \in I_H \cup I_{GH}, \quad \text{and} \quad \lambda_i^H = 0, \quad i \in I_G \cup I_{GH}. \quad (6)$$

*Proof.* Since  $\hat{x}$  is a minimizer for (P), employing Theorem 1, we have

$$0_n \in \{\nabla f(\hat{x})\} + N(S, \hat{x}) = \{\nabla f(\hat{x})\} + (\Gamma(S, \hat{x}))^0. \quad (7)$$

On the other hand, the GGCQ at  $\hat{x}$  and (2)-(3) imply that

$$(\Gamma(S, \hat{x}))^0 = \left( \overline{\text{cone}}(\Gamma(S, \hat{x})) \right)^0 \subseteq (\mathcal{Z}_{I_H}^{I_G})^{00}.$$

The above inclusion, the bipolar theorem (1), the closedness assumption of  $\text{cone}(\mathcal{Z}_{I_H}^{I_G})$ , and (7) conclude that

$$0_n \in \{\nabla f(\hat{x})\} + \overline{\text{cone}}(\mathcal{Z}_{I_H}^{I_G}) = \{\nabla f(\hat{x})\} + \text{cone}(\mathcal{Z}_{I_H}^{I_G}). \quad (8)$$

According to Lemma 1, we obtain from (8) that

$$-\nabla f(\hat{x}) \in \bigcup_{(\mu_r) \in \mathbb{R}^{|I_G|}} \bigcup_{(\eta_s) \in \mathbb{R}^{|I_H|}} \left( \sum_{r \in I_G} \mu_r \partial_c G_r(\hat{x}) + \sum_{s \in I_H} \eta_s \partial_c H_s(\hat{x}) \right),$$

which concludes that there exist some  $\mu_r \in \mathbb{R}$  and  $\eta_s \in \mathbb{R}$  as  $r \in I_G$  and  $s \in I_H$  such that

$$-\nabla f(\hat{x}) \in \left( \sum_{r \in I_G} \mu_r \partial_c G_r(\hat{x}) + \sum_{s \in I_H} \eta_s \partial_c H_s(\hat{x}) \right).$$

For each

$$r \in I \setminus I_G = I_H \cup I_{GH} \quad \text{and} \quad s \in I \setminus I_H = I_G \cup I_{GH},$$

put  $\mu_r := 0$  and  $\eta_s := 0$ . Thus,

$$-\nabla f(\hat{x}) \in \left( \sum_{r \in I} \mu_r \partial_c G_r(\hat{x}) + \sum_{s \in I} \eta_s \partial_c H_s(\hat{x}) \right).$$

Changing the indices  $r$  and  $s$  to  $i$  in the above inclusion, and setting  $\lambda_i^G := \mu_i$  and  $\lambda_i^H := \eta_i$  as  $i \in I$ , we deduce that

$$\begin{cases} -\nabla f(\hat{x}) \in \sum_{i \in I} \left( \lambda_i^G \partial_c G_i(\hat{x}) + \lambda_i^H \partial_c H_i(\hat{x}) \right), \\ \lambda_i^G = 0, \quad i \in I_H \cup I_{GH}, \quad \text{and} \quad \lambda_i^H = 0, \quad i \in I_G \cup I_{GH}, \end{cases}$$

as required.  $\square$

When the functions  $G_i$  and  $H_i$  as  $i \in I$  are continuously differentiable, (5)-(6) were named the strongly stationary condition for (P) in [9]. Hence we also call them strongly stationary condition.

Now, we state a new optimality condition for (P), and we call it parametric stationary (P-stationary, in short) condition.

**Theorem 3. (P-Stationary Condition):** Suppose that  $\hat{x}$  is an optimal solution of (P) and the PGCQ $_{I_2}^{I_1}$  holds at  $\hat{x}$ . If  $\text{cone}(\mathcal{Z}_{I_H \cup I_2}^{I_G \cup I_1})$  is closed, then there exist some multipliers  $\lambda_i^G, \lambda_i^H \in \mathbb{R}$  as  $i \in I$ , such that

$$-\nabla f(\hat{x}) \in \sum_{i \in I} \left( \lambda_i^G \partial_c G_i(\hat{x}) + \lambda_i^H \partial_c H_i(\hat{x}) \right), \quad (9)$$

$$\lambda_i^G = 0, \quad i \in I_H \cup I_2, \quad \text{and} \quad \lambda_i^H = 0, \quad i \in I_G \cup I_1. \quad (10)$$

*Proof.* Repeating the proof of (8), we get

$$0_n \in \{\nabla f(\hat{x})\} + \overline{\text{cone}}\left(\mathcal{Z}_{I_H \cup I_2}^{I_G \cup I_1}\right) = \{\nabla f(\hat{x})\} + \text{cone}\left(\mathcal{Z}_{I_H \cup I_2}^{I_G \cup I_1}\right),$$

and according to Lemma 1, we obtain

$$\text{cone}\left(\mathcal{Z}_{I_H \cup I_2}^{I_G \cup I_1}\right) = \bigcup_{(\mu_r) \in \mathbb{R}^{|I_G \cup I_1|}} \bigcup_{(\eta_s) \in \mathbb{R}^{|I_H \cup I_2|}} \left( \sum_{r \in I_G \cup I_1} \mu_r \partial_c G_r(\hat{x}) + \sum_{s \in I_H \cup I_2} \eta_s \partial_c H_s(\hat{x}) \right).$$

Using the above two relations and following the proof of Theorem 2 lead us to the required result.  $\square$

In what follows, we will show that the parametric stationary condition, presented in Theorem 3, gives rise to two other stationary conditions that are presented in [9] for smooth MPSCs. First, we present the M-stationary condition as follows (“M” is an abbreviation for Mordukhovich):

**Theorem 4. (M-Stationary Condition):** Suppose that  $\hat{x}$  is an optimal solution of (P) and the  $\text{PGCQ}_{I_2}^{I_1}$  holds at  $\hat{x}$ . If  $\text{cone}\left(\mathcal{Z}_{I_H \cup I_2}^{I_G \cup I_1}\right)$  is closed, then there exist some multipliers  $\lambda_i^G, \lambda_i^H \in \mathbb{R}$  as  $i \in I$ , such that

$$-\nabla f(\hat{x}) \in \sum_{i \in I} \left( \lambda_i^G \partial_c G_i(\hat{x}) + \lambda_i^H \partial_c H_i(\hat{x}) \right), \quad (11)$$

$$\lambda_i^G = 0, \quad i \in I_H, \quad \text{and} \quad \lambda_i^H = 0, \quad i \in I_G, \quad (12)$$

$$\lambda_i^G \lambda_i^H = 0, \quad i \in I_{GH}. \quad (13)$$

*Proof.* Since the inclusion (11) is the same as inclusion (9), and the relation (12) obviously results from relation (10), it suffices to prove only equation (13). Let  $i \in I$ . Owing to  $I = I_1 \cup I_2$ , we conclude that  $i \in I_1$  or  $i \in I_2$ , and so,  $\lambda_i^H = 0$  or  $\lambda_i^G = 0$ , respectively. Thus,  $\lambda_i^G \lambda_i^H = 0$ , and the proof is complete.  $\square$

If in Theorem 3 we put  $I_1 = I_2 = I_{GH}$ , we get the following theorem, named weakly stationary (W-stationary, in short) condition [9] in smooth case.

**Theorem 5. (W-Stationary Condition):** Suppose that  $\hat{x}$  is an optimal solution of (P) and the  $\text{PGCQ}_{I_{GH}}^{I_{GH}}$  are satisfied at  $\hat{x}$ . If  $\text{cone}\left(\mathcal{Z}_{I_H \cup I_{GH}}^{I_G \cup I_{GH}}\right)$  is closed, then there exist some multipliers  $\lambda_i^G, \lambda_i^H \in \mathbb{R}$  as  $i \in I$ , such that

$$-\nabla f(\hat{x}) \in \sum_{i \in I} \left( \lambda_i^G \partial_c G_i(\hat{x}) + \lambda_i^H \partial_c H_i(\hat{x}) \right),$$

$$\lambda_i^G = 0, \quad i \in I_H \cup I_{GH}, \quad \text{and} \quad \lambda_i^H = 0, \quad i \in I_G \cup I_{GH}.$$

The following implications are straightforward consequences of the aforementioned definitions of stationary conditions:

$$S\text{-Stationarity} \Rightarrow P\text{-Stationarity} \Rightarrow M\text{-Stationarity} \Rightarrow W\text{-Stationarity}.$$

The following example thoroughly and accurately analyzes the strict relationships between the various constraint qualifications and different stationary conditions expressed in the present article.

**Example 1.** Put in problem (P),

$$n := 2, \quad x := (x_1, x_2) \in \mathbb{R}^2, \quad f(x) := 2x_1 + 3x_2,$$

$$G_1(x) := x_1, \quad H_1(x) := x_2,$$

$$G_2(x) := 1, \quad H_2(x) := (x_1^2 - x_2) + |x_1^2 - x_2|.$$

It is easy to see that  $S = \{0\} \times [0, +\infty)$  and that  $\hat{x} := 0_2$  is an optimal solution to the problem. Also, a short calculation shows that:

$$I_G = \emptyset, \quad I_H = \{2\}, \quad I_{GH} = \{1\},$$

$$\nabla f(0_2) = (2, 3), \quad \partial_c G_1(0_2) = \{(1, 0)\}, \quad \partial_c H_1(0_2) = \{(0, 1)\},$$

$$\partial_c G_2(0_2) = \{0_2\}, \quad \partial_c H_2(0_2) = \{0\} \times (-1 + [-1, 1]) = \{0\} \times [-2, 0].$$

$$(\mathcal{G}^{I_G \cup I_1})^\perp = \{(1, 0)\}^\perp = \{0\} \times \mathbb{R},$$

$$(\mathcal{H}^{I_H \cup I_2})^\perp = (\{0\} \times [-2, 0])^\perp = \mathbb{R} \times \{0\},$$

$$\text{cone}(\mathcal{Z}_{I_H \cup I_2}^{I_G \cup I_1}) = \mathbb{R}^2,$$

$$(\mathcal{G}^{I_G \cup I_1})^\perp \cap (\mathcal{H}^{I_H \cup I_2})^\perp = \{0_2\} \subseteq S = \overline{\text{cone}}(\Gamma(S, 0_2)).$$

Thus,  $\text{PGCQ}_{I_2}^{I_1}$  holds at  $\hat{x}$  and  $\text{cone}(\mathcal{Z}_{I_H \cup I_2}^{I_G \cup I_1})$  is closed, i.e., all hypotheses of Theorem 3 hold. Obviously, we can find some scalars  $\lambda_i^G$  and  $\lambda_i^H$  as  $i = 1, 2$  satisfying (9)-(10). In fact, taking

$$\lambda_1^G := -2, \quad \lambda_1^H := 0, \quad \lambda_2^G := 0, \quad \lambda_2^H := \frac{3}{2},$$

we have

$$(-2, -3) \in \lambda_1^G \{(1, 0)\} + \lambda_1^H \{(0, 1)\} + \lambda_2^G \{0_2\} + \lambda_2^H (\{0\} \times [-2, 0]).$$

This means the P-stationary condition, M-stationary condition, and W-stationary condition are satisfied at  $\hat{x}$ . It should be observed that since

$$(\mathcal{G}^{I_G})^\perp \cap (\mathcal{H}^{I_H})^\perp = \mathbb{R}^2 \cap (\mathbb{R} \times \{0\}) = \mathbb{R} \times \{0\} \not\subseteq S = \overline{\text{cone}}(\Gamma(S, 0_2)),$$

the GGCQ does not hold at  $\hat{x}$ , and the S-stationary condition (5)-(6) is not valid. In fact, there are not  $\lambda_i^G$  and  $\lambda_i^H$  as  $i = 1, 2$  satisfying

$$(-2, -3) \in \lambda_1^G \{(1, 0)\} + \lambda_1^H \{(0, 1)\} + \lambda_2^G \{0_2\} + \lambda_2^H (\{0\} \times [-2, 0]),$$

$$\lambda_1^G = \lambda_2^G = \lambda_1^H = 0.$$

As the final point of this article, we introduce a broad and important class of MPSCs that satisfy parametric Guignard constraint qualification at all of their feasible points but do not necessarily satisfy generalized Guignard constraint qualification. It is noteworthy that in this category of MPSCs, none of the appearing functions are necessarily convex.

Consider the following optimization problem with fractional quadratic constraints on  $\mathbb{R}$ :

$$(Q) \quad \begin{aligned} \min \quad & f(x) \\ \text{s.t.} \quad & \frac{(a_i x + b_i)(a'_i x + b'_i)}{(c_i x + d_i)(c'_i x + d'_i)} = 0, \quad i \in I, \\ & x \in \mathbb{R}, \end{aligned}$$

where the numbers  $a_i, a'_i, c_i, c'_i, b_i, b'_i, d_i, d'_i \in \mathbb{R}$  are fixed such that  $(a_i, b_i) \neq 0_2 \neq (c_i, d_i)$  as  $i \in I := \{1, \dots, m\}$ , and where  $f : \mathbb{R} \rightarrow \mathbb{R}$  is continuously differentiable. The feasible set of (Q) is denoted by  $\hat{S}$ . This problem is a MPSC with the following data:

$$G_i(x) = \frac{a_i x + b_i}{c_i x + d_i}, \quad \text{and} \quad H_i(x) = \frac{a'_i x + b'_i}{c'_i x + d'_i}.$$

Since  $G_i$  and  $H_i$ , for  $i \in I$ , are continuously differentiable on their open domain, they are locally Lipschitz near each point on their domains. Let  $\hat{x} \in \mathbb{R}^n$  be a feasible point for (Q), and  $J_1, J_2 \subseteq I_{GH}$  be given with  $J_1 \cup J_2 = I_{GH}$ . The definition of polar cones implies that  $0 \in A^0$  for all  $A \subseteq \mathbb{R}$ . Thus,  $(\mathcal{Z}_{I_H \cup I_{GH} \setminus J}^{I_G \cup J})^0 \neq \emptyset$ . Let  $w \in (\mathcal{Z}_{I_H \cup I_{GH} \setminus J}^{I_G \cup J})^0$  be chosen arbitrarily. According to

$$w \in (\mathcal{G}^{I_G \cup J_1})^\perp \cap (\mathcal{H}^{I_H \cup J_2})^\perp,$$

and

$$\nabla G_i(\hat{x}) = \frac{a_i d_i - b_i c_i}{(c_i \hat{x} + d_i)^2}, \quad \text{and} \quad \nabla H_i(\hat{x}) = \frac{a'_i d'_i - b'_i c'_i}{(c'_i \hat{x} + d'_i)^2},$$

we have

$$\begin{cases} \left( \frac{a_i d_i - b_i c_i}{(c_i \hat{x} + d_i)^2} \right) w = 0, & \text{for } i \in I_G \cup J_1, \\ \left( \frac{a'_i d'_i - b'_i c'_i}{(c'_i \hat{x} + d'_i)^2} \right) w = 0, & \text{for } i \in I_H \cup J_2. \end{cases} \quad (14)$$

The first equality in (14) concludes, for each  $t \geq 0$  and for  $i \in I_G \cup J_1$ , that

$$(a_i d_i - b_i c_i)(\hat{x} + t w - \hat{x}) = 0 \implies a_i d_i(\hat{x} + t w) + b_i c_i \hat{x} = b_i c_i(\hat{x} + t w) + a_i d_i \hat{x}.$$

By adding the two sides of latter equality with  $a_i c_i \hat{x}(\hat{x} + t w) + b_i d_i$  and factoring in the appropriate expressions, we obtain that

$$a_i(\hat{x} + t w)(c_i \hat{x} + d_i) + b_i(c_i \hat{x} + d_i) = c_i(\hat{x} + t w)(a_i \hat{x} + b_i) + d_i(a_i \hat{x} + b_i),$$

and so



$$\left(a_i(\hat{x} + tw) + b_i\right)(c_i\hat{x} + d_i) = \left(c_i(\hat{x} + tw) + d_i\right)(a_i\hat{x} + b_i).$$

This means that

$$\frac{a_i(\hat{x} + tw) + b_i}{c_i(\hat{x} + tw) + d_i} = \frac{a_i\hat{x} + b_i}{c_i\hat{x} + d_i} = 0, \quad (15)$$

where the last equality holds for  $i \in I_G \cup J_1$ . Similarly, from the second equality of (14), for each  $i \in I_H \cup J_2$  we deduce that

$$\frac{a'_i(\hat{x} + tw) + b'_i}{c'_i(\hat{x} + tw) + d'_i} = \frac{a'_i\hat{x} + b'_i}{c'_i\hat{x} + d'_i} = 0. \quad (16)$$

Owing to (15)-(16) and the fact that  $I = I_G \cup I_H \cup J_1 \cup J_2$ , we have

$$\frac{a_i(\hat{x} + tw) + b_i}{c_i(\hat{x} + tw) + d_i} \cdot \frac{a'_i(\hat{x} + tw) + b'_i}{c'_i(\hat{x} + tw) + d'_i} = 0, \quad \text{for all } i \in I.$$

Thus,  $\hat{x} + tw \in \hat{S}$  for all  $t \geq 0$ , and so  $w \in \Gamma(\hat{S}, \hat{x})$ . Summarizing, we proved that

$$\left(\mathcal{Z}_{I_H \cup J_2}^{I_G \cup J_1}\right)^0 \subseteq \Gamma(\hat{S}, \hat{x}) \subseteq \overline{\text{cone}}(\Gamma(\hat{S}, \hat{x})).$$

Therefore,  $\text{PGCQ}_{J_2}^1$  holds at every point in  $\hat{S}$ . On the other hand, since

$$\mathcal{Z}_{I_H \cup J_2}^{I_G \cup J_1} = \left\{ \pm \frac{a_i d_i - b_i c_i}{(c_i \hat{x} + d_i)^2} \mid i \in I_G \cup J_1 \right\} \cup \left\{ \pm \frac{a'_i d'_i - b'_i c'_i}{(c'_i \hat{x} + d'_i)^2} \mid i \in I_H \cup J_2 \right\},$$

then, the number of members of  $\mathcal{Z}_{I_H \cup J_2}^{I_G \cup J_1}$  is not more than  $2m$ . So, according to the well-known result that says “the convex cone of each finite set in  $\mathbb{R}^n$  is closed” [4], we conclude that  $\text{cone}(\mathcal{Z}_{I_H \cup J_2}^{I_G \cup J_1})$  is closed. Thus, P-stationary condition is satisfied at each optimal solution of (Q) by Theorems 3 and 4, respectively. It should be noted that the GGCQ does not necessarily hold at all feasible points of (Q) and S-stationary condition is not necessarily satisfied at all optimal solutions of (Q).

**Remark 3.** Here we present another proof to reach (15)-(16) out of (14).

If  $w = 0$ , then (15)-(16) hold clearly. Thus, we suppose that  $w \neq 0$  satisfies (14). Hence,

$$\begin{cases} \frac{a_i d_i - b_i c_i}{(c_i \hat{x} + d_i)^2} = 0, & i \in I_G \cup J_1, \\ \frac{a'_i d'_i - b'_i c'_i}{(c'_i \hat{x} + d'_i)^2} = 0, & i \in I_H \cup J_2, \end{cases} \implies \begin{cases} a_i d_i = b_i c_i, & i \in I_G \cup J_1, \\ a'_i d'_i = b'_i c'_i, & i \in I_H \cup J_2. \end{cases}$$

This means that there exist  $k, k' \in \mathbb{R}$  such that

$$\begin{cases} \frac{a_i x + b_i}{c_i x + d_i} = k, & i \in I_G \cup J_1, x \in \hat{S}, \\ \frac{a'_i x + b'_i}{c'_i x + d'_i} = k', & i \in I_H \cup J_2, x \in \hat{S}. \end{cases}$$

This means that  $G_i(x)$  as  $i \in I_G \cup J_1$  and  $H_i(x)$  as  $i \in I_H \cup J_2$  are independent of  $x$ , and since

$$\begin{cases} \frac{a_i \hat{x} + b_i}{c_i \hat{x} + d_i} = 0, & i \in I_G \cup J_1, \\ \frac{a'_i \hat{x} + b'_i}{c'_i \hat{x} + d'_i} = 0, & i \in I_H \cup J_2, \end{cases}$$

we have  $k = k' = 0$ , and so

$$\begin{cases} \frac{a_i(\hat{x} + tw) + b_i}{c_i(\hat{x} + tw) + d_i} = 0, & i \in I_G \cup J_1, \\ \frac{a'_i(\hat{x} + tw) + b'_i}{c'_i(\hat{x} + tw) + d'_i} = 0, & i \in I_H \cup J_2. \end{cases}$$

#### 4 Conclusion

Since MPSC, like “mathematical programming with equilibrium constraints” (MPEC) and “mathematical programming with vanishing constraints” (MPVC), is in the class of optimization problems that include multiplicative constraints, in order to present similar works [1, 2], and [10, 11] which consider nonsmooth MPECs and MPVCs, respectively, this article deals with the nonsmoothness of the results of [9].

#### Acknowledgment

The authors are very grateful to the referees for their constructive comments, especially correcting an incorrect remark from the first version of the article.

#### References

- [1] Ansari Ardali A., Movahedian N., Nobakhtian S. (2016). “Optimality conditions for non-smooth mathematical programs with equilibrium constraints, using convexificators”, *Optimization*, 65, 67-85.
- [2] Ansari Ardali A., Movahedian N., Nobakhtian S. (2016). ”Optimality conditions for non-smooth equilibrium problems via Hadamard directional derivative”, *Set-Valued and Variational Analysis*, 24, 483-497.
- [3] Clarke F. H. (1983). “Optimization and non-smooth analysis”, Wiley, Interscience.
- [4] Giorgi G., Gwirraggio A., Thierselder J. (2004). “Mathematics of optimization”, Smooth and Nonsmooth cases, Elsevier.

- [5] Kanzow C., Mehlitz P., Steck D. (2019). “Relaxation schemes for mathematical programs with switching constraints”, Optimization Methods and Software.
- [6] Kazemi S., Kanzi N. (2018). “Constraint qualifications and stationary conditions for mathematical programming with non-differentiable vanishing constraints”, Journal of Optimization Theory and Applications, 179(3), 800-819.
- [7] Kazemi S., Kanzi N., Ebadian A. (2019). “Estimating the Frechet normal cone in optimization problems with non-smooth vanishing constraints”, Iranian Journal of Science and Technology, Transactions A Science, 43(5), 2299-2306.
- [8] Liang Y. C., Ye J. J. (2021). “Optimality conditions and exact penalty for mathematical programs with switching constraints”, Journal of Optimization Theory and Applications, 190, 1-31.
- [9] Mehlitz P. (2020). “Stationarity conditions and constraint qualifications for mathematical programs with switching constraints”, Mathematical Programming, 180(1), 149-186.
- [10] Mokhtavayi H., Heydari A., Kanzi N. (2020). “First-order optimality conditions for Lipschitz optimization problems with vanishing constraints”, Iranian Journal of Science and Technology, Transactions A Science, 44 (6), 1853-1861.
- [11] Shaker A. J., Kanzi N., Farahmand R. S., Reyhani A. P. (2018). “Characterization of properly efficient solutions for convex multi-objective programming with non-differentiable vanishing constraints”, Control and Optimization in Applied Mathematics, 3(2), 49-58.
- [12] Shikhman V. (2021). “Topological approach to mathematical programs with switching constraints”, Set-Valued and Variational Analysis.

#### How to Cite this Article:

Gorgini Shabankareh, F., Kanzi, N., Izadi, J., Fallahi, K., (2022). “Guignard qualifications and stationary conditions for mathematical programming with nonsmooth switching constraints”, Control and Optimization in Applied Mathematics, 6(2): 23-35. doi: 10.30473/coam.2021.60747.1176



#### COPYRIGHTS

© 2021 by the authors. Licensee PNU, Tehran, Iran. This article is an open access article distributed under the terms and conditions of the Creative Commons Attribution 4.0 International (CC BY4.0) (<http://creativecommons.org/licenses/by/4.0>)





Payame Noor University



Control and Optimization in Applied Mathematics (COAM)  
Vol. 6, No. 2, Summer-Autumn 2021 (37-52), ©2016 Payame Noor University, Iran

DOI. [10.30473/coam.2021.60849.1177](https://doi.org/10.30473/coam.2021.60849.1177) (Cited this article) 

## Research Article

# Multi-Label Classification with Meta-Label-Specific Features and Q-Learning

Seyed Hossein Seyed Ebrahimi<sup>1</sup>, Kambiz Majidzadeh<sup>2,\*</sup>, Farhad Soleimanian Gharehchopogh<sup>3</sup>

<sup>1,2,3</sup>Department of IT and Computer Engineering, Urmia Branch, Islamic Azad University, Urmia, Iran.

**Received:** September 15, 2021; **Accepted:** January 01, 2022.

**Abstract.** Classification is a crucial process in data mining, data science, machine learning, and the applications of natural language processing. Classification methods distinguish the correlation between the data and the output classes. In single-label classification (SLC), each input sample is associated with only one class label. In certain real-world applications, data instances may be assigned to more than one class. The type of classification which is required in such applications is known as multi-label classification (MLC). In MLC, each sample of data is associated with a set of labels. Due to the presence of multiple class labels, the SLC learning process is not applicable to MLC tasks. Many solutions to the multi-label classification problem have been proposed, including BR, FS-DR, and LLSF. But, these methods are not as accurate as they could be. In this paper, a new multi-label classification method is proposed based on graph representation. A feature selection technique and the Q-learning method are employed to increase the accuracy of the proposed algorithm. The proposed multi-label classification algorithm is applied to various standard multi-label datasets. The results are compared with state-of-the-art algorithms based on the well-known performance evaluation metrics. Experimental results demonstrated the effectiveness of the proposed model and its superiority over the other methods.

**Keywords.** Machine learning, Classification, Multi-label, Meta-label specific features.

**MSC.** 00A15.

---

\* Corresponding author

[h.seyedebrahimi@iaurmia.ac.ir](mailto:h.seyedebrahimi@iaurmia.ac.ir), [k.majidzadeh@iaurmia.ac.ir](mailto:k.majidzadeh@iaurmia.ac.ir), [bonab.farhad@gmail.com](mailto:bonab.farhad@gmail.com)  
<http://mathco.journals.pnu.ac.ir>

## 1 Introduction

Classification is one of the most important applications of statistical methods in various sciences. One of the main purposes of modeling and classification in statistics is to forecast based on the facts, available features and available information on a particular topic [1, 14, 16]. In statistics, this task is mainly the responsibility of methods such as regression, audit analysis, time series, classification, and tree regression. Classification is one of the most widely used methods in data analysis. The aim of classification methods is to extract the patterns in the data by grouping people and variables [2, 12, 13, 24]. Classification involves a wide variety of methods that are used in many sciences. These methods differ in terms of their purposes, the algorithm they use, and the way they display the results. Classification is the assignment of records or any set of objects to a specific set of categories. It has many applications in various commercial, economic and medical contexts.

Classification is one of the principles of data mining. Classification algorithms, through samples stored in the training dataset, produce general models that can be used to predict class predictions for new samples [10, 20, 22, 36]. Each instance of a training dataset is assigned to a set of attributes. Each attribute specifies a class associated with the instance. There are several classification algorithms based on the number of available classes as well as the number of classes to which each instance can belong.

In multi-label classification, each instance belongs to several classes. This type of classification originated from the field of text classification; simply because each text can belong to several predefined titles at the same time [11, 34, 9, 29]. Multi-label classification has been widely used in real-world applications such as music classification, protein function classification, photo interpretation, video classification, landscape semantic classification, and more. The purpose of multi-label classification is to create a function that maps each multi-label data to a related class set [6, 7, 28, 32, 37]. This division is shown in Figure 1.

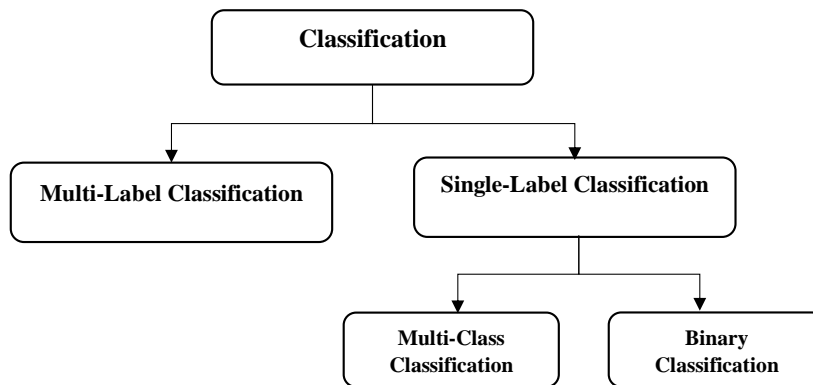


**Figure 1:** Categorization of the classification algorithms.

Due to the importance and widespread use of multi-label classifiers, in what follows, we introduce three important criteria that allow us to classify and compare them.

The first criterion is based on the way the learning algorithm deals with the multi-label dataset. All supervised-based learning methods, which are presented on multi-label data, can be divided into two general categories. The first group consists of *transitional problems*, and the second group involves *adaptation methods*.

A transitional problem is one that maps the problem to single-label learners, and this is why it is named so. But, the second category includes methods that can directly apply multi-label data.

Another important criterion is classification based on the output of multi-label learners. The output of any multi-label learner is either a model that classifies multiple labels or performs the label rating operation. Each test sample can be labeled with relevant and unrelated labels in a multi-label classification model. However, label ratings rank all possible labels for each sample.

In this paper, a novel classification method is presented for multi-label classification problems. In the proposed method, the Q-Learning approach and a feature selection technique are employed. Moreover, in the proposed model, the feature space is encoded as a graph, and the Q-learning is utilized to select the most appropriate feature subset.

The main novelty of this paper is the integration of Q-learning and feature weighting to improve the accuracy of classification. In fact, this research utilizes a Q-learning-based model for final feature selection, what makes it different from previous methods.

The remainder of this paper is organized as follows. Section 2 is devoted to a review of the related works. In Section 3, the details of our proposed method are explained. The performance of the proposed method is evaluated in Section 4. Finally, the achievements of our research are outlined in a brief conclusion.

## 2 Related Works

In this section, we review the research literature of the field of multi-classification.

### 2.1 Transfer Methods

The methods in this category strive to transfer a multi-label dataset into a single-label one. This is done by breaking down the original multi-label dataset into several single-label datasets. Single-label classifiers are then applied to these datasets. Finally, all classifiers are combined to produce a multi-label classifier.

Six methods are suggested in [4] that convert any multi-label dataset into a single-label one. These methods can be described as follows.

- For each instance, select the label with the highest index, among the associated label sets.

- For each sample, select the label with the lowest index among the associated label sets.
- Copy each sample to the number of labels, and assign only one sample label to each copy.
- This is the same as the previous one, except that we assign a weight to each pair (sample, label).
- Randomly select one of the sample labels.
- Delete samples that have more than one label in the collection.

The problem with the aforementioned methods is that they destroy a lot of information involved in the initial multi-label dataset, because the samples lose some of their labels. As a result, the learning algorithm will not use all the information in the initial dataset to generate the model. It is evident that the model created in this case is less efficient than the model created using the entire initial training dataset.

In [19], a novel method called “*K*-way Tree-based eXtreme Multi-Label Classifier (KTXMLC)” is proposed. To maintain the correlations, this method operates on a tree-based classifier utilizing a clustering algorithm.

Moreover, in the multi-label classification problem, a novel method is developed to reweight examples in [38]. In [35], for multi-label classification, dual aggregated network is proposed on pyramidal convolutional features. To learn discriminant multi-scale information of different intended objects within the image data, this approach consists of both classifier-level aggregation and feature. In [33], even at low prior probabilities, a new label dependence criterion demonstrates values from a full range to develop a data-driven label clustering.

The method proposed in [31] describes four commonly used tricks in data analysis. Each of them converts multi-label datasets into a number of single-label ones. These methods include One by One (OBO), One Versus One (OVO), One Versus Rest (OVR), and Label Powerset (LP). Moreover, in [23] an approach based on deep learning is proposed with label-attention and domain-specific pre-training for multi-label legal document classification. In [5], an algorithm of multi-label feature selection is proposed on the basis of many-objective optimization.

In this paper, an enhanced NSGA III algorithm is employed with two archives with the aim of improving the convergence and diversity of NSGA III.

## 2.2 Adaptation Methods

In adaptation methods, the existing algorithms are modified or are combined with other models. Algorithms in the first category produce a special multi-label classifier that considers all instances and all classes of the training dataset at once. But the second category improves an existing single-label classifier method, while multi-label datasets are implicitly or explicitly subdivided into a sequence of subsets. Several efficient and



effective multi-label classification algorithms have been produced and designed by the second method.

Existing adaptation methods are based on the development of dependency rule learners, decision trees, sample-based methods, neural networks, cumulative methods, and SVM classifiers.

In [26], a method called MMAC is presented. This method explores the rules of dependency to create a set of classification rules. Then, it deletes the instances that follow these rules, and repeats the rule search on the remaining data. This continues until all the samples follow at least one rule. The disadvantage of this method is that it is very suitable for training samples, because the flexibility of the method on new data is reduced.

### 3 The Proposed Method

This section presents the details of the proposed  $Q$ -learning multi-label classification algorithm. In the proposed algorithm, the  $Q$ -learning approach is utilized to improve classification accuracy in multi-label data. Moreover, in the proposed method, a new graph-based feature selection method is introduced to reduce the dimension of data.

To describe the data, a large number of attributes are used. A majority of the so-called features may be redundant and irrelevant to the application of the intended data mining. Due to the redundant and unrelated features in the data, the performance of the machine learning algorithm may be negatively affected. Additionally, these features can also increase the complexity of computation, which is why reducing the size of dataset is one of the first steps in data mining and machine learning. The model, which is based on reduced features, has a higher generalizability than the original model. Based on a widely accepted rule, a minimum of  $10 \times n \times C$  educational data is essential in order to classify a problem with dimension  $n$  and  $C$  classes. The reduction in the number of features could lead to a diminish in the amount of required training data, once it is practically impossible to present the required amount of training data. Subsequently, there would be an upsurge in the overall performance of the classification algorithm [17, 8, 18].

In higher dimensions, managing the data is difficult, and the computational and analytical capabilities reduce compared to lower dimensions. Therefore, dimensionality is an essential part of the knowledge discovery process. Multi-dimensional data platforms pose many computational challenges despite the opportunities they create. One of the problems with large datasets is that most of the time, all data features are not important for finding the knowledge that lies in the data. For this reason, in many areas, dimensionality reduction is one of the most significant issues.

The methods of dimensionality reduction are divided into two categories.

- **Feature-based extraction methods:** These methods map a multi-dimensional space into a smaller one. In fact, they form less attributes through the combination of existing attribute values, so that the so-called attributes hold all (or most) of the information included in the original attributes. These methods in turn are

divided into two categories: linear and non-linear methods. Linear methods are simpler and easier to understand and seek to find a sub-public space. The non-linear methods, which are more complex and more difficult to analyze, seek to find a subliminal subspace.

- **Methods based on feature selection:** These methods try to reduce the dimension of the data by selecting a subset of the primary features. Sometimes, data analytic techniques such as classification, work better on the reduced space. One of the main solutions to the problem of reducing the dimension is to use feature selection. During the attribute selection process, a subset of the primary attributes is selected by removing the irrelevant and redundant attributes. The entire search space investigates to find the most appropriate feature subset.

In this paper, the initial dimension of a dataset is reduced using a graph-based feature selection method. Figure 2 shows the general flowchart of the proposed method.

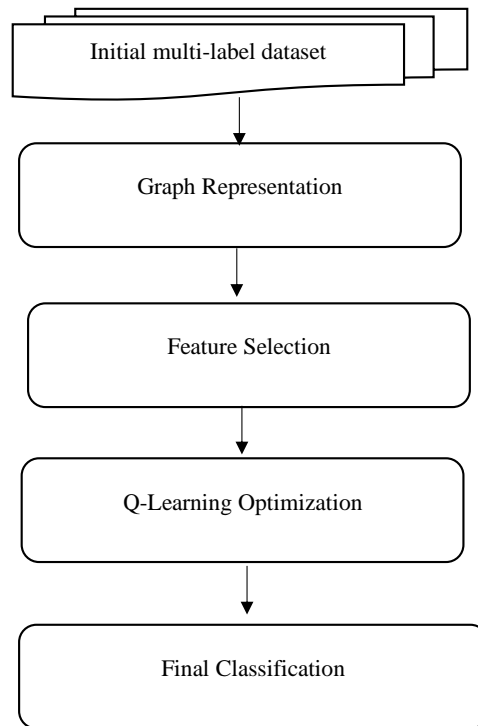


**Figure 2:** The flowchart of the proposed method.

To apply the graph-based method, the solution space of feature selection must be demonstrated by a weighted graph. To this end, in the first step, the initial features are shown with the  $\text{Graph} = \langle G, E, w_{ij} \rangle$ , where  $G = \{G_1, G_2, \dots, G_n\}$  is a set of original features in which each feature shows a node in the graph,  $E = \{(G_i, G_j) : G_i, G_j \in G\}$  denotes the set of edges of the graph, and  $w_{ij}$  indicates the similarity between two features  $G_i$  and  $G_j$  that are linked by the edge  $(G_i, G_j)$ . This study employs the Pearson similarity criteria [15] to compute the similarity value of different features. The Pearson similarity

between two features  $G_i$  and  $G_j$  is shown by

$$W_{ij} = \left| \frac{\sum_p (x_i - \bar{x}_i)(x_j - \bar{x}_j)}{\sqrt{\sum_p (x_i - \bar{x}_i)^2 \sum_p (x_j - \bar{x}_j)^2}} \right|, \quad (1)$$

where  $x_i$  and  $x_j$  signify the feature vectors  $G_i$  and  $G_j$ , respectively. Variables  $\bar{x}_i$  and  $\bar{x}_j$  indicate the averages of vectors  $x_i$  and  $x_j$  over  $p$  samples. Greater similarity between the two features makes the Pearson criterion between the two features closer to 1, and reciprocally, the dissimilarity of the two features makes the Pearson criterion of the two features closer to 0.

Once the Pearson correlation coefficient is calculated, a normalization technique called SoftMax scaling [27] can be utilized to normalize these similarity values into the range from 0 to 1:

$$\widehat{w}_{ij} = \frac{1}{1 + \exp\left(-\frac{w_{ij} - \bar{w}}{\sigma}\right)}. \quad (2)$$

Here,  $w_{ij}$  is the similarity value between features  $G_i$  and  $G_j$ ,  $\bar{w}$  and  $\sigma$  are the average and variance of all of the Pearson correlations, respectively, and  $\widehat{w}_{ij}$  denotes the normalized correlation between features  $G_i$  and  $G_j$ .

In the second stage of the proposed feature selection, the weighted features are grouped in several clusters. The main purpose of feature clustering is to divide the primary features into a number of different clusters based on their similarity. Therefore, the features in each cluster are more similar to each other, and the features in different clusters are less similar to each other. In most feature clustering methods, the number of clusters must be determined before performing the clustering algorithm [21]. In other words, in most of these methods, the parameter  $k$ , which specifies the number of clusters, must be specified by the user. In general, it is difficult to determine the number of clusters for the initial characteristics of the work, and the number of optimal clusters can be determined only by trial and error.

For this reason, in this paper, a community detection algorithm called *Louvain* [3] is used for feature clustering. The present algorithm could detect the available communities existing in the graph through the maximization of a modularity function. This method is uncomplicated, effective, and easy-to-implement; one that could be utilized for the identification of communities in large networks. The complexity of computation for the algorithm is  $O(n \log n)$ , where  $n$  is the number of nodes in the graph. Therefore, it has the potential to be utilized in the detection of communities in extra-large networks in a short computing timespan. To maximize the specific network modularity, in the first step, each of the nodes is allocated to a selected community. In the second step, a new network is being made simply through the merging of previously detected communities. Then, until an imperative enhancement in the network modularity is achieved, the so-called process iterates. The present method has two main advantages. The first advantage is its intuitive and easy-to-implement stages, while the second is that it is exceedingly fast.

In the third stage, the appropriate features of each cluster are selected. The aim of this stage of the proposed method is to search for the optimal feature subset using

the concept of term variance (TV). In other words, in this step, an attempt is made to select each cluster of a number of features that are well able to represent all the features of that cluster. Clustering features and selecting the most effective features from each cluster ensure that the selected features provide a good representation of all the primary features. To select the most important features from each cluster, the TV criterion is utilized. This is a widely used criterion having low computational complexity and high efficiency. The TV criterion indicates the power of the attributes. Therefore, attributes having high scores provide valuable information. The TV criterion is defined by

$$TV(i) = \frac{1}{|G|} \sum_{j=1}^{|G|} \left( Attr(j, i) - \overline{Attr(i)} \right)^2, \quad (3)$$

where  $Attr(j, i)$  indicates attribute  $j$  of sample  $i$  in the dataset, and  $|G|$  denotes the number of all features in the dataset.

After the feature selection step, it is time for the final classification step. At this stage, the learning algorithm is used to deal with the problem of multi-label classification. The Q-learning algorithm is an extended version of the iterative value algorithm that is also used for uncertain problems. The Q-learning is a type of non-model reinforcement learning techniques that is based on dynamic random planning. In Q-learning, instead of defining a mapping from states to their values, a mapping is defined from the state/action pair to values called Q-values. Moreover, instead of defining a mapping from states to their values, a mapping is defined from the state/operation pair to the Q-values.

In this paper, we use Q-learning in multi-label classification problems by making changes to the algorithm structure. In the proposed algorithm, the search space is divided into several parts. Additionally, three new features are defined in the proposed algorithm.

In this paper, for the first time, using a combination of the TV feature selection algorithm and Q-learning, as a novel method, is proposed for feature selection. In the proposed method, unlike the existing methods, the final features in the problem of multi-label classification are optimally selected. The next steps will be decided by the agent, following  $\Delta t$  steps into the future. The weight for this step is calculated as  $\gamma^{\Delta t}$ , where  $\gamma$  is the discount factor whose value lies between 0 and 1 ( $0 \leq \gamma \leq 1$ ), and demonstrates the valuing reward impacts which are received earlier and are more than the ones received later (reflecting a “good start” value). Additionally,  $\gamma$  might also be construed as the success (or survive) probability at each step  $\Delta t$ .

After selecting an appropriate subset of features, these features are used as the inputs of the classification model. It is worth mentioning that accurate feature selection and the use of an efficient prediction model to analyze the data lead to a better classification. A variety of machine learning algorithms, discussed in the previous section, have been proposed for classification. Machine learning classification algorithms such as support vector machine, artificial neural networks, deep learning, fuzzy systems, and ensemble learning models are used for multi-label classification.

The appropriate choice of a classifier is a vital step in classification. In the proposed method, a hybrid prediction model combining six different classifiers is used to take

advantage of all these classifiers. The hybrid model is an efficient prediction model that improves the total classification accuracy. In other words, the main idea of this paper is to use multiple classifiers in data classification. Consequently, the proposed hybrid model is very reliable when working with multi-label datasets.

In the proposed method, a combination of Q-learning, Support Vector Machine (SVM), Naïve Bayes (NB), Random Forest (RF), Decision Tree (DT) and K-Nearest Neighbors (KNN) classifiers is used in the classification process. Each of the classifiers makes its own prediction independently, and finally, based on the majority prediction, the final prediction is made. Given that each of the classifiers contributes to the final prediction, and according to the predicted emotional state by the majority, the final human state is recognized. This method is called Majority-Voting Classification (MVC). The pseudo-code of the proposed method is as follows.

---

**Algorithm 1**

---

**Input**     $D_T$ : Dataset  
               $\theta$ : Threshold for similarity

**Output**    Predicted labels

1:    **Begin algorithm**

2:    **Graph** = Create a graph using Pearson similarity

3:    **Graph** = Apply the threshold value  $\theta$  to a primary graph

4:     $G'$  = An empty set

5:    **Do**

6:        **Calculate Feature Relevance**

7:        Sort features

8:        **Select the Best Feature  $G'$**

13        Remove  $G'$  from the **Original Features**

14:    **While** (at least one feature has been found)

15:        Report  $G'$  as a final feature set

16:        Send the selected features to the Multi-Voting Classification

17:        Specify the final classification using the Multi-Voting Classification

16:    **End algorithm**

---

**Figure 3:** Pseudo-code of the proposed classification model

## 4 Experimental Results

To evaluate the performance of the proposed classification model on the multi-label classification problem, the proposed method was applied to various multi-label datasets. Furthermore, the obtained results were compared with those of the state-of-the-art works based on different metrics. The experiments were conducted in two parts.

MATLAB programming language was used to implement the feature selection method and other methods, and the results were derived based on these implementations. Also, all the tests were performed on a system with a 2.3 GHz Corei3 processor and 2 GB of internal memory (RAM).

In experiments on the proposed method, the dataset was randomly divided into training data and test data. For this purpose, 70% of the dataset was considered as the training data, and the remaining 30% as the test data. Also, in all the experiments, after identifying the train and test sets, each classification method was performed ten

times, and an average of the ten different executions was used to compare different methods.

#### 4.1 The First Part of Experiments

In the first part, the algorithms were evaluated on the Emotions, Scene, Yeast and Genbase datasets according to the Sensitivity (%), Specificity (%), and Classification (%) metrics [32].

Another criterion used in this set of experiments was *average execution time*. In fact, we used this criterion to examine the complexity of the proposed method and the competitor methods. It is clear that less execution time indicates lower complexity and higher efficiency.

In Tables 1-4, the proposed method, which uses the graph-based feature selection method and Q-Learning, is compared with Multi-Label Classification with weighted classifier [30]. In these tables, Sensitivity, Specificity, and Classification rates are used to investigate the performance of the proposed method and the base methods existing in the literature.

**Table 1:** Comparison of the proposed method with multi-label classification with weighted classifier on the Emotions dataset

	Multi-label classification with weighted classifier			The proposed method		
	Best	Worst	Average	Best	Worst	Average
Sensitivity (%)	84.71	81.48	83.721	86.08	81.92	85.19
Specificity (%)	86.79	83.92	85.99	87.12	83.38	86.73
Classification (%)	85.51	81.31	84.42	86.39	82.54	85.62

**Table 2:** Comparison of the proposed method with multi-label classification with weighted classifier on the Scene dataset

	Multi-label classification with weighted classifier			The proposed method		
	Best	Worst	Average	Best	Worst	Average
Sensitivity (%)	82.62	81.54	83.71	86.89	80.38	85.54
Specificity (%)	87.78	83.29	84.28	87.99	85.82	84.71
Classification (%)	86.12	82.31	84.09	87.08	83.64	84.52

According to the results of Tables 1-4, the proposed method outperformed competitor algorithms and obtained better results.

Moreover, Figure 4 shows the average accuracy of the proposed method on different datasets. As shown in the figure, the proposed method has a higher average accuracy compared to the base methods existing in the literature.

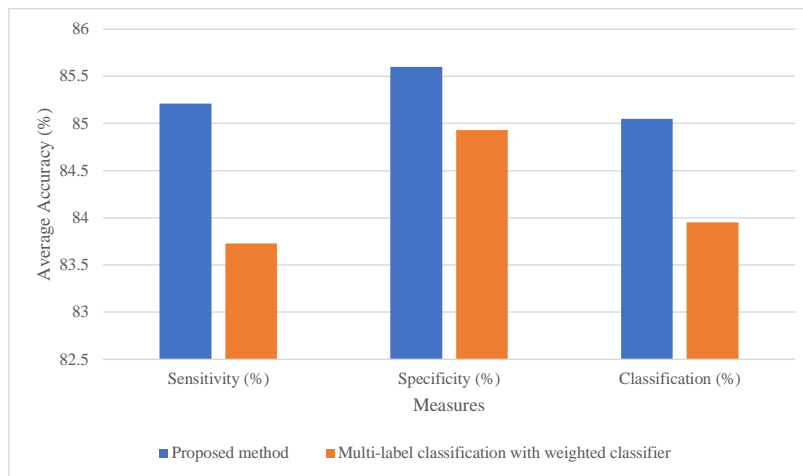
Also, Table 5 allows us to compare the average execution time of the proposed method with that of multi-label classification with weighted classifier.

**Table 3:** Comparison of the proposed method with multi-label classification with weighted classifier on the Yeast dataset

	Multi-label classification with weighted classifier			The proposed method		
	Best	Worst	Average	Best	Worst	Average
Sensitivity (%)	84.61	81.41	83.22	86.28	82.91	84.12
Specificity (%)	86.89	82.04	84.21	87.46	83.87	84.23
Classification (%)	85.09	80.28	83.08	86.39	84.48	85.62

**Table 4:** Comparison of the proposed method with multi-label classification with weighted classifier on the Genbase dataset

	Multi-label classification with weighted classifier			The proposed method		
	Best	Worst	Average	Best	Worst	Average
Sensitivity (%)	84.72	80.42	83.71	86.87	81.91	85.98
Specificity (%)	85.38	82.35	84.72	88.59	84.87	86.71
Classification (%)	84.51	80.87	82.32	86.02	82.43	84.43

**Figure 4:** Comparison of the algorithms according to the average accuracy

The results of this experiment show that the proposed method has less execution time.

#### 4.2 The Second Part of Experiments

In this subsection, the proposed multi-label classification is compared with the BR, MDDM, LIFT, LLSF, and MLSF methods in terms of Exact-Match, Hamming-Score, Macro-F1, and Micro-F1 metrics. The results of the competitor algorithms are adopted from the original paper which is reported by the authors, namely, [25]. It is worth

**Table 5:** Comparison of the expectation time for the proposed method and multi-label classification with weighted classifier

<b>Execution Time</b>	<b>Multi-label classification with weighted classifier</b>	<b>The proposed method</b>
<b>1</b>	119	89
<b>2</b>	118	82
<b>3</b>	112	80
<b>4</b>	115	85
<b>5</b>	118	91
<b>6</b>	125	79
<b>7</b>	113	83
<b>8</b>	108	84
<b>9</b>	118	92
<b>10</b>	121	81
Average	114.7	84.6

mentioning that all the details of the methods and datasets can be found in [25]. Tables 6-9 present the comparison results.

**Table 6:** Results obtained by the algorithms regarding the Exact-Math metric

Dataset	Methods					
	BR	MDDM	LIFT	LLSF	MLSF	Proposed
Emotions	0.285	0.263	0.184	0.285	0.315	<b>0.3305</b>
Scene	0.533	0.529	0.637	0.531	0.637	<b>0.7006</b>
Yeast	0.148	0.137	0.154	0.148	0.212	<b>0.2187</b>
Genbase	<b>0.982</b>	0.980	0.953	<b>0.982</b>	<b>0.982</b>	0.9474
Medical	0.665	0.609	0.574	0.662	0.689	<b>0.7013</b>
Enron	0.111	0.121	0.116	0.111	0.122	<b>0.1301</b>
Mediamill	0.066	0.068	0.069	0.066	0.070	<b>0.0715</b>
Bibtex	0.143	0.143	0.139	0.144	0.143	<b>0.1474</b>
Corel16k1	0.006	0.000	0.000	0.006	0.008	<b>0.0104</b>
Corel16k2	0.004	0.001	0.000	0.004	0.007	<b>0.0091</b>

According to Tables 6-9, the proposed multi-label classification model obtained better results compared to the competitor algorithms regarding the Exact-Match, Hamming-Score, Macro-F1, and Micro-F1 metrics.

A more detailed examination of the tables demonstrates that in the Genbase dataset, some competitor algorithms obtained better results compared to the proposed algorithm. Additionally, in the Enron and Mediamill datasets, the LIFT and MDDM methods obtained better values for the Hamming-Score and Micro-F1 metrics, respectively.



**Table 7:** Results obtained by the algorithms regarding the Hamming-Score metric

Dataset	Methods					
	BR	MDDM	LIFT	LLSF	MLSF	Proposed
Emotions	0.805	0.788	0.755	0.805	0.793	<b>0.8136</b>
Scene	0.895	0.899	0.919	0.895	0.891	<b>0.9356</b>
Yeast	0.801	0.798	0.804	0.801	0.789	<b>0.8195</b>
Genbase	<b>0.999</b>	<b>0.999</b>	0.998	<b>0.999</b>	<b>0.999</b>	0.9964
Medical	0.990	0.988	0.987	0.990	0.990	<b>0.9931</b>
Enron	0.940	0.953	<b>0.955</b>	0.940	0.940	0.9504
Mediamill	0.968	0.969	0.969	0.968	0.968	<b>0.9706</b>
Bibtex	0.984	0.988	0.988	0.984	0.984	<b>0.9901</b>
Corel16k1	0.980	0.981	0.981	0.980	0.980	<b>0.9901</b>
Corel16k2	0.981	0.983	0.983	0.981	0.981	<b>0.9900</b>

**Table 8:** Results obtained by the algorithms regarding the Hamming-Score metric

Dataset	Methods					
	BR	MDDM	LIFT	LLSF	MLSF	Proposed
Emotions	0.633	0.583	0.496	0.633	<b>0.657</b>	0.6438
Scene	0.694	0.684	0.759	0.693	0.699	<b>0.8080</b>
Yeast	0.322	0.318	0.319	0.322	0.346	<b>0.3869</b>
Genbase	0.761	0.754	0.704	<b>0.769</b>	<b>0.769</b>	0.6080
Medical	0.366	0.323	0.240	0.370	0.387	<b>0.4094</b>
Enron	0.222	0.201	0.136	0.222	0.221	<b>0.2455</b>
Mediamill	0.028	0.035	0.035	0.028	0.029	<b>0.0364</b>
Bibtex	0.328	0.159	0.145	0.329	0.328	<b>0.3331</b>
Corel16k1	0.047	0.008	0.003	0.045	0.047	<b>0.0548</b>
Corel16k2	0.051	0.012	0.004	0.049	0.051	<b>0.0534</b>

**Table 9:** Results obtained by the algorithms regarding the Hamming-Score metric

Dataset	Methods					
	BR	MDDM	LIFT	LLSF	MLSF	Proposed
Emotions	0.661	0.627	0.557	0.661	0.665	<b>0.6749</b>
Scene	0.688	0.682	0.755	0.686	0.692	<b>0.8009</b>
Yeast	0.631	0.627	0.632	0.631	0.639	<b>0.6726</b>
Genbase	<b>0.993</b>	0.992	0.980	<b>0.993</b>	<b>0.993</b>	0.9664
Medical	0.810	0.780	0.679	0.804	0.815	<b>0.8331</b>
Enron	0.515	0.579	0.570	0.515	0.515	<b>0.5987</b>
Mediamill	0.510	<b>0.528</b>	0.519	0.510	0.491	0.5179
Bibtex	0.422	0.364	0.338	0.423	0.423	<b>0.4481</b>
Corel16k1	0.072	0.007	0.005	0.069	0.070	<b>0.0759</b>
Corel16k2	0.079	0.016	0.012	0.079	0.076	<b>0.0840</b>

## 5 Conclusion

Data mining refers to the study and analysis of large amounts of data in order to discover hidden and meaningful patterns and rules within them. Any dataset can be thought of as a valuable source of information, and the important point here is that the valuable information is hidden among a large amount of data, and we need to analyze the data to access that information. Classification is a form of data analysis that can be used to create a model to describe the data or to conceive directional mirror data. In multi-label classification, each data is associated with a subset of labels. This is called a set of related labels for that data. The aim of a multi-label learner is to create a function that maps each multi-label data to a set of related labels. Today, multi-label classifiers provide an important learning pattern among data mining learning algorithms. In this paper, a combination of graph-based feature selection and Q-learning, a new method was proposed to improve classification accuracy. The proposed algorithm was applied to ten well-known datasets, and the results were compared with those of the widely-used, state-of-the-art methods. The obtained results demonstrated that the proposed method had higher accuracy compared to the previous methods, and also had less computational complexity.

## References

- [1] Alizadeh J., Khaloozadeh H. (2019). "Enlarging the region of attraction for nonlinear systems through the sum-of-squares programming", *Control and Optimization in Applied Mathematics*, 4(2), 19-37.
- [2] Al-Makhadmeh Z., Tolba A. (2019). "Utilizing IoT wearable medical device for heart disease prediction using higher order Boltzmann model: A classification approach", *Measurement*, 147, 106815.
- [3] Blondel V., et al. (2008). "Fast unfolding of communities in large networks", *Journal of Statistical Mechanics: Theory and Experiment*, 10008, 1-12.
- [4] Boutell M.R., Luo J., Shen X., Brown C.M. (2004). "Learning multi-label scene classification", *Pattern Recognition*, 1757-1771.
- [5] Dong H., et al. (2020). "A many-objective feature selection for multi-label classification", *Knowledge-Based Systems*, 208, 106456.
- [6] Hashemi A., Dowlatshahi M.B., Nezamabadi-pour H. (2020). "MGFS: A multi-label graph-based feature selection algorithm via PageRank centrality", *Expert Systems with Applications*, 142, 113024.
- [7] Hu J., et al. (2020). "Robust multi-label feature selection with dual-graph regularization", *Knowledge-Based Systems*, 203, 106126.
- [8] Jayaraman V., Sultana H.P. (2019). "Artificial gravitational cuckoo search algorithm along with particle bee optimized associative memory neural network for feature selection in heart disease classification", *Journal of Ambient Intelligence and Humanized Computing*.
- [9] Ji Z., et al. (2020). "Deep ranking for image zero-shot multi-label classification", *IEEE Transactions on Image Processing*, 29, 6549-6560.

- [10] Khammassi C., Krichen S. (2017). "A GA-LR wrapper approach for feature selection in network intrusion detection", *Computers & Security*, 70, 255-277.
- [11] Khandagale S., Xiao H., Babbar R. (2020). "Bonsai: diverse and shallow trees for extreme multi-label classification", *Machine Learning*, 109(11), 2099-2119.
- [12] Mafarja M., Mirjalili S. (2018). "Whale optimization approaches for wrapper feature selection", *Applied Soft Computing*, 62, 441-453.
- [13] Makki I., Alhalabi W., Adham R.S. (2019). "Using emotion analysis to define human factors of virtual reality wearables", *Procedia Computer Science*, 163, 154-164.
- [14] Mansourinasab S., Sojoodi M., Moghadasi S.R. (2019). "Model predictive control for a 3D pendulum on SO (3) manifold using convex optimization", *Control and Optimization in Applied Mathematics*, 4(2), 69-80.
- [15] MonirulKabir Md., Shahjahan Md., Murase K. (2011). "A new local search based hybrid genetic algorithm for feature selection", *Neurocomputing*, 74(17), 2914-2928.
- [16] Morais-Rodrigues F., et al. (2020). "Analysis of the microarray gene expression for breast cancer progression after the application modified logistic regression", *Gene*, 726, 144168.
- [17] Naem A.A., Ghali N.I., Saleh A.A. (2018). "Antlion optimization and boosting classifier for spam email detection", *Future Computing and Informatics Journal*, 3(2), 436-442.
- [18] Nasarian E., et al. (2020). "Association between work-related features and coronary artery disease: A heterogeneous hybrid feature selection integrated with balancing approach", *Pattern Recognition Letters*, 133, 33-40.
- [19] Prajapati P., Thakkar A. (2021). "Performance improvement of extreme multi-label classification using K-way tree construction with parallel clustering algorithm", *Journal of King Saud University - Computer and Information Sciences*.
- [20] Rejer I., Twardochleb M. (2018). "Gamers' involvement detection from EEG data with cGAAM – A method for feature selection for clustering", *Expert Systems with Applications*, 101, 196-204.
- [21] Rostami M., Berahmand K., Forouzandeh S. (2020). "A novel method of constrained feature selection by the measurement of pairwise constraints uncertainty", *Journal of Big Data*, 7(1), 83.
- [22] Salman M.S., et al. (2019). "Group ICA for identifying biomarkers in schizophrenia: 'Adaptive' networks via spatially constrained ICA show more sensitivity to group differences than spatio-temporal regression", *NeuroImage: Clinical*, 22, 101747.
- [23] Song D., et al. (2021). "Multi-label legal document classification: A deep learning-based approach with label-attention and domain-specific pre-training", *Information Systems*, 101718.
- [24] Song Q., et al. (2017). "Using deep learning for classification of lung nodules on computed tomography images", *Journal of healthcare engineering*, 2017.
- [25] Sun L., Kudo M., Kimura, K. (2016, December). "Multi-label classification with meta-label-specific features", In 2016 23rd International Conference on Pattern Recognition (ICPR) (1612-1617). IEEE.
- [26] Thabtah F.A., Cowling P., Peng Y., Rastogi R., Morik K., Bramer M., Wu X. (2004). "MMAC: A new multi-class, multi-label associative classification approach", *Proc. Proceedings of Fourth IEEE International Conference on Data Mining, ICDM 2004*, 217-224.

- [27] Theodoridis S., Koutroumbas K. (2008). "Pattern recognition", Academic Press, Oxford.
- [28] Wang W., et al. (2020). "MLCForest: Multi-label classification with deep forest in disease prediction for long non-coding RNAs", Briefings in Bioinformatics.
- [29] Wu T., et al. (2020). "Distribution-balanced loss for multi-label classification in long-tailed datasets", in European Conference on Computer Vision, Springer.
- [30] Xia Y., Chen K., Yang Y. (2021). "Multi-label classification with weighted classifier selection and stacked ensemble", Information Sciences, 557, 421-442.
- [31] Xu J. (2011). "An extended one-versus-rest support vector machine for multi-label classification", Neurocomputing, 3114-3124.
- [32] Yang M., et al. (2019). "Investigating the transferring capability of capsule networks for text classification", Neural Networks, 118, 247-261.
- [33] Yap X.H., Raymer M. (2021). "Multi-label classification and label dependence in in silico toxicity prediction", Toxicology in Vitro, 105157.
- [34] You R., et al. (2020). "Cross-modality attention with semantic graph embedding for multi-label classification", in Proceedings of the AAAI Conference on Artificial Intelligence.
- [35] Yun D., Ryu J., Lim J. (2021). "Dual aggregated feature pyramid network for multi label classification", Pattern Recognition Letters, 144, 75-81.
- [36] Zheng X., et al. (2019). "Gene selection for microarray data classification via adaptive hypergraph embedded dictionary learning", Gene, 706, 188-200.
- [37] Zhang Y., et al. (2020). "Large-scale multi-label classification using unknown streaming images", Pattern Recognition, 99, 107100.
- [38] Zhong Y., Du B., Xu C. (2021). "Learning to reweight examples in multi-label classification", Neural Networks.

#### How to Cite this Article:

Seyed Ebrahimi, S.H., Majidzadeh, K., Soleimanian Gharehchopogh, F. (2022). "Multi-label classification with meta-label-specific features and Q-learning", Control and Optimization in Applied Mathematics, 6(2): 37-52. doi: 10.30473/coam.2021.60849.1177



#### COPYRIGHTS

© 2021 by the authors. Licensee PNU, Tehran, Iran. This article is an open access article distributed under the terms and conditions of the Creative Commons Attribution 4.0 International (CC BY4.0) (<http://creativecommons.org/licenses/by/4.0>)



Payame Noor University



Control and Optimization in Applied Mathematics (COAM)  
Vol. 6, No. 2, Summer-Autumn 2021 (53-77), ©2016 Payame Noor University, Iran

DOI. [10.30473/coam.2022.59267.1164](https://doi.org/10.30473/coam.2022.59267.1164) (Cited this article) 

## Research Article

# Optimal Control Problems: Convergence and Error Analysis in Reproducing Kernel Hilbert Spaces

Ebrahim Amini\*

Department of Mathematics, Payame Noor University (PNU),  
P.O. Box. 19395-3697, Tehran, Iran.

**Received:** June 01, 2021; **Accepted:** January 30, 2022.

**Abstract.** In this article, we offer an efficient method to find an approximate solution for quadratic optimal control problems. The approximate solution is offered in a finite series form in reproducing kernel space. The convergence of proposed method is analyzed under some hypotheses which provide the theoretical basis of the proposed method for solving quadratic optimal control problems. Furthermore, in this study, we investigate the application of the proposed method to obtain the solution of equations that have formally been solved using Pontryagin's maximum principle. Moreover, many different types of quadratic optimal control problems are considered prototype examples. The obtained results demonstrate that the proposed method is truly effective and convenient to obtain the analytic and approximate solutions of quadratic optimal control problems.

**Keywords.** Optimal control problem, Pontryagin's maximum principle, Convergence, Reproducing kernel Hilbert space.

**MSC.** 90C34; 90C40.

---

\* Corresponding author  
eb.amini.s@pnu.ac.ir  
<http://mathco.journals.pnu.ac.ir>

## 1 Introduction

Optimal control is a particular branch of modern control theory which has been broadly applied in various fields including aviation systems [12], robotic [40], biomedicine [21], etc. Recently, different types of computational techniques have been expounded for solving optimal control problems (OCPs). For instance, we can mention the following papers. Salim [35] presented a method based on the parameterization of both state and control variables, the authors of [5] applied the relaxed descent method to approximate solutions for OCPs, Nemati et al. [29] applied the Bernstein polynomials with the fractional operational matrix to obtain the solution of a class of fractional (OCPs), Ghomami Baladezaei [20] applied a  $1/G'$ -expansion technique for solving nonlinear (OCPs), Nezhadhossein [30] used the Haar matrix equations to obtain the solution of continuous time-variant linear-quadratic OCPs, Chrysosoverghi et al. [6] applied discretization methods to solve the OCPs with some state constraints, in [22] the authors applied the modal series method to study infinite horizon nonlinear control problems, EL-Gindy et al. [10] presented an alternative technique for solving controlled Duffing oscillator problems, the authors of [34] applied the differential transform method to approximate solutions for the linear OCPs. In [24], Kafash et al. applied Chebyshev polynomials to obtain some suitable algorithms for solving the OCPs, authors of [38] applied a Chebyshev technique for solving nonlinear OCPs, Betts et al. [2] used techniques to show that a nonconvergent Runge–Kutta method converges for OCPs, the authors of [25] applied the pseudospectral method to analyze the solution of OCPs, Canuto et al. [4] applied a pseudospectral method for solving infinitely smooth and well-behaved problems, the examples of Radau pseudospectral method to numerically solve OCPs are given in [11]. Also, the authors of [41] used the basic variational iteration method to obtain approximate solution of linear quadratic OCPs.

The concept of reproducing kernel was first applied by Zaremba [42] to obtain the approximate solution of boundary value problems for harmonic functions (see [1] for more details). Researchers have been investigating this theory for constructing approximate solutions to fractal interpolation [39, 3], second-order three-point boundary value problems with the property of singularity [13], singularly perturbed boundary value problems [14], nonlocal fractional boundary value problems [17], Riccati differential equations [18], nonlinear delay differential equations of fractional order [19], Black-Scholes equation [37], and nonlinear differential-difference equations. The authors of [8, 27, 7] examined the reproducing kernel to derive solution of some partial differential equations. The book [9] provides a wide range of reproducing kernel methods which have been used to solve various model problems.

The main idea of this study is to find an approximate solution of a quadratic OCPs in reproducing kernel spaces. Some ordinary capabilities of the method lie in the following formations. The current method is mesh-free, easily executed and useful for various boundary conditions and the obtained approximate solution converges uniformly to the exact solution.

This paper is organized as follows. The statement of quadratic OCPs is described in Section 2. In Section 3, we express some nearly new definitions used in this paper. In Section 4, we investigate and analyze the derived results to the proposed method.

In Section 5, four numerical examples are presented to illustrate the accuracy and efficiency of our method. Eventually, we provide some concluding remarks in Section 6.

## 2 Statement of the Problem

Consider the following single-input  $n$ -state dynamic system

$$\begin{cases} \dot{x}(t) = f(t, x(t)) + Bv(t), & 0 \leq t \leq T, \\ x(0) = x_0, \end{cases} \quad (1)$$

where  $x(t) = (x_1(t), \dots, x_n(t))^T \in \mathcal{R}^n$  is the state vector,  $v(t) \in \mathcal{R}$  is the control function and  $x_0 \in \mathcal{R}^n$  is the initial state vector at  $t = 0$ . Moreover,  $f(t, x(t)) \in \mathcal{R}^n$  is a continuously differentiable function in all arguments and  $B \in \mathcal{R}^{n \times 1}$  is a real constant vector.

Now the unconstrained OCP can be stated as finding the optimal control law  $v(t)$ , minimizing the quadratic objective functional

$$U[x(t), v(t)] = \frac{1}{2}x^T(t)Kx(t) + \frac{1}{2} \int_0^t (x^T(s)Sx(s) + v^T(s)Rv(s))ds. \quad (2)$$

Now the unconstrained optimal control problem can be stated as finding the optimal control law  $v(\cdot)$  that minimizes the quadratic objective functional (2) subject to the control system (1), where  $K$  and  $S$  are symmetric positive semi-definite  $n \times n$  matrices and  $R$  is a positive constant.

Consider Hamiltonian control system (1) as

$$H[t, x(t), v(t), p(t)] = \frac{1}{2}[x^T(t)Sx(t) + v^T(t)Rv(t)] + p^T(t)[f(t, x(t)) + Bv(t)],$$

where  $p(t) \in \mathcal{R}^n$  is the co-state vector with the  $i$ -th component  $p_i(t)$ ,  $i = 1, 2, \dots, n$ .

Using Pontryagin's maximum principle [31], the optimality condition for system (1) can be described by the subsequent equations

$$\begin{cases} \dot{x}(t) = f(t, x(t)) - (BR^{-1}B^T)p(t), \\ \dot{p}(t) = -Sx(t) - g(t, x(t), p(t)), \quad g(t, x(t), p(t)) = \left[ \frac{\partial f(t, x(t))}{\partial x} \right]^T p(t), \\ x(0) = x_0, \quad 0 \leq t \leq T, \end{cases} \quad (3)$$

with the terminal condition  $p(T) = Kx(T)$ . From this the optimal control law is determined by  $v(t) = -R^{-1}B^T p(t)$ .

Using change of variables  $y(t) = x(t) - x_0$  and  $z(t) = p(t) - p(T)$ , the aforementioned system can further be converted into the following form

$$\begin{cases} \dot{y}(t) + (BR^{-1}B^T)z(t) = F(t, y(t)) - (BR^{-1}B^T)p(T), \\ \dot{z}(t) + Sy(t) = -Sx_0 - G(t, y(t), z(t)), \\ y(0) = 0, \quad z(T) = 0, \quad 0 \leq t \leq T, \end{cases} \quad (4)$$

where

$$\begin{cases} y(t) = (y_1(t), \dots, y_n(t))^T, \\ z(t) = (z_1(t), \dots, z_n(t))^T, \\ F(t, y(t)) = (F_1(t, y(t)), \dots, F_n(t, y(t)))^T = f(t, y(t) + x_0), \\ G(t, y(t), z(t)) = (G_1(t, y(t), z(t)), \dots, G_n(t, y(t), z(t)))^T \\ \quad = g(t, y(t) + x_0, z(t) + p(T)). \end{cases} \quad (5)$$

The functions  $F(t, y(t))$  and  $G(t, y(t), z(t))$  can be divided into two parts, a linear part and a nonlinear part and therefore (4) can be rewritten in the following form

$$\begin{cases} \dot{y}(t) + (BR^{-1}B^T)z(t) = F_0(t) + F_L(t, y(t)) + F_N(t, y(t)), \\ \dot{z}(t) + Sy(t) = G_0(t) + G_L(t, y(t), z(t)) + G_N(t, y(t), z(t)), \\ y(0) = 0, z(T) = 0, \quad 0 \leq t \leq T, \end{cases} \quad (6)$$

where  $F_N$  and  $G_N$  are two nonlinear functions and  $F_L$  and  $G_L$  are two linear functions and

$$\begin{cases} F(t, y(t)) - (BR^{-1}B^T)p(T) = F_0(t) + F_L(t, y(t)) + F_N(t, y(t)), \\ -Sx_0 - G(t, y(t), z(t)) = G_0(t) + G_L(t, y(t), z(t)) + G_N(t, y(t), z(t)). \end{cases} \quad (7)$$

### 3 Hilbert Function Spaces

We give some basic definitions and properties of Hilbert function spaces, and then we construct some Hilbert function spaces which are used in the proceeding sections.

**Definition 1.** (see [15]). A Hilbert space  $H$  of functions  $y : E \rightarrow \mathfrak{R}$  is called a Hilbert function space if for each  $t \in E$ , there exists a positive constant  $c_t$  such that  $|y(t)| \leq c_t \|y\|_H$  for all  $y$  in  $H$ .

**Definition 2.** (see [15]). The inner product spaces  $W_2^{2,i}[0, T], i = 0, 1$ , of real-valued functions are defined as

$$W_2^{2,1}[0, T] = \{y(t) \mid \text{where } y \text{ and } \dot{y} \text{ are absolutely continuous functions, } \dot{y} \in L^2[0, T], y(0) = 0, t \in [0, T]\}, \quad (8)$$

and

$$W_2^{2,2}[0, T] = \{y(t) \mid \text{where } y \text{ and } \dot{y} \text{ are absolutely continuous functions, } \dot{y} \in L^2[0, T], y(T) = 0, t \in [0, T]\}. \quad (9)$$

Also, the specific inner product in  $W_2^{2,i}[0, T], i = 0, 1$  is of the subsequent form

$$\langle y(t), \tilde{y}(t) \rangle = y(0)\tilde{y}(0) + \int_0^t \dot{y}(s)\tilde{\dot{y}}(s)ds, \quad (10)$$

and the norm in the inner product space  $\|y(t)\|_{W_2^{2,i}}$  is given by

$$\|y(t)\|_{W_2^{2,i}} = \sqrt{\langle y(t), y(t) \rangle_{W_2^{2,i}}}, \quad (11)$$

where  $y, \tilde{y} \in W_2^{2,i}[0, T]$ .



It is clear that  $W_2^{2,i}[0, T]$  is a Hilbert space.

**Definition 3.** (see [15]). The inner product space  $W_2^1[0, T]$  is defined as

$$W_2^1[0, T] = \{y(t) \mid y \text{ is an absolutely continuous real-valued function, } y, \dot{y} \in L^2[0, T], t \in [0, T]\}. \quad (12)$$

The inner product in  $W_2^1[0, T]$  is of the form

$$\langle y(t), \tilde{y}(t) \rangle = \int_0^t (y(s)\tilde{y}(s) + \dot{y}(s)\tilde{\dot{y}}(s))ds, \quad (13)$$

and the norm  $\|y(t)\|_{W_2^1}$  is defined by

$$\|y(t)\|_{W_2^1} = \sqrt{\langle y(t), y(t) \rangle_{W_2^1}}, \quad (14)$$

where  $y(t), \tilde{y}(t) \in W_2^1[0, T]$ .

**Definition 4.** (see [9]). Let  $H$  be a real Hilbert space of functions defined on a set  $E$ . The specific product is denoted by  $\langle x, x \rangle_H$ . Let  $\|x\| = \sqrt{\langle x, x \rangle_H}$  be the norm in the Hilbert space  $H$ , for  $x, y \in H$ . The function  $R: E \times E \rightarrow \mathcal{R}$  is called a reproducing kernel of  $H$  if the following conditions are satisfied:

- (i)  $t, R_t(s) = R(t, s)$  as a real-valued function of  $s$  belongs to  $H$ .
- (ii) For every  $x \in H$  and  $t \in E$ , we have  $\langle x(\cdot), R_t(\cdot) \rangle_H$ . This is called a reproducing property.

**Theorem 1.** (see [15]). The space  $W_2^{2,0}[0, T]$  consisting of real-valued functions is a Hilbert function space and the reproducing kernel for this space can be explained as follows

$$R_s^0(t) = \begin{cases} C_s^0(t) = \sum_{i=1}^4 c_i(s)t^{i-1}, & t \leq s, \\ D_s^0(t) = \sum_{i=1}^4 d_i(s)t^{i-1}, & t > s, \end{cases} \quad (15)$$

where, the coefficients  $c_i(s), d_i(s), i = 1, \dots, 4$ , are characterized as follows

- $R_s^0(0) = 0, \frac{\partial R_s^0(0)}{\partial t} - \frac{\partial^2 R_s^0(0)}{\partial t^2} = 0, (\frac{\partial^3 C_s^0(t)}{\partial t^3}|_{t=s} - \frac{\partial^3 D_s^0(t)}{\partial t^3}|_{t=s}) = 1,$
- $\frac{\partial^{3-i} R_s^0(T)}{\partial t^{3-i}} = 0, i = 0, 1,$
- $\frac{\partial^i C_s^0(t)}{\partial t^i}|_{t=s} = \frac{\partial^i D_s^0(t)}{\partial t^i}|_{t=s}, i = 0, 1, 2.$

Then, by using the features of the reproducing kernel  $R_i^0(s)$ , the solution of above derivative equations is computed.

**Theorem 2.** (see [39]). The space  $W_2^{2,1}[0, T]$  consisting of real-valued functions is a Hilbert function space and the corresponding kernel for this space can be explained as follows

$$R_s^1(t) = \begin{cases} \tilde{C}_s^1(t) = \sum_{i=1}^4 \tilde{c}_i(s)t^{i-1}, & t \leq s, \\ \tilde{D}_s^1(t) = \sum_{i=1}^4 \tilde{d}_i(s)t^{i-1}, & t > s, \end{cases} \quad (16)$$

where, the coefficients  $\tilde{c}_i(s), \tilde{d}_i(s), i = 1, \dots, 4$ , are characterized as follows

- $R_s^1(T) = 0, \frac{\partial^3 R_s^1(T)}{\partial t^3} = 0, (\frac{\partial^3 \widetilde{C}_s^1(t)}{\partial t^3}|_{t=s} - \frac{\partial^3 \widetilde{D}_s^1(t)}{\partial t^3}|_{t=s}) = 1,$
- $\frac{\partial^i R_s^1(0)}{\partial t^i} - (-1)^{1-i} \frac{\partial^{3-i} R_s^1(0)}{\partial t^{3-i}} = 0, i = 0, 1,$
- $\frac{\partial^i \widetilde{C}_s^1(t)}{\partial t^i}|_{t=s} = \frac{\partial^i \widetilde{D}_s^1(t)}{\partial t^i}|_{t=s}, i = 0, 1, 2.$

Then, by using the features of the reproducing kernel  $R_i^1(s)$ , the solution of above drivative equations is computed.

### 3.1 The inner product space $\widetilde{W}[0, T]$

The inner product space  $\widetilde{W}[0, T]$  is defined as

$$\begin{aligned} \widetilde{W}[0, T] &= \underbrace{W_2^{2,0}[0, T] \oplus \dots \oplus W_2^{2,0}[0, T]}_n \oplus \underbrace{W_2^{2,1}[0, T] \oplus \dots \oplus W_2^{2,1}[0, T]}_n, \\ \widetilde{W}[0, T] &= \{(y_1, \dots, y_n, z_1, \dots, z_n)^T | y_i \in W_2^{2,0}[0, T], z_i \in W_2^{2,1}[0, T], i = 1, \dots, n\}. \end{aligned}$$

The specific inner product in  $\widetilde{W}[0, T]$  is of the subsequent form

$$\begin{aligned} &\langle (y_1, \dots, y_n, z_1, \dots, z_n)^T, (\widetilde{y}_1, \dots, \widetilde{y}_n, \widetilde{z}_1, \dots, \widetilde{z}_n)^T \rangle_{\widetilde{W}} \\ &= \sum_{i=1}^n \langle y_i, \widetilde{y}_i \rangle_{W_2^{2,0}} + \sum_{i=1}^n \langle z_i, \widetilde{z}_i \rangle_{W_2^{2,1}}, \end{aligned} \quad (17)$$

and the norm  $\|(y_1, \dots, y_n, z_1, \dots, z_n)^T\|_{\widetilde{W}}$  is denoted by

$$\begin{aligned} &\|(y_1, \dots, y_n, z_1, \dots, z_n)^T\|_{\widetilde{W}} \\ &= \sqrt{\sum_{i=1}^n \|y_i\|_{W_2^{2,0}}^2 + \sum_{i=1}^n \|z_i\|_{W_2^{2,1}}^2}. \end{aligned} \quad (18)$$

It is easy to verify that  $\widetilde{W}[0, T]$  is a Hilbert space.

Also,  $\overline{W}[0, T] = \bigoplus_{i=1}^{2n} W_2^1$  is a Hilbert space in a similar procedure.

## 4 Analytical Solution of the System

In this section, we will characterize the analytical solution of system (6) in the space  $\widetilde{W}[0, T]$ .

First, consider the following assumptions:

- (I) Suppose that the problem (6) has a unique solution.
- (II) Let  $\Lambda \left( \begin{matrix} l_{ij} \\ \end{matrix} \right)_{2n \times 2n} : \widetilde{W}[0, T] \longrightarrow \overline{W}[0, T]$  be a linear operator, where

$$\Lambda(y(t), z(t)) = (\dot{y}(t) + (BR^{-1}B)z(t) - F_L(t, y(t)), \dot{z}(t) + Sy(t) - G_L(t, y(t), z(t))). \quad (19)$$

Then (6) can be converted into the following form

$$\Lambda(y(t), z(t)) = (F_0(t) + F_N(t, y(t)), G_0(t) + G_N(t, y(t), z(t))). \tag{20}$$

**Theorem 3.** The operator  $(l_{ij})_{2n \times 2n}$  is a linear and bounded operator. Since  $(l_{ij})_{2n \times 2n}$  is a linear and bounded operator, then the adjoint operator of  $(l_{ij})_{2n \times 2n}$  defined as subsequent form  $(l_{ij})_{2n \times 2n}^* : \widetilde{W}[0, T] \rightarrow \widetilde{W}[0, T]$  is uniquely determined. Let a countable set  $\{t_i\}_{i=1}^\infty$  be dense in the interval  $[0, T]$  and  $R_s(t)$  be the reproducing kernel of  $W_2^1[0, T]$ . Now, we set  $\rho_{ij}(t) = (l_{ij})_{2n \times 2n}^* \Phi_{ij}(t)$ ,  $i = 1, 2, \dots, j = 1, 2, \dots, 2n$ , where

$$\Phi_{ij}(t) = R_{t_i}(t) \vec{e}_j = \begin{cases} (R_t(t_i), \underbrace{0, 0, \dots, 0}_{2n-1})^T, & j = 1, \\ (0, \underbrace{R_t(t_i), 0, \dots, 0}_{2n-2})^T, & j = 2, \\ \vdots \\ (0, \underbrace{0, \dots, 0, R_t(t_i)}_{2n-1})^T, & j = 2n. \end{cases} \tag{21}$$

**Lemma 1.** (see [16]). For each  $i \in \{1, 2, 3, \dots\}$  and each  $j \in \{1, 2, \dots, 2n\}$ ,  $\rho_{ij} \in \widetilde{W}[0, T]$ .

**Lemma 2.** (see [23]) If the set  $\{t_i\}_{i=1}^\infty$  is dense in the interval  $[0, T]$ , then the system  $\{\rho_{ij}(t)\}_{(1,1)}^{(\infty, 2n)}$  is independent in  $\widetilde{W}[0, T]$ .

**Theorem 4.** (see [23]) Suppose that the set  $\{t_i\}_{i=1}^\infty$  is dense in the interval  $[0, T]$  and the solution of system (20) is unique, then  $\{\rho_{ij}(t)\}_{(1,1)}^{(\infty, 2n)}$  is the complete system of  $\widetilde{W}[0, T]$  and

$$\rho_{ij}(t) = ((l_{j1})_s R_s^0(t)|_{s=t_i}, \dots, (l_{jn})_s R_s^0(t)|_{s=t_i}, (l_{j(n+1)})_s R_s^1(t)|_{s=t_i}, \dots, (l_{j2n})_s R_s^1(t)|_{s=t_i})^T,$$

and the subscript  $s$  of the operator  $l_{jj}, j = 1, 2, \dots, 2n$ , indicates that we can apply this operator to the function of  $s$ .

#### 4.1 The Linear problem

If (20) is linear, that is  $F_N(t, y(t)) = G_N(t, y(t), z(t)) = \underbrace{(0, 0, \dots, 0)}_n$ , then (20) can be rewritten as follows.

$$\Lambda(y(t), z(t)) = (F_0(t), G_0(t)). \tag{22}$$

The exact solution and approximate solution can be derived by using the following theorem.

**Theorem 5.** Suppose that  $(y(t), z(t)) \in \widetilde{W}[0, T]$ , then

$$(y(t), z(t)) = \sum_{i=1}^{\infty} \sum_{j=1}^{2n} C_{ij} \rho_{ij}(t), \quad (23)$$

where

$$\sum_{i=1}^m \sum_{j=1}^{2n} C_{ij} \Lambda \rho_{ij}(t_k) = (F_0(t_k), G_0(t_k)), \quad k = 1, 2, \dots, m, \quad (24)$$

*Proof.* The system  $\{\rho_{ij}(t)\}_{(1,1)}^{(\infty, 2n)}$  is complete in  $\widetilde{W}[0, T]$ , then

$$(y(t), z(t)) = \sum_{i=1}^{\infty} \sum_{j=1}^{2n} C_{ij} \rho_{ij}(t). \quad (25)$$

Now, by the  $m$ -term intercept of (25), the approximate solution is presented by

$$Q_m(y(t), z(t)) = (y^m(t), z^m(t)) = \sum_{i=1}^m \sum_{j=1}^{2n} C_{ij} \rho_{ij}(t), \quad (26)$$

where  $Q_m : \widetilde{W}[0, T] \rightarrow \{\rho_{ij}(t)\}_{(1,1)}^{(m, 2n)}$  is an orthogonal projection operator.

It follows that

$$\begin{aligned} \Lambda(y^m(t_k), z^m(t_k)) &= \sum_{j=1}^{2n} \langle \Lambda(y^m(t), z^m(t)), \Phi_{kj}(t) \rangle_{\widetilde{W}} \vec{e}_j \\ &= \sum_{j=1}^{2n} \langle (y^m(t), z^m(t)), \Lambda^* \Phi_{kj}(t) \rangle_{\widetilde{W}} \vec{e}_j = \sum_{j=1}^{2n} \langle Q_m(y(t), z(t)), \rho_{kj}(t) \rangle_{\widetilde{W}} \vec{e}_j \\ &= \sum_{j=1}^{2n} \langle (y(t), z(t)), Q_m \rho_{kj}(t) \rangle_{\widetilde{W}} \vec{e}_j = \sum_{j=1}^{2n} \langle (y(t), z(t)), \rho_{kj}(t) \rangle_{\widetilde{W}} \vec{e}_j \\ &= \sum_{j=1}^{2n} \langle \Lambda(y(t), z(t)), \Phi_{kj}(t) \rangle_{\widetilde{W}} \vec{e}_j = \Lambda(y(t_k), z(t_k)), \quad k = 1, 2, \dots, m. \end{aligned} \quad (27)$$

Therefore,

$$\sum_{i=1}^m \sum_{j=1}^{2n} C_{ij} \Lambda \rho_{ij}(t_k) = (F_0(t_k), G_0(t_k)), \quad k = 1, 2, \dots, m. \quad (28)$$

Then, the approximate solution  $(y(t), z(t))$  can be obtained by

$$(y^m(t), z^m(t)) = Q_m(y(t), z(t)) = \sum_{i=1}^m \sum_{j=1}^{2n} C_{ij} \rho_{ij}(t), \quad (29)$$

where the coefficients  $C_{ij}$ ,  $i = 1, 2, \dots, n$ ,  $j = 1, 2, \dots, 2n$ , can be determined by (28).  $\square$

### 4.1.1 Convergence analysis

**Theorem 6.** Let  $\{t_i\}_{i=1}^\infty$  be dense in the interval  $[0, T]$  and  $(y(t), z(t))$  be the solution of (22), then the approximate solution  $(y^m(t), z^m(t))$  and its derivative  $(\dot{y}^m(t), \dot{z}^m(t))$  are uniformly convergent to the exact solution  $(y(t), z(t))$  and  $(\dot{y}(t), \dot{z}(t))$ , respectively.

*Proof.* Noting that  $\widetilde{W}[0, T]$  is a Hilbert space, we obtain

$$\|y_i(t) - y_i^m(t)\|_{W_2^{2,0}} \rightarrow 0, \quad \text{as } m \rightarrow \infty, \quad i = 1, \dots, n, \tag{30}$$

$$\|z_i(t) - z_i^m(t)\|_{W_2^{2,1}} \rightarrow 0, \quad \text{as } m \rightarrow \infty, \quad i = 1, \dots, n. \tag{31}$$

On the other hand, it holds that

$$\begin{aligned} |y_i(s) - y_i^m(s)| &= | \langle y_i(\cdot) - y_i^m(\cdot), R_s^0(\cdot) \rangle_{W_2^{2,0}} | \\ &\leq v_i^1 \|y_i - y_i^m\|_{W_2^{2,0}}, \quad i = 1, \dots, n, \end{aligned} \tag{32}$$

$$\begin{aligned} |\dot{y}_i(s) - \dot{y}_i^m(s)| &= | \langle y_i(\cdot) - y_i^m(\cdot), \frac{\partial}{\partial s} R_s^0(\cdot) \rangle_{W_2^{2,0}} | \\ &\leq v_i^2 \|y_i - y_i^m\|_{W_2^{2,0}}, \quad i = 1, \dots, n, \end{aligned} \tag{33}$$

and

$$\begin{aligned} |z_i(s) - z_i^m(s)| &= | \langle z_i(\cdot) - z_i^m(\cdot), R_s^1(\cdot) \rangle_{W_2^{2,1}} | \\ &\leq \theta_i^1 \|z_i - z_i^m\|_{W_2^{2,1}}, \quad i = 1, \dots, n, \end{aligned} \tag{34}$$

$$\begin{aligned} |\dot{z}_i(s) - \dot{z}_i^m(s)| &= | \langle z_i(\cdot) - z_i^m(\cdot), \frac{\partial}{\partial s} R_s^1(\cdot) \rangle_{W_2^{2,1}} | \\ &\leq \theta_i^2 \|z_i - z_i^m\|_{W_2^{2,1}}, \quad i = 1, \dots, n, \end{aligned} \tag{35}$$

where  $v_i^1, v_i^2, \theta_i^1$ , and  $\theta_i^2$  are real constants.

Hence, we deduce that  $\|y - y^m\| \rightarrow 0, \|z - z^m\| \rightarrow 0, \|\dot{y} - \dot{y}^m\| \rightarrow 0$  and  $\|\dot{z} - \dot{z}^m\| \rightarrow 0$  as  $m \rightarrow \infty$ , where  $\|y\|^2 = \sum_{i=1}^n \|y_i\|_\infty^2$  and  $\|z\|^2 = \sum_{i=1}^n \|z_i\|_\infty^2$ . Thus the proof is completed.  $\square$

### 4.1.2 Error analysis

In the following, we obtain the error estimates for the approximate solution of (22) in  $\widetilde{W}[0, T]$ .

**Theorem 7.** Let the partition for the interval  $[0, 1]$  be denoted by  $P_m = \{0 = t_1 < t_2 < \dots < t_m = T\}$ , also, suppose that  $(y(t), z(t))$  and the problem (22) has an approximate solution  $(y^m(t), z^m(t))$  in the space  $\widetilde{W}[0, T]$ . The following relation holds,

$$\|(y(t), z(t)) - (y^m(t), z^m(t))\| \leq c h_t, \quad h_t = \max_{1 \leq i \leq m-1} (t_{i+1} - t_i), \tag{36}$$

where  $c$  is a real constant and

$$\|(y(t), z(t)) - (y^m(t), z^m(t))\|^2 = \sum_{i=1}^n \|y_i - y_i^m\|_\infty^2 + \sum_{i=1}^n \|z_i - z_i^m\|_\infty^2.$$

*Proof.* Assume that  $t \in [t_i, t_{i+1}]$ , for some  $i = 1, \dots, m-1$ . We can write

$$\begin{aligned} (y(t), z(t)) - (y^m(t), z^m(t)) &= (y(t), z(t)) - (y(t_i), z(t_i)) \\ &+ (y^m(t_i), z^m(t_i)) - (y^m(t), z^m(t)) \\ &+ (y(t_i), z(t_i)) - (y^m(t_i), z^m(t_i)). \end{aligned} \quad (37)$$

According to the mean value theorem, there exists  $\xi_i \in (t_i, t_{i+1})$  such that

$$(y(t), z(t)) - (y(t_i), z(t_i)) = (t - t_i)(\dot{y}(\xi_i), \dot{z}(\xi_i)), \quad (38)$$

where  $\dot{y} = (\dot{y}_1, \dots, \dot{y}_n)^T$  and  $\dot{z} = (\dot{z}_1, \dots, \dot{z}_n)^T$ .

Since  $(y(t), z(t)) \in \widetilde{W}[0, T]$  then for some  $d > 0$

$$\|(\dot{y}(t), \dot{z}(t))\| \leq d, \quad \forall t \in [t_i, t_{i+1}], \quad (39)$$

and therefore

$$\|(y(t), z(t)) - (y(t_i), z(t_i))\| \leq d h_t. \quad (40)$$

We know

$$\begin{cases} |y^m(t) - y^m(t_i)| \leq \int_{t_i}^t |\dot{y}^m(s)| ds, \\ |z^m(t) - z^m(t_i)| \leq \int_{t_i}^t |\dot{z}^m(s)| ds, \end{cases} \quad (41)$$

where

$$\int_{t_i}^t |\dot{y}^m(s)| ds = \left( \int_{t_i}^t |\dot{y}_1^m(s)| ds, \dots, \int_{t_i}^t |\dot{y}_n^m(s)| ds \right)^T,$$

and

$$\int_{t_i}^t |\dot{z}^m(s)| ds = \left( \int_{t_i}^t |\dot{z}_1^m(s)| ds, \dots, \int_{t_i}^t |\dot{z}_n^m(s)| ds \right)^T.$$

Since  $(y^m(t), z^m(t)) \in \widetilde{W}[0, T]$ , it follows that

$$\|(y^m(t), z^m(t)) - (y^m(t_i), z^m(t_i))\| \leq e h_t, \quad (42)$$

where  $e$  is a positive constant.

Using Theorem 6, for large  $m$  we have

$$\|(y(t_i), z(t_i)) - (y^m(t_i), z^m(t_i))\| \leq \epsilon. \quad (43)$$

Since  $\epsilon$  is arbitrary, we can combine (37)-(43), for the chosen value of  $m$ , thus

$$\|(y(t), z(t)) - (y^m(t), z^m(t))\| \leq c h_t, \quad h_t = \max_{1 \leq i \leq m-1} (t_{i+1} - t_i), \quad (44)$$

where  $c$  is a positive constant and this completes the proof.  $\square$

**Theorem 8.** Consider the partition of the interval  $[0, 1]$ , denoted by  $P_m = \{0 = t_1 < t_2 < \dots < t_m = T\}$ , also, suppose that the problem (22) has an approximate solution  $(y^m(t), z^m(t))$  in the space  $\widetilde{W}[0, T]$  such that  $\|\dot{y}^m(t)\|_\infty$  and  $\|\dot{z}^m(t)\|_\infty$  are bounded. If  $(y(t), z(t)) \in \bigoplus_{i=1}^{2n} C^2[0, T]$ , then the following relations hold,

$$\|(\mathbf{y}(t), \mathbf{z}(t)) - (\mathbf{y}^m(t), \mathbf{z}^m(t))\| \leq c h_t^2, \tag{45}$$

$$\|(\dot{\mathbf{y}}(t), \dot{\mathbf{z}}(t)) - (\dot{\mathbf{y}}^m(t), \dot{\mathbf{z}}^m(t))\| \leq e h_t, \quad h_t = \max_{1 \leq i \leq m-1} (t_{i+1} - t_i), \tag{46}$$

where  $c$  and  $e$  are real constants.

*Proof.* In each subinterval  $[t_i, t_{i+1}]$ , we can write

$$\begin{aligned} (\mathbf{y}(t), \mathbf{z}(t)) - (\mathbf{y}^m(t), \mathbf{z}^m(t)) &= (\mathbf{y}(t), \mathbf{z}(t)) - (\mathbf{y}(t_i), \mathbf{z}(t_i)) \\ &+ (\mathbf{y}^m(t_i), \mathbf{z}^m(t_i)) - (\mathbf{y}^m(t), \mathbf{z}^m(t)) \\ &+ (\mathbf{y}(t_i), \mathbf{z}(t_i)) - (\mathbf{y}^m(t_i), \mathbf{z}^m(t_i)). \end{aligned} \tag{47}$$

According to the mean value theorem, there exists  $\xi_i \in (t_i, t_{i+1})$  such that

$$(\mathbf{y}(t), \mathbf{z}(t)) - (\mathbf{y}(t_i), \mathbf{z}(t_i)) = (t - t_i)(\ddot{\mathbf{y}}(\xi_i), \ddot{\mathbf{z}}(\xi_i)). \tag{48}$$

Since  $(\mathbf{y}(t), \mathbf{z}(t)) \in \bigoplus_{i=1}^{2n} C^2[0, T]$  then for some  $d > 0$

$$\|(\ddot{\mathbf{y}}(t), \ddot{\mathbf{z}}(t))\| \leq d, \quad \forall t \in [0, T], \tag{49}$$

and therefore

$$\|(\mathbf{y}(t), \mathbf{z}(t)) - (\mathbf{y}(t_i), \mathbf{z}(t_i))\| \leq d h_t. \tag{50}$$

Note that

$$\begin{cases} |\dot{\mathbf{y}}^m(t) - \dot{\mathbf{y}}^m(t_i)| \leq \int_{t_i}^t |\ddot{\mathbf{y}}^m(s)| ds, \\ |\dot{\mathbf{z}}^m(t) - \dot{\mathbf{z}}^m(t_i)| \leq \int_{t_i}^t |\ddot{\mathbf{z}}^m(s)| ds, \end{cases} \tag{51}$$

where

$$\int_{t_i}^t |\ddot{\mathbf{y}}^m(s)| ds = \left( \int_{t_i}^t |\ddot{y}_1^m(s)| ds, \dots, \int_{t_i}^t |\ddot{y}_n^m(s)| ds \right)^T,$$

and

$$\int_{t_i}^t |\ddot{\mathbf{z}}^m(s)| ds = \left( \int_{t_i}^t |\ddot{z}_1^m(s)| ds, \dots, \int_{t_i}^t |\ddot{z}_n^m(s)| ds \right)^T.$$

Hence

$$\|(\mathbf{y}^m(t), \mathbf{z}^m(t)) - (\mathbf{y}^m(t_i), \mathbf{z}^m(t_i))\| \leq k h_t. \tag{52}$$

Using Theorem 6 for large  $m$ , we have

$$\|(\mathbf{y}(t_i), \mathbf{z}(t_i)) - (\mathbf{y}^m(t_i), \mathbf{z}^m(t_i))\| \leq \epsilon, \tag{53}$$

and

$$\|(\mathbf{y}(t_i), \dot{\mathbf{z}}(t_i)) - (\mathbf{y}^m(t_i), \dot{\mathbf{z}}^m(t_i))\| \leq \epsilon. \tag{54}$$

Since  $\epsilon$  is arbitrary, we can combine the equations (47)-(54), for the chosen value of  $m$ , thus

$$\|(\dot{y}(t), \dot{z}(t)) - (\dot{y}^m(t), \dot{z}^m(t))\| \leq d h_t, \quad h_t = \max_{1 \leq i \leq m-1} (t_{i+1} - t_i). \quad (55)$$

We know that

$$y(t) - y^m(t) = y(t_i) - y^m(t_i) + \int_{t_i}^t (\dot{y}(s) - \dot{y}^m(s)) ds, \quad (56)$$

$$z(t) - z^m(t) = z(t_i) - z^m(t_i) + \int_{t_i}^t (\dot{z}(s) - \dot{z}^m(s)) ds. \quad (57)$$

By using (53)- (57) for large  $m$ , it is straightforward to see that

$$\|(y(t), z(t)) - (y^m(t), z^m(t))\| \leq c h_t^2, \quad h_t = \max_{1 \leq i \leq m-1} (t_{i+1} - t_i), \quad (58)$$

and this completes the proof.  $\square$

## 4.2 The Nonlinear Problem

If (20) is nonlinear, then the approximate solution can be obtained using the following method.

The system  $\{\rho_{ij}(t)\}_{(1,1)}^{(\infty, 2n)}$  is complete in  $\widetilde{W}[0, T]$ , then

$$(y(t), z(t)) = \sum_{i=1}^{\infty} \sum_{j=1}^{2n} C_{ij} \rho_{ij}(t). \quad (59)$$

Now, by the  $m$ -term intercept of (59), the approximate solution is presented by

$$Q_m(y(t), z(t)) = (y^m(t), z^m(t)) = \sum_{i=1}^m \sum_{j=1}^{2n} C_{ij} \rho_{ij}(t), \quad (60)$$

where  $Q_m : \widetilde{W}[0, T] \rightarrow \{\rho_{ij}(t)\}_{(1,1)}^{(m, 2n)}$  is an orthogonal projection operator.

For numerical computation, we give  $m$  and initial function  $(y_0^m(t), z_0^m(t)) \in \widetilde{W}[0, T]$  and suppose that

$$\begin{aligned} (y_l^m(t), z_l^m(t)) &= (y_{1,l}^m(t), \dots, y_{n,l}^m(t), z_{1,l}^m(t), \dots, z_{n,l}^m(t))^T \\ &= \sum_{i=1}^m \sum_{j=1}^{2n} C_{ij,l} \rho_{ij}(t), \quad l = 1, 2, \dots, \end{aligned} \quad (61)$$

where the coefficients  $C_{ij,l}, i = 1, \dots, m, j = 1, \dots, 2n, l = 1, 2, \dots$  can be obtained by using

$$\Lambda(y_l^m(t_k), z_l^m(t_k)) = (F_0(t_k) + F_N(t_k, y_{l-1}^m(t_k)), G_0(t_k) + G_N(t_k, y_{l-1}^m(t_k), z_{l-1}^m(t_k))), \quad (62)$$

for  $k = 1, \dots, m, l = 1, 2, \dots$ .



### 4.2.1 The existence of solution and convergence analysis

In the following lemma, we find the solution of equation (20), and then show that the sequence  $\{(y_i^m(t), z_i^m(t))\}_{i=1}^\infty$  is convergent.

**Lemma 3.** (see [28]) For any  $y_i \in W_2^{2,0}$ ,  $i = 1, 2, \dots, n$ , and  $z_i \in W_2^{2,1}$ ,  $i = 1, 2, \dots, n$ , we have the following statements

$$\|y_i(t)\|_\infty \leq \alpha_i^1 \|y_i(t)\|_{W_2^{2,0}}, \|\dot{y}_i(t)\|_\infty \leq \alpha_i^2 \|y_i(t)\|_{W_2^{2,0}}, \tag{63}$$

$$\|z_i(t)\|_\infty \leq \beta_i^1 \|z_i(t)\|_{W_2^{2,1}}, \|\dot{z}_i(t)\|_\infty \leq \beta_i^2 \|z_i(t)\|_{W_2^{2,1}}, \tag{64}$$

where  $\alpha_i^1, \alpha_i^2, \beta_i^1$  and  $\beta_i^2$  are real constants.

**Lemma 4.** Suppose that,  $\|y_i(t)\|_{W_2^{2,0}}$ ,  $i = 1, \dots, n$ , and  $\|z_i(t)\|_{W_2^{2,1}}$ ,  $i = 1, \dots, n$ , are bounded, then there exist constants  $\gamma_i^1, \gamma_i^2, \delta_i^1$  and  $\delta_i^2$  such that

$$\|y_i(t)\|_\infty \leq \gamma_i^1, \|\dot{y}_i(t)\|_\infty \leq \gamma_i^2, \tag{65}$$

$$\|z_i(t)\|_\infty \leq \delta_i^1, \|\dot{z}_i(t)\|_\infty \leq \delta_i^2. \tag{66}$$

*Proof.* Since  $\|y_i(t)\|_{W_2^{2,0}}$  and  $\|z_i(t)\|_{W_2^{2,1}}$  are bounded, by Lemma 3,  $\|y_i(t)\|_\infty$  and  $\|z_i(t)\|_\infty$  are also bounded.  $\square$

**Lemma 5.** If  $\gamma_i, i = 1, \dots, n$ , and  $\delta_i, i = 1, \dots, n$ , are real constants then  $\Pi_i = \{y_{i,l}^m(t) \mid \|y_{i,l}^m(t)\|_{W_2^{2,0}} \leq \gamma_i\} \subset C[0, T]$ ,  $i = 1, \dots, n$ , and  $\tilde{\Pi}_i = \{z_{i,l}^m(t) \mid \|z_{i,l}^m(t)\|_{W_2^{2,1}} \leq \delta_i\} \subset C[0, T]$ ,  $i = 1, \dots, n$ , are bounded sets.

*Proof.* By Lemma 4, there exist positive constants  $\gamma_i < \infty, i = 1, \dots, n$ , such that  $\|y_{i,l}^m(t)\|_\infty \leq \gamma_i$ , for each  $t \in [0, T]$  and each  $y_{i,l}^m(t) \in \Pi_i$ . A similar argument shows that  $\tilde{\Pi}_i, i = 1, \dots, n$  are bounded sets.  $\square$

**Lemma 6.** If  $\gamma_i, i = 1, \dots, n$ , and  $\delta_i, i = 1, \dots, n$ , are real constants then  $\Pi_i = \{y_{i,l}^m(t) \mid \|y_{i,l}^m(t)\|_{W_2^{2,0}} \leq \gamma_i\} \subset C[0, T]$ ,  $i = 1, \dots, n$ , and  $\tilde{\Pi}_i = \{z_{i,l}^m(t) \mid \|z_{i,l}^m(t)\|_{W_2^{2,1}} \leq \delta_i\} \subset C[0, T]$ ,  $i = 1, 2, \dots, n$ , are equicontinuous.

*Proof.* Based on Lemma 5, for an arbitrary  $y_{i,l}^m \in \Pi_i, i = 1, \dots, n$ , we deduce

$$\begin{aligned} |y_{i,l}^m(t') - y_{i,l}^m(t)| &= |\langle y_{i,l}^m(s), R_t^0(s) - R_{t'}^0(s) \rangle_{W_2^{2,0}}| \\ &\leq \|y_{i,l}^m(t)\|_{W_2^{2,0}} \|R_t^0(s) - R_{t'}^0(s)\|_{W_2^{2,0}} \\ &\leq \|y_{i,l}^m(t)\|_{W_2^{2,0}} \left\| \frac{d}{dt} R_t^0(s) \Big|_{t=\zeta \in [t', t]} \right\|_{W_2^{2,0}} |t' - t| \\ &\leq \omega_i |t' - t|, \end{aligned} \tag{67}$$

where  $\omega_i, i = 1, \dots, n$ , are positive constants.

Choosing

$$\delta_i = \frac{\epsilon}{\omega_i},$$

gives that for all  $t, t' \in [0, T]$  with  $|t' - t| < \delta_i$ , we have

$$|y_{i,l}^m(t') - y_{i,l}^m(t)| < \epsilon, \quad (68)$$

hence  $\Pi_i$ ,  $i = 1, \dots, n$  are equicontinuous sets.

A similar argument shows that  $\widetilde{\Pi}_i$ ,  $i = 1, \dots, n$ , are equicontinuous sets.  $\square$

**Theorem 9.** Suppose that the following statements are true.

- (i)  $\{t_i\}_{i=1}^\infty$  is a countable dense subset in the domain  $[0, T]$ .
- (ii)  $\Pi_i = \{y_{i,l}^m(t) \mid \|y_{i,l}^m(t)\|_{W_2^{2,0}} \leq \gamma_i\} \subset C[0, T]$ ,  $i = 1, \dots, n$ ,  
and  $\widetilde{\Pi}_i = \{z_{i,l}^m(t) \mid \|z_{i,l}^m(t)\|_{W_2^{2,1}} \leq \delta_i\} \subset C[0, T]$ ,  $i = 1, \dots, n$ .
- (iii)  $(l_{ij})_{2n \times 2n}$  is an invertible operator of  $(y(t), z(t))$ .
- (iv)  $F_N(t, y(t))$  and  $G_N(t, y(t), z(t))$  are continuous as  $t \in [0, T]$ .

Then, there exist subsequences  $\{y_{l_p}^m(t)\}_{p=1}^\infty \subseteq \bigoplus_{i=1}^n \Pi_i$ , and  $\{z_{l_p}^m(t)\}_{p=1}^\infty \subseteq \bigoplus_{i=1}^n \widetilde{\Pi}_i$ , which  $\{(y_{l_p}^m(t), z_{l_p}^m(t))\}_{p=1}^\infty$ , converges uniformly to  $(y(t), z(t))$ , as  $m \rightarrow \infty, p \rightarrow \infty$ , where

$$(y(t), z(t)) = (l_{ij})_{2n \times 2n}^{-1} (F_0(t) + F_N(t, y(t)), G_0(t) + G_N(t, y(t), z(t))).$$

*Proof.* Using (62), we have

$$\Lambda(y_{l_p}^m(t_k), z_{l_p}^m(t_k)) = (F_0(t_k) + F_N(t_k, y_{l_{p-1}}^m(t_k)), G_0(t_k) + G_N(t_k, y_{l_{p-1}}^m(t_k), z_{l_{p-1}}^m(t_k))), \quad (69)$$

for  $k = 1, \dots, m$ ,  $l = 1, 2, \dots$ .

It follows from Lemma 5 that  $\Pi_i$ ,  $i = 1, \dots, n$ , are precompact sets. Then, any sequence in  $\Pi_i$ , has a subsequence such that uniformly convergent and the limit of subsequence belongs to  $\Pi_i$ . Hence, by this principle, we show that there exists a sequence  $\{l_p\}_{p=1}^\infty$ , such that subsequences  $\{y_{l_p}^m(t)\}_{p=1}^\infty$  and  $\{z_{l_p}^m(t)\}_{p=1}^\infty$ , are uniformly convergent and  $(y(t), z(t)) = \lim_{p \rightarrow \infty, m \rightarrow \infty} (y_{l_p}^m(t), z_{l_p}^m(t))$ . Using (69), we also have

$$\Lambda(y_{l_p}^m(t_k), z_{l_p}^m(t_k)) = (F_0(t_k) + F_N(t_k, y_{l_{p-1}}^m(t_k)), G_0(t_k) + G_N(t_k, y_{l_{p-1}}^m(t_k), z_{l_{p-1}}^m(t_k))), \quad (70)$$

for  $k = 1, \dots, m$ ,  $l = 1, 2, \dots$ .

Since  $\Lambda$ ,  $F_N$  and  $G_N$  are continuous and  $\{t_i\}_{i=1}^\infty$  is dense in  $[0, T]$ , after taking limits from both sides of (70), we have

$$m \rightarrow \infty, p \rightarrow \infty \Rightarrow \Lambda(y(t), z(t)) = (F_0(t) + F_N(t, y(t)), G_0(t) + G_N(t, y(t), z(t))).$$

It follows that

$$(y(t), z(t)) = \Lambda^{-1} (F_0(t) + F_N(t, y(t)), G_0(t) + G_N(t, y(t), z(t))),$$

from the existence of  $\Lambda^{-1}$ .

This completes the proof of the theorem.  $\square$

**Theorem 10.** Suppose that the assumptions of Theorem 9 are valid, then there exist subsequences  $\{y_{l_p}^m(t)\}_{p=1}^\infty \subseteq \bigoplus_{i=1}^n \Pi_i$ , and  $\{z_{l_p}^m(t)\}_{p=1}^\infty \subseteq \bigoplus_{i=1}^n \widetilde{\Pi}_i$ , in which  $\{(\dot{y}_{l_p}^m(t), \dot{z}_{l_p}^m(t))\}_{p=1}^\infty$  converges uniformly to  $(\dot{y}(t), \dot{z}(t))$ , as  $m \rightarrow \infty, p \rightarrow \infty$ , where

$$(y(t), z(t)) = \Lambda^{-1}(F_0(t) + F_N(t, y(t)), G_0(t) + G_N(t, y(t), z(t))).$$

*Proof.* By Theorem 9, there exist subsequences  $\{y_{l_p}^m(t)\}_{p=1}^\infty \subseteq \bigoplus_{i=1}^n \Pi_i$ , and  $\{z_{l_p}^m(t)\}_{p=1}^\infty \subseteq \bigoplus_{i=1}^n \widetilde{\Pi}_i$ , in which  $\{(y_{l_p}^m(t), z_{l_p}^m(t))\}$  converges uniformly to  $(y(t), z(t))$ , as  $m \rightarrow \infty, p \rightarrow \infty$ , where

$$(y(t), z(t)) = \Lambda^{-1}(F_0(t) + F_N(t, y(t)), G_0(t) + G_N(t, y(t), z(t))).$$

It follows from Lemma 4 that the sequences  $\{y_{i,l_p}^m(t)\}_{p=1}^\infty, i = 1, \dots, n, \{\dot{y}_{i,l_p}^m(t)\}_{p=1}^\infty, i = 1, \dots, n, \{z_{i,l_p}^m(t)\}_{p=1}^\infty, i = 1, \dots, n,$  and  $\{\dot{z}_{i,l_p}^m(t)\}_{p=1}^\infty, i = 1, \dots, n,$  are bounded. Then, there exist subsequences  $\{y_{i,l_{p_s}}^m(t)\}_{s=1}^\infty, i = 1, \dots, n, \{\dot{y}_{i,l_{p_s}}^m(t)\}_{s=1}^\infty, i = 1, \dots, n, \{z_{i,l_{p_s}}^m(t)\}_{s=1}^\infty, i = 1, \dots, n,$  and  $\{\dot{z}_{i,l_{p_s}}^m(t)\}_{s=1}^\infty, i = 1, \dots, n,$  such that

$$\|y_{i,l_{p_s}}^m(t) - y_i(t)\|_\infty \rightarrow 0, \|\dot{y}_{i,l_{p_s}}^m(t) - \dot{y}_i(t)\|_\infty \rightarrow 0, \text{ as } s \rightarrow \infty, m \rightarrow \infty, i = 1, \dots, n,$$

$$\|z_{i,l_{p_s}}^m(t) - z_i(t)\|_\infty \rightarrow 0, \|\dot{z}_{i,l_{p_s}}^m(t) - \dot{z}_i(t)\|_\infty \rightarrow 0, \text{ as } s \rightarrow \infty, m \rightarrow \infty, i = 1, \dots, n.$$

Now, without loss of generality, we replace  $\{y_{i,l_{p_s}}^m(t)\}_{s=1}^\infty, i = 1, \dots, n,$  and  $\{z_{i,l_{p_s}}^m(t)\}_{s=1}^\infty, i = 1, \dots, n,$  with  $\{y_{i,l_p}^m(t)\}_{p=1}^\infty, i = 1, \dots, n,$  and  $\{z_{i,l_p}^m(t)\}_{p=1}^\infty, i = 1, \dots, n,$  respectively, which completes the proof of the theorem.  $\square$

**Theorem 11.** Suppose that the assumptions of Theorem 9 are valid, and there exists a unique solution for (20), then

$$\|(y_l^m(t), z_l^m(t)) - (y(t), z(t))\| \rightarrow 0, \text{ as } l \rightarrow \infty, m \rightarrow \infty, \tag{71}$$

$$\|(\dot{y}_l^m(t), \dot{z}_l^m(t)) - (\dot{y}(t), \dot{z}(t))\| \rightarrow 0, \text{ as } l \rightarrow \infty, m \rightarrow \infty. \tag{72}$$

*Proof.* Suppose that there exists  $k \in \{1, 2, \dots, n\}$  such that  $\{y_{k,l}^m(t)\}_{l \geq 1} \subset \Pi_k$  does not converge to  $y_k$ . Then there exists a positive number  $\epsilon_{k,0}$ , and a subsequence  $\{y_{k,l_p}^m(t)\}_{p \geq 1} \subset \Pi_k$ , such that

$$\|y_{k,l_p}^m(t) - y_k(t)\|_\infty \geq \epsilon_{k,0}, \quad p = 1, 2, \dots, \text{ as } m \rightarrow \infty. \tag{73}$$

Since  $\{y_{k,l}^m(t)\}_{l \geq 1} \subset \Pi_k$  is a precompact set, there exists a subsequence of  $\{y_{k,l_p}^m(t)\}_{p \geq 1}$  which converges uniformly to  $\widehat{y}_k(t)$ . Without loss of generality, we may assume that  $\{y_{k,l_p}^m(t)\}_{p \geq 1}$  converges uniformly to  $\widehat{y}_k(t)$ :

$$\|y_{k,l_p}^m(t) - \widehat{y}_k(t)\|_\infty \rightarrow 0, \text{ as } p \rightarrow \infty, m \rightarrow \infty, \tag{74}$$

Since the solution of Equation (20) is unique, we have  $y_k(t) = \widehat{y}_k(t)$ , and so (74) contradicts (73). This completes the proof of Theorem 11.  $\square$

### 4.2.2 Error analysis

To demonstrate the error analysis, we present two following theorems.

**Theorem 12.** Suppose that the assumptions of Theorem 9 are valid and the partition of the interval  $[0, 1]$ , denoted by  $P_m = \{0 = t_1 < t_2 < \dots < t_m = T\}$ , also suppose that  $(y(t), z(t))$  and  $(y_l^m(t), z_l^m(t))$  are respectively the exact solution and the approximate solution of the problem (20) in the space  $\widetilde{W}[0, T]$ . The following relation holds,

$$\|(y(t), z(t)) - (y_l^m(t), z_l^m(t))\| \leq c h_t, \text{ as } m \rightarrow \infty, l \rightarrow \infty, \quad (75)$$

where  $c$  is a real constant and  $h_t = \max_{1 \leq i \leq m-1} (t_{i+1} - t_i)$ .

**Theorem 13.** Suppose that the assumptions of Theorem 9 are valid and  $(y^m(t), z^m(t))$  is the approximate solution of the problem (20) in the space  $\widetilde{W}[0, T]$  such that  $\|\dot{y}_l^m(t)\|$  and  $\|\dot{z}_l^m(t)\|$  are bounded and also suppose that the partition of the interval  $[0, 1]$ , denoted by  $P_m = \{0 = t_1 < t_2 < \dots < t_m = T\}$ . If  $(y(t), z(t)) \in \bigoplus_{i=1}^{2n} C^2[0, T]$ , then the following relations hold,

$$\|(y(t), z(t)) - (y_l^m(t), z_l^m(t))\| \leq c h_t^2, \text{ as } m \rightarrow \infty, l \rightarrow \infty, \quad (76)$$

$$\|(\dot{y}(t), \dot{z}(t)) - (\dot{y}_l^m(t), \dot{z}_l^m(t))\| \leq e h_t, \text{ as } m \rightarrow \infty, l \rightarrow \infty, \quad (77)$$

where  $c$  and  $e$  are real constants and  $h_t = \max_{1 \leq i \leq m-1} (t_{i+1} - t_i)$ .

## 5 Numerical Experiment

To indicate the performance of the current method, we present four examples. For each example, we choose the subset  $t_i = \frac{i-1}{m-1}$ ,  $i = 1, \dots, m$  to construct the orthogonal  $\{\rho_{ij}(t)\}_{(1,1)}^{(m,2n)}$  in  $\widetilde{W}$ .

To illustrate the efficiency of the proposed method for Examples 1 and 3, we report error  $|v(t) - v^m(t)|$  where  $v^m(t) = -R^{-1}B(z^m(t) + p(T))$  and for Examples 2 and 4, we report error  $|v(t) - v_l^m(t)|$  where  $v_l^m(t) = -R^{-1}B(z_l^m(t) + p(T))$ .

For the computational work we select the following examples from [10, 36, 32]. In the process of computation, all the calculations are done by using Maple 12 and Matlab 2012 software packages.

**Example 1.** The control problem is as follows:

$$\dot{x}(t) = v(t) - x(t), \quad 0 \leq t \leq 1, \quad (78)$$

where  $x(0) = 1$ . The quadratic objective functional to be minimized is as follows:

$$J[x(1), v(1)] = \frac{1}{2} \int_0^1 (x^2(t) + v^2(t)) dt. \quad (79)$$

The exact solutions have been given in [10] by

$$x(t) = Ae^{\sqrt{2}t} + (1 - A)e^{-\sqrt{2}t},$$

$$v(t) = A(\sqrt{2} + 1)e^{\sqrt{2}t} - (1 - A)(\sqrt{2} - 1)e^{-\sqrt{2}t},$$

where  $A = \frac{(2\sqrt{2}-3)}{-(e^{\sqrt{2}})^2+2\sqrt{2}-3}$ .

In Table 1, the values of  $v^m(t)$ , by using the expressed method, for  $m = 10, 50, 100, 150$  are compared with the exact solutions at selected values of time  $t$ . In Table 2, a comparison is made between the obtained results for  $m = 10, 50, 100, 150$  together with the solutions obtained by Kafash et al. [24], Mehne et al. [26] for the optimal cost functional and the exact solution. In Figure 1, the values of  $x(t)$  and  $\dot{x}(t)$ , by using the expressed method for  $m = 150$  are compared with the exact solutions.

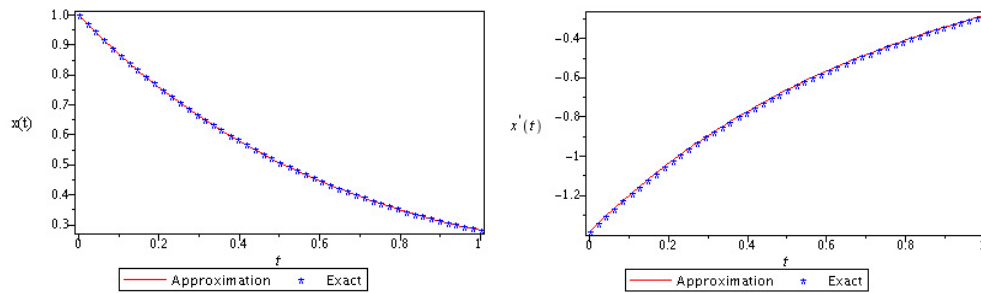


**Figure 1:** Estimated and exact values of  $x(t)$  and  $\dot{x}(t)$  for  $m = 150$  (Example 1)

**Table 1:** Numerical comparison between the values of  $v^m(t)$  for  $m = 10, 50, 100, 150$  and the exact solutions at selected values of time  $t$  (Example 1)

$t$	$m = 10$	$m = 50$	$m = 100$	$m = 150$	<i>Exact</i>
0.0	-0.38495473	-0.38578941	-0.38581144	-0.38581543	-0.38581859
0.1	-0.32730314	-0.32803424	-0.32805378	-0.32805733	-0.32806014
0.2	-0.27621086	-0.27685108	-0.27686825	-0.27687137	-0.27687384
0.3	-0.23065788	-0.23121453	-0.23122941	-0.23123211	-0.23123424
0.4	-0.18973342	-0.19021029	-0.19022294	-0.19022523	-0.19022705
0.5	-0.15261816	-0.15301687	-0.15302734	-0.15302924	-0.15303074
0.6	-0.11856830	-0.11888911	-0.11889745	-0.11889895	-0.11890015
0.7	-0.08690088	-0.08714327	-0.08714951	-0.08715063	-0.08715152
0.8	-0.05698034	-0.05714335	-0.05714750	-0.05714825	-0.05714883
0.9	-0.02820598	-0.02828829	-0.02829036	-0.02829074	-0.02829104
1.0	0.00000000	0.00000000	0.00000000	0.00000000	0.00000000

**Table 2:** The optimal cost functional  $J$  (Example 1)

Methods	$J$	$Error$	$CPU-time$ (s)
Method of Kafash et al. [24]			
Iteration $n = 1$	0.194298642	$1.3e-3$	
Iteration $n = 2$	0.192931607	$2.2e-5$	
Iteration $n = 3$	0.192909776	$4.7e-7$	
Method of Mehne et al. [26]			
Iteration $n = 1$	0.251362736	$5.8e-2$	
Iteration $n = 2$	0.194298642	$1.3e-3$	
Iteration $n = 3$	0.193828723	$9.1e-4$	
The proposed method			
$m = 10$	0.19267632	$2.3e-4$	1.82 (s)
$m = 50$	0.19290141	$7.9e-6$	7.11 (s)
$m = 100$	0.19290737	$1.9e-6$	19.14 (s)
$m = 150$	0.19290844	$8.5e-7$	58.42 (s)

**Table 3:** Numerical comparison between the values of  $v^m(t)$  for  $m = 200, 220, 240, 260$ ,  $l = 25$  and the exact solutions at selected values of time  $t$  Estimated values of  $v(t)$  for  $m = 200, 220, 240, 260$  (Example 2)

$t$	$m = 200$	$m = 220$	$m = 240$	$m = 260$	$bvp4c$
0.0	-0.59775621	-0.59789871	-0.59834627	-0.59850812	-0.59869334
0.1	-0.56028712	-0.56037123	-0.56054103	-0.56056310	-0.56085005
0.2	-0.51860934	-0.51870638	-0.51884131	-0.51887531	-0.51888020
0.3	-0.47214962	-0.47217091	-0.47225834	-0.47230698	-0.47230918
0.4	-0.42035982	-0.42058920	-0.42067862	-0.42070901	-0.42071582
0.5	-0.36372467	-0.36373451	-0.36374529	-0.36375687	-0.36376888
0.6	-0.30124533	-0.30125321	-0.30126587	-0.30126809	-0.30127343
0.7	-0.23320118	-0.23320672	-0.23321234	-0.23322998	-0.23322692
0.8	-0.15984387	-0.15985391	-0.15986524	-0.15987193	-0.15988291
0.9	-0.08181139	-0.08181389	-0.08181512	-0.08181734	-0.08181862
1.0	0.00000000	0.00000000	0.00000000	0.00000000	0.00000000

**Example 2.** Consider the OCP

$$J[x_1(1), x_2(1), v(1)] = \frac{1}{2} \int_0^1 (x_1^2(t) + x_2^2(t) + v^2(t)) dt, \quad (80)$$

provided with

$$\begin{cases} \dot{x}_1(t) = x_2(t) + x_1(t)x_2(t), \\ \dot{x}_2(t) = -x_1(t) + x_2(t) + x_2^2(t) + v(t), \\ x_1(0) = -0.8, \quad x_2(0) = 0. \end{cases} \quad (81)$$

Table 3 presents the values of  $v_l^m(t)$  using the proposed method for  $m = 200, 220, 240, 260$ ,  $l = 25$ , and the solutions obtained by the Matlab package `bvp4c`. The cost functional values at the different methods are listed in Table 4.

**Table 4:** The optimal cost functional  $J$  (Example 2)

Methods	$J$	CPU-time (s)
Method of Shirazian et al. [36]		
n=10	0.44488	–
Method of Saberi Nik et al. [32]		
n=10	0.44488	–
The proposed method		
$m = 200, l = 25$	0.44424381	870.09 (s)
$m = 220, l = 25$	0.44445346	896.98 (s)
$m = 240, l = 25$	0.44477691	908.23 (s)
$m = 260, l = 25$	0.44484805	968.95 (s)

**Example 3.** In the following example, there is only one control function,  $v(t)$ , and two state functions,  $x_1(t), x_2(t)$ , and we are concerned with the minimization of

$$J[x(1), v(1)] = \frac{1}{2} \int_0^1 (x(t) \begin{pmatrix} 0 & 0 \\ 0 & 2\pi \end{pmatrix} x(t) + \frac{\pi}{2} v^2(t)) dt, \quad (82)$$

provided with

$$\begin{cases} \dot{x}(t) = \begin{pmatrix} 0 & 0 \\ \frac{\pi}{2} & 0 \end{pmatrix} x(t) + \begin{pmatrix} \frac{\pi}{2} \\ 0 \end{pmatrix} v(t), & 0 \leq t \leq 1, \\ x(0) = \begin{pmatrix} 1 \\ 1 \end{pmatrix}, \end{cases} \quad (83)$$

where  $x(t) = (x_1(t), x_2(t))^T$ . The exact solutions have been given by

$$\begin{aligned} x_1(t) &= \frac{\cos(\frac{\pi}{2}t)e^{2\pi-\frac{\pi}{2}t} - 3\sin(\frac{\pi}{2}t)e^{2\pi-\frac{\pi}{2}t} + \cos(\frac{\pi}{2}t)e^{\pi+\frac{\pi}{2}t} - \sin(\frac{\pi}{2}t)e^{\pi+\frac{\pi}{2}t}}{e^{\pi} + e^{2\pi}}, \\ x_2(t) &= \frac{2\sin(\frac{\pi}{2}t)e^{2\pi-\frac{\pi}{2}t} + \cos(\frac{\pi}{2}t)e^{2\pi-\frac{\pi}{2}t} + \cos(\frac{\pi}{2}t)e^{\pi+\frac{\pi}{2}t}}{e^{\pi} + e^{2\pi}}, \\ v(t) &= \frac{2\sin(\frac{\pi}{2}t)e^{2\pi-\frac{\pi}{2}t} - 4\cos(\frac{\pi}{2}t)e^{2\pi-\frac{\pi}{2}t} - 2\sin(\frac{\pi}{2}t)e^{\pi+\frac{\pi}{2}t}}{e^{\pi} + e^{2\pi}}. \end{aligned}$$

Table 5 presents the approximation of  $v^m(t)$  using the expressed method for  $m = 60, 200, 220$  and  $240$ , compared with the exact solution. In Table 6, we give the absolute errors for the optimal cost functional, taking  $m = 60, 200, 220, 240$  which proves the accuracy of the solution. In Figure 2, the values of  $x_i(t)$  and  $\dot{x}_i(t)$ ,  $i = 1, 2$  using the expressed method for  $m = 200$  are compared with the exact solutions.

### 5.1 The Controlled Van der Pol oscillator

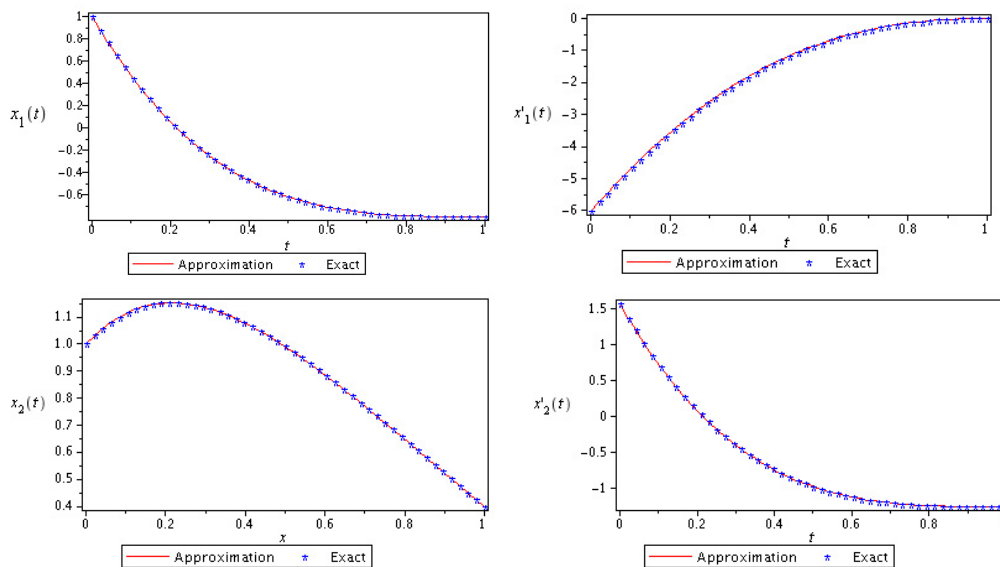
**Example 4.** Consider the optimal control of the Van der Pol oscillator as given in [33]:  
Minimize

**Table 5:** Numerical comparison between the values of  $v^m(t)$  for  $m = 65, 75, 85, 150$  and the exact solutions at selected values of time  $t$  (Example 3)

$t$	$m = 60$	$m = 200$	$m = 220$	$m = 240$	<i>Exact</i>
0.0	-3.83117212	-3.83398029	-3.83411316	-3.83416097	-3.83430467
0.1	-2.99300554	-2.99519508	-2.99529627	-2.99533269	-2.99544214
0.2	-2.26411644	-2.26567275	-2.26574640	-2.26577291	-2.26585257
0.3	-1.64835768	-1.64942895	-1.64947964	-1.64949788	-1.64955269
0.4	-1.14423126	-1.14491626	-1.14494867	-1.14496033	-1.14499538
0.5	-0.74613098	-0.74652552	-0.74654419	-0.74655090	-0.74657110
0.6	-0.44562472	-0.44581671	-0.44582580	-0.44582906	-0.44583890
0.7	-0.23242578	-0.23249247	-0.23249560	-0.23249674	-0.23250013
0.8	-0.09513159	-0.09513455	-0.09513469	-0.09513476	-0.09513492
0.9	-0.02174069	-0.02172789	-0.02172726	-0.02172704	-0.02172638
1.0	0.00000000	0.00000000	0.00000000	0.00000000	0.00000000

**Table 6:** The optimal cost functional  $J$  (Example 3)

$m$	$J$	<i>Error</i>	<i>CPU-time (s)</i>
60	4.74390944	$7.5e-3$	35.53 (s)
200	4.75079233	$6.6e-4$	166.65 (s)
220	4.75106701	$3.9e-4$	215.47 (s)
240	4.75116701	$2.9e-4$	287.59 (s)

**Figure 2:** Estimated and exact values of  $x_i(t)$ ,  $i = 1, 2$ , and  $\dot{x}_i(t)$ ,  $i = 1, 2$ , for  $m = 200$  (Example 3)



**Table 7:** Comparison of bvp4c, DTM and the expressed method for  $v(t)$

$t$	$m = 400, l = 40$	DTM	bvp4c
0.0	0.01125972	-0.010732	-0.011266
0.4	0.51481165	0.51524	0.51484
0.8	0.72141451	0.72165	0.72142
1.2	0.64601920	0.64615	0.64604
1.6	0.37309510	0.37309	0.37310
2.0	$-2.9298e-7$	$-1.5363e-6$	0.00000

**Table 8:** Numerical comparison of bvp4c, DTM and the proposed method

$x_1(t)$				$x_2(t)$		
t	$m = 400, l = 40$	DTM	bvp4c	$m = 400, l = 40$	DTM	bvp4c
0.0	0.99964932	0.99951	1.00000	$-3.0347e-9$	$-2.0587e-7$	0.000000
0.4	0.93585385	0.93584	0.93587	-0.28348142	-0.28344	-0.28349
0.8	0.79427145	0.79432	0.79430	-0.40884291	-0.40875	-0.40894
1.2	0.61307301	0.61321	0.61313	-0.50071973	-0.50061	-0.50093
1.6	0.38381050	0.38414	0.38390	-0.66461615	-0.66458	-0.66498
2.0	0.05994144	0.05927	0.05981	-0.98676550	-0.98677	-0.98678

$$J[x(2), v(2)] = \frac{1}{2} \int_0^2 (x^2(t) + \dot{x}^2(t) + v^2(t))dt, \tag{84}$$

provided with

$$\begin{cases} \ddot{x}(t) = \epsilon\omega(1 - x^2(t))\dot{x}(t) - \omega^2x(t) + v(t), & t \in [0, 2], \\ x(0) = 1, \dot{x}(0) = 0. \end{cases} \tag{85}$$

The OCP in Eqs. (84)-(85) may be restated as follows:

Minimize

$$J[x_1(2), x_2(2), v(2)] = \frac{1}{2} \int_0^2 (x_1^2(t) + x_2^2(t) + v^2(t))dt, \tag{86}$$

provided with

$$\begin{cases} \dot{x}_1(t) = x_2(t), \\ \dot{x}_2(t) = \epsilon\omega(1 - x_1^2(t))x_2(t) - \omega^2x_1(t) + v(t), & t \in [0, 2], \\ x_1(0) = 1, x_2(0) = 0. \end{cases} \tag{87}$$

Consider (87) with  $\omega = 1$  and  $\epsilon = 1$ . Table 7 presents the approximation of  $v_1^m(t)$  using the proposed method for  $m = 400, l = 40$  compared with the results obtained using the Matlab package bvp4c and results given in [32] (DTM). In Table 8, a comparison is made between the values of  $x_1(t)$  and  $x_2(t)$  using the present method for  $m = 400, l = 40$ , together with the results obtained using the Matlab package bvp4c and results given in [32].

## 6 Conclusion

The objective of this paper was to propose a new semi-analytical technique to estimate the solution of quadratic OCPs. This method enabled us to solve the quadratic OCPs. The proposed method provided the solution in a convergent series with components that could be easily computed. Furthermore, the accuracy of the proposed technique was evaluated through numerical tests. The results from the numerical examples confirmed the accuracy and reliability of the analytical method for this equation.

## References

- [1] Aronszajn, N. (1950). "Theory of reproducing kernels", *Transactions of the American Mathematical Society*, 68, 337-404.
- [2] Betts, J. T., Biehn, N., and Campbell, S. L., (2002). "Convergence of non-convergent IRK discretization of optimal control problems with state inequality constraints", *SIAM Journal on Scientific Computing*, 23( 6), 1981–2007.
- [3] Bouboulis, P., and Mavroforakis, M. (2011). "Reproducing Kernel Hilbert spaces and fractal interpolation", *Journal of Computational and Applied Mathematics*, 235(12), 3425-3434.
- [4] Canuto, C., Hussaini, M. Y., Quarteroni, A. and Zang, T. A. (1988). "Spectral methods in fluid dynamics", *Spinger-Verlag, Heidelberg, Germany*.
- [5] Chrysoverghi, I., Coletsos, J., and Kokkinis B., (2001). "Approximate relaxed descent method for optimal control problems", *Control and Cybernetics*, 30(4), 385-404.
- [6] Chrysoverghi, I., Coletsos I., and Kokkinis, B., (2006). "Discretization methods for optimal control problems with state constraints", *Journal of Computational and Applied Mathematics*, 19(1), 1-31.
- [7] Cialenco, I., Fasshauer, G. E., and Ye, Q. (2012). "Approximation of stochastic partial differential equations by a kernel-based collocation method", *International Journal of Computer Mathematics*, 89(18), 2543–2561.
- [8] Cui, M., and Geng, F. (2007). "A computational method for solving one-dimensional variable-coefficient Burgers equation. *Applied Mathematics and Computation*, 188(2), 1389–1401.
- [9] Cui, M., and Lin, Y. (2009). "Nonlinear Numerical Analysis in Reproducing Kernel Space", (UK ed.). *Nova Science Publishers, Inc.*
- [10] EL-Gindy, T. M., EL-Hawary, H. M., Salim, M. S. and EL-Kady, M. (1995). "A Chebyshev approximation for solving optimal control problems", *Computers & Mathematical with Application*, 29(6), 35-45.
- [11] Garg, D., Patterson, M., Hager, W. W., Rao, A. V., Benson, D. A., and Huntington, G. T. (2010). "A unified framework for the numerical solution of optimal control problems using pseudo spectral methods", *Automatica*, 46(11), 1843–1851.
- [12] Garrard, W. L., and Jordan, J. M. (1977). "Design of nonlinear automatic flight control systems", *Automatica*, 13(5), 497–505.

- [13] Geng, F. (2009). "Solving singular second-order three-point boundary value problems using reproducing kernel Hilbert space method", *Applied Mathematics and Computation*, 215(6), 2095–2102.
- [14] Geng, F. (2011). "A novel method for solving a class of singularly perturbed boundary value problems based on reproducing kernel method", *Applied Mathematics and Computation*, 218(8), 4211–4215.
- [15] Geng, F., and Cui, M. (2007). "Solving singular nonlinear second-order periodic boundary value problems in the reproducing kernel space", *Applied Mathematics and Computation*, 192(2), 389–398.
- [16] Geng, F., and Cui, M., (2007). "Solving a nonlinear system of second order boundary value problems", *Journal of Mathematical Analysis and Applications*, 327, 1167-1181.
- [17] Geng, F., and Cui, M. (2012). "A reproducing kernel method for solving nonlocal fractional boundary value problems", *Applied Mathematics Letters*, 25(5), 818–823.
- [18] Geng, F. Z., and Li, X. M. (2012). "A new method for Riccati differential equations based on reproducing kernel and quasi-linearization methods", *Abstract and Applied Analysis*, 2012, 1–8.
- [19] Ghasemi, M., Fardi, M., and Khoshsiar Ghaziani, R. (2015). "Numerical solution of nonlinear delay differential equations of fractional order in reproducing kernel Hilbert space", *Applied Mathematics and Computation*, 268, 815–831.
- [20] Gholami Baladezaei, M., Ghachpazan, M., and Hashemi Borzabadi, A., (2020). "Extraction of approximate solution for a class of nonlinear optimal control problems using  $1/G'$ -expansion technique", *Control and Optimization in Applied Mathematics*, 5(2), 56-82.
- [21] Itik, M., Salameci, M. U., and Banks, S. P. (2009). "Optimal control of drug therapy in cancer treatment", *Nonlinear Analysis: Theory, Methods and Applications*, 71(12), e1473–e1486.
- [22] Jajarmi, A., Pariz, N., S. Effati, S., and Vahidian Kamyad A., (2011), "Solving infinite horizon nonlinear optimal control problems using an extended modal series method", *Journal of Zhejiang University Science B.*, 12( 8), 667-677.
- [23] Jiang, W., and Chen, Z. (2013). "A collocation method based on reproducing kernel for a modified anomalous subdiffusion equation", *Numerical Methods for Partial Differential Equations*, 30(1), 289–300.
- [24] Kafash, B., Delavarkhalafi, A., and Karbassi, S. M., (2012). "Application of chebyshev polynomials to derive efficient algorithms for the solution of optimal control problems", *Scientia Iranica*, 19(3), 795-805.
- [25] Kameswaran, S., and Biegler, L. T., (2008). "Convergence rates for direct transcription of optimal control problems using collocation at Radau points", *Computational Optimization and Applications*, 41(1), 81–126.
- [26] Mehne, H. H., and Borzabadi, A. H. (2006). A numerical method for solving optimal control problems using state parametrization. *Numerical Algorithms*, 42(2), 165–169.
- [27] Mohammadi, M., and Mokhtari, R. (2011). "Solving the generalized regularized long wave equation on the basis of a reproducing kernel space", *Journal of Computational and Applied Mathematics*, 235(14), 4003–4014.
- [28] Momani, S., Abu Arqub, O., Hayat, T., and Al-Sulami, H. (2014). A computational method for solving periodic boundary value problems for integro-differential equations of Fredholm–Volterra type. *Applied Mathematics and Computation*, 240, 229–239.

- [29] Nemati, A., Alizadeh, A. and F. Soltanian, F., (2020). "Solution of fractional optimal control problems with noise function using the Bernstein functions", *Control and Optimization in Applied Mathematics*, 4(1), 37-51.
- [30] Nezhadhossein, S., (2017). "Haar matrix equations for solving time-variant linear-quadratic optimal control problems", *Control and Optimization in Applied Mathematics*, 2(2), 1-14.
- [31] Pinch, E.R., (1993). "Optimal control and calculus of variations", Oxford University Press.
- [32] Saberi Nik, H., and Effati, S. (2014). An approximate method for solving a class of nonlinear optimal control problems, *Optimal Control Applications and Methods*, 35, 324-339.
- [33] Saberi Nik, S. Effati, H., Mostafa, S. S., and Shirazian, M., (2014). Spectral homotopy analysis method and its convergence for solving a class of nonlinear optimal control problems, *Numerical Algorithms*, 65, 171-194.
- [34] Saberi Nik, H., Effati, S., and Yildirim, A. (2012). "Solution of linear optimal control systems by differential transform method", *Neural Computing and Applications*, 23(5), 1311-1317.
- [35] Salim, M. S. (1994). "Numerical studies for optimal control problems and its applications", Ph.D Thesis, Assiut University, Assiut, Egypt.
- [36] Shirazian, M., and Effati, S. (2012). Solving a class of nonlinear optimal control problems via He's variational iteration method. *International Journal of Control, Automation and Systems*, 10(2), 249-256. <https://doi.org/10.1007/s12555-012-0205-z>
- [37] Vahdati, S., Fardi, M., and Ghasemi, M. (2018). "Option pricing using a computational method based on reproducing kernel", *Journal of Computational and Applied Mathematics*, 328, 252-266.
- [38] Vlassenbroeck, J., van Dooren, R. (1988). "A Chebyshev technique for solving nonlinear optimal control problems", *IEEE Transactions on Automatic Control*, 33(4), 333-340.
- [39] Wang, Y., Du, M., Tan, F., Li, Z., and Nie, T. (2013). "Using reproducing kernel for solving a class of fractional partial differential equation with non-classical conditions", *Applied Mathematics and Computation*, 219(11), 5918-5925.
- [40] Wei, S. M., Zefran, S. M., and DeCarlo, R. A. (2008). "Optimal control of robotic system with logical constraints: application to UAV path planning", *IEEE International Conference on Robotic and Automation*, Pasadena, 176-181.
- [41] Yousefi, S. A., Dehghan, M., and Lotfi, A., (2010). "Finding the optimal control of linear systems via He's variational iteration method", *International Journal of Computer Mathematics*, 87(5), 1042-1050.
- [42] Zarembo, S. (1907). "L'équation biharmonique et une classe remarquable de fonctions fondamentales harmoniques". *Bulletin International de l'Academie des Sciences de Cracovie*, 147-196.

**How to Cite this Article:**

Amini, A., (2022). “Optimal control problems: Convergence and error analysis in reproducing kernel Hilbert spaces”, *Control and Optimization in Applied Mathematics*, 6(2): 53-76. doi: 10.30473/coam.2022.59267.1164

**COPYRIGHTS**



© 2021 by the authors. Licensee PNU, Tehran, Iran. This article is an open access article distributed under the terms and conditions of the Creative Commons Attribution 4.0 International (CC BY4.0) (<http://creativecommons.org/licenses/by/4.0>)





Payame Noor University



Control and Optimization in Applied Mathematics (COAM)

Vol. 6, No. 2, Summer-Autumn 2021 (79-96), ©2016 Payame Noor University, Iran

DOI: [10.30473/COAM.2022.61195.1181](https://doi.org/10.30473/COAM.2022.61195.1181) (Cited this article)

## Research Article

# On Grey Graphs and their Applications in Optimization

Mohammad Hamidi<sup>1,\*</sup> , Kamal Norouzi<sup>2</sup>, Akbar Rezaei<sup>3</sup>

<sup>1,2,3</sup>Department of Mathematics, Payame Noor University (PNU),  
P.O. Box. 19395-4697, Tehran, Iran.

**Received:** October 10, 2021; **Accepted:** March 17, 2022.

**Abstract.** In this research, we use averages and relative measures of interval grey numbers to introduce *grey vertices*, *grey edges*, and *grey graphs* (*graphs are based on interval grey numbers*). To do so, we design a grey graph based on a *graph* (as the underlying graph). Also, we find a relation between grey vertices and grey edges of a grey graph. The primary method used in this research is based on linear inequalities related to grey vertices and grey edges. We find some necessary and sufficient conditions on the *grey vertex* (as *(non-)discrete grey vertices*) connectivity of grey graphs based on interval grey numbers and *linear inequality systems*. The paper includes implications for the development of *(non-)weighted graphs*, and the modeling of uncertainty problems by grey vertices, grey edges, and their relations in a *grey model* as a grey graph. As a weighted graph, a fuzzy graph is a vital graph that has some applications in the real world, but with changes in conditions, it loses its efficiency. On the other hand, the efficiency of a grey graph is stable under changes in the conditions. So, grey graphs cover the weaknesses of fuzzy graphs. The new conception of *grey graphs based on grey numbers* is introduced in this study. We propose an optimization method that can be applied for grey numbers in an extension of graphs, and apply it for grey numbers in the real world, especially for optimization problems and via grey graphs.

**Keywords.** (Interval) Grey number, Polar position, Optimization, Grey graph, Grey vertex, Grey edge.

**MSC.** 05C35; 05C78.

---

\* Corresponding author

m.hamidi@pnu.ac.ir, k.norouzi@student.pnu.ac.ir, rezaei@pnu.ac.ir  
<http://mathco.journals.pnu.ac.ir>

## 1 Introduction

As an essential approach to the study of uncertainty, *grey system theory* provides applied models for systems with both known and unknown data. Today, the theory has found many critical applications [6]. The introduction of grey systems was inspired by the *vagueness* of real-world data. Although fuzzy sets or rough sets have also been applied in the study of ambiguity or incompleteness of information, grey systems and fuzzy sets provide entirely different representations, and there is a fundamental difference between grey numbers and fuzzy subsets.

Recently, some researchers have studied grey systems and their subsystems known as *interval grey numbers*. Several types of interval grey numbers exist; for instance, according to Lin et al. [10, 11], a grey number is a number that belongs to a known range, but its exact value is unknown. Moreover, a grey number according to Yang et al. [18], is a number for which upper bound and lower bound are specified, whose exact position is unknown within the specified bounds.

In some other studies, interval grey numbers such as black and white numbers have been defined. Recall that a *black number* is a number for which one of the following conditions is satisfied.

- The number has neither an upper limit nor a lower limit.
- The upper limit and lower limit of the number are grey numbers.

Also, a number whose upper limit is equal to its lower limit is a *white number*.

Further details on grey numbers can be found in [1, 8, 12, 13, 19, 20]. To extend grey systems, some researchers studied grey (logical) algebraic systems and introduced some operations on grey algebraic systems and interval grey numbers. These include [3, 4, 5, 15, 16].

In general, complex systems are made of several interacting elements, and it is accordingly natural to associate a node to each element and a link to each interaction, which yields to a graph. As a result, graph theory is an important tool in modeling that enables us to utilize the rich information that lies in complex network structures, including food webs, scientific citations, social networks, communication networks, company links in a stock portfolio, the internet, and the world wide web. We refer the reader to [2] and [7] for instances of research carried out in this regard.

Another application of graph theory is in data structures, where data is transformed into information. For example, it is possible to use graph theory to provide a nonlinear representation of data in memory. Also, a graph and its adjacency matrix can represent the arbitrary relationships among data. Recently, graph theory has been combined with fuzzy subsets and neutrosophic subsets. The resulting techniques have found many applications in the real world. See [9] and [17] for more details.

In the present research, we introduce grey graphs as graphs that are supported by interval grey numbers. Indeed, we use interval grey numbers to define the notions of grey vertex and grey edge. Also, we extend them to graphs based on the relations between grey vertices and grey edges. The main motivation of this system comes from fuzzy vertices and fuzzy edges but in the different form of an (interval-valued) fuzzy graph.



Since there is a fundamental difference between grey numbers and fuzzy subsets, we find that graphs based on interval grey numbers are different from (interval-valued) fuzzy graphs. We try to find some results for equivalence conditions of connected vertices and one-valued edges. The solutions of linear inequalities play a crucial role in our work on the relation between grey vertices and grey edges. So, we find some algorithms for graphs based on interval grey numbers. Section 2 is devoted to reviewing those results and definitions that will be needed in the following sections. In Section 3, we present the novel concept of a grey graph and prove some of its properties. Finally, in Section 4, we present some applications of our results in the real world.

## 2 Notations and Preliminaries

This section is devoted to a review of those results and definitions that will be needed in what follows.

**Definition 1.** [21] Let  $U$  be an arbitrary set. A fuzzy subset of  $U$  is a set  $F = \{(x, \mu_F(x)) : x \in U\}$ , where  $\mu_F : U \rightarrow [0, 1]$  as the membership function of  $F$  and  $\mu_F(x)$  represents the grade of belongingness of  $x$  into  $F$ .

**Definition 2.** [14] Assume  $V$  is an arbitrary set,  $x, y \in V$ ,  $\sigma : V \rightarrow [0, 1]$  and  $\mu : V \times V \rightarrow [0, 1]$ , where  $\mu(x, y) \leq \sigma(x) \wedge \sigma(y)$ . Then,  $G = (V, \sigma, \mu)$  is a fuzzy graph,  $\sigma$  is as the fuzzy vertex set, and  $\mu$  is as the fuzzy edge set of  $G$ .

**Definition 3.** [3] Consider a universal set  $U$ ,  $\Omega \subseteq \mathbb{R}$  and  $a \in U$ . A grey number is a number for which upper and lower bounds are specified, but whose exact position is unknown within the specified bounds. A discrete grey number is one for which a countable number of potential values is known. On the other hand, a continuous grey number is one which has the potential to take any value within an interval. A grey number expressed as  $(a^\pm \in [a^-, a^+], a^- \leq a^+)$  is known as an interval grey number, where  $[a^-, a^+] = \{s \mid a^- \leq s \leq a^+\}$ ,  $t$  is an information,  $a^\pm$  is a grey number and,  $a^-$  and  $a^+$  denote the lower and upper limits of the information. If  $a^\pm \in [a^-, +\infty)$ , we call it a lower-limit grey number, we refer to  $a^\pm \in (-\infty, a^+]$  as an upper-limit grey number, and we call  $a^\pm \in (-\infty, +\infty)$  a black number (that is, a number for which neither the exact value nor the range is known). Finally, a one-valued number  $a$  is one for which  $a^- = a^+$  (that is, it is an exact value).

## 3 Graphs Based on Grey Numbers

The goal of this section is to define the notions of grey number-based vertex set (or grey vertex), grey number-based edge set (or grey edge), and grey number-based graph.

From now on, we consider  $T_{min}(x, y) = \min\{x, y\}$  and  $T_{pr}(x, y) = xy$ , where  $x, y \in \Omega \subseteq \mathbb{R}$ .

**Definition 4.** Assume  $\Omega = [a, b]$  is a universe,  $\mu(\Omega) = b - a$  and  $G^\pm = (V, E)$  is a graph. Given  $xy \in E$ , define  $\mu^-(xy) = T_{\min}(g^\circ(x^\pm), g^\circ(y^\pm))$  and  $\mu^+(xy) = T_{\min}(|Av(x^\pm)|, |Av(y^\pm)|)$ , where  $Av(x^\pm) = \frac{x^+ + x^-}{2}$  and  $g^\circ(x^\pm) = \frac{x^+ - x^-}{b - a}$  denote the *average* and *relative measure* of the *grey number*  $x^\pm$ , respectively. Take

$$\sigma^\pm = \{x^\pm \in [\sigma^-(x), \sigma^+(x)] : x \in V\}, \mu^\pm = \{(xy)^\pm \in [\mu^-(xy), \mu^+(xy)] : xy \in E\}$$

and for all  $x, y \in V$ ,  $x^\pm, y^\pm$  and  $(xy)^\pm$  are *grey numbers*.

An algebraic structure  $G = (\Omega, \sigma^\pm, \mu^\pm)$  is a *grey number-based graph* on  $G^\pm$  (or more briefly, a *grey graph*), if for all  $xy \in E$ ,  $\mu^-(xy) \leq \mu^+(xy)$ . If  $\mu^-(xy) = \mu^+(xy) = 0$ , we say that no link exists between the vertices  $x^\pm$  and  $y^\pm$ . We call  $\sigma^\pm$  the set of *grey number-based vertices* or *grey vertices*, and we refer to  $\mu^\pm$  as the set of *grey number-based edges* or *grey edges* of  $G$ .

In what follows, we present an example of a grey number-based graph.

**Example 1.** Let  $\Omega = [0, 1000]$  and consider the cycle graph  $C_4$ . Then,  $G = (\Omega, \sigma^\pm, \mu^\pm)$  is a grey number-based graph on  $C_4$ , depicted in Figure 1. Computations show that

$$g^\circ(a^\pm) = \frac{2-1}{1000}, g^\circ(b^\pm) = \frac{7-2}{1000}, |Av(a^\pm)| = \frac{1+2}{2} \text{ and } |Av(b^\pm)| = \frac{7+2}{2}.$$

Thus,

$$\begin{aligned} \mu^-(ab) &= T_{\min}(g^\circ(a^\pm), g^\circ(b^\pm)) \\ &= T_{\min}\left(\frac{1}{1000}, \frac{5}{1000}\right) \\ &= \frac{1}{1000} \mu^+(ab) \\ &= T_{\min}(|Av(a^\pm)|, |Av(b^\pm)|) \\ &= T_{\min}\left(\frac{3}{2}, \frac{9}{2}\right) \\ &= \frac{3}{2}. \end{aligned}$$

Therefore,

$$(ab)^\pm \in [\mu^-(ab), \mu^+(ab)] = \left[\frac{1}{1000}, \frac{3}{2}\right].$$

By a similar argument,

$$(ac)^\pm \in [\mu^-(ac), \mu^+(ac)] = \left[\frac{1}{1000}, \frac{3}{2}\right], (bd)^\pm \in [\mu^-(bd), \mu^+(bd)] = \left[\frac{1}{1000}, \frac{7}{2}\right],$$

and

$$(cd)^\pm \in [\mu^-(cd), \mu^+(cd)] = \left[\frac{4}{1000}, \frac{9}{2}\right].$$

From now on, let  $\Omega$  be a universe and consider a graph  $G^\pm = (V, E)$ . Also, let  $xy \in E$  and  $G = (\Omega, \sigma^\pm, \mu^\pm)$  be a grey graph.

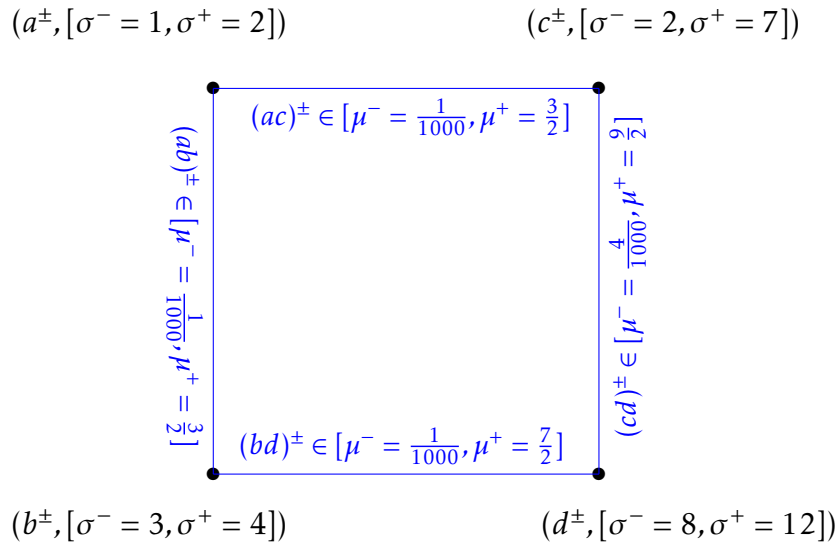


**Figure 1:** The grey graph  $G = (\Omega, \sigma^\pm, \mu^\pm)$  on  $C_4$ .

**Theorem 1.** *The following statements are true.*

- (i) If  $g^\circ(x^\pm) > |Av(x^\pm)|$ , then  $0 \leq |Av(x^\pm)| \leq 1$ .
- (ii)  $\mu(\Omega) < \frac{\mu(x^\pm)}{|Av(x^\pm)|} \Leftrightarrow g^\circ(x^\pm) > |Av(x^\pm)|$ .
- (iii)  $(|x^-| < x^+ \text{ and } g^\circ(x^\pm) > |Av(x^\pm)|) \Leftrightarrow \mu(\Omega) < \frac{\mu(x^\pm)}{|Av(x^\pm)|}$ .
- (iv) If  $|Av(x^\pm)| \geq 1$ , then  $g^\circ(x^\pm) \leq |Av(x^\pm)|$ .

*Proof.* Parts (i), (ii) and (iii) can be easily proved.

Also, (iv) can be deduced from (i). □

**Theorem 2.** *If  $\mu^\pm$  is one-valued, then one of the following statements is true.*

- (i)  $g^\circ(x^\pm) \leq g^\circ(y^\pm)$  and  $|Av(x^\pm)| \leq |Av(y^\pm)|$ .
- (ii)  $g^\circ(y^\pm) \leq g^\circ(x^\pm)$  and  $|Av(x^\pm)| \leq |Av(y^\pm)|$ .
- (iii)  $g^\circ(x^\pm) \leq g^\circ(y^\pm)$  and  $|Av(y^\pm)| \leq |Av(x^\pm)|$ .
- (iv)  $g^\circ(y^\pm) \leq g^\circ(x^\pm)$  and  $|Av(y^\pm)| \leq |Av(x^\pm)|$ .

*Proof.* Let  $xy \in E$ . Since  $\mu^\pm$  is one-valued, there is  $t \in \mathbb{R}^+$  that  $[\mu^-(xy), \mu^+(xy)] = \{t\}$ . Let us denote this set by  $t$  for the sake of simplicity. Thus,  $\mu^-(xy) = t = \mu^+(xy)$ .

Now,  $\mu^-(xy) = t$  implies  $T_{min}(g^\circ(x^\pm), g^\circ(y^\pm)) = t$ , and so  $g^\circ(x^\pm) = t < g^\circ(y^\pm)$ ,  $g^\circ(y^\pm) = t < g^\circ(x^\pm)$  or  $g^\circ(x^\pm) = t = g^\circ(y^\pm)$ . In addition,  $\mu^+(xy) = t$  implies  $T_{min}(|Av(x^\pm)|, |Av(y^\pm)|) = t$ , and so  $|Av(x^\pm)| = t < |Av(y^\pm)|$ ,  $|Av(y^\pm)| = t < |Av(x^\pm)|$  or  $|Av(y^\pm)| = t = |Av(x^\pm)|$ .

Therefore,

$$\begin{aligned}
 & (g^\circ(x^\pm) = t \leq g^\circ(y^\pm) \text{ and } |Av(x^\pm)| = t \leq |Av(y^\pm)|), \\
 & (g^\circ(y^\pm) = t \leq g^\circ(x^\pm) \text{ and } |Av(x^\pm)| = t \leq |Av(y^\pm)|), \\
 & (g^\circ(x^\pm) = t \leq g^\circ(y^\pm) \text{ and } |Av(y^\pm)| = t \leq |Av(x^\pm)|),
 \end{aligned}$$

or

$$(g^\circ(y^\pm) = t \leq g^\circ(x^\pm) \text{ and } |Av(y^\pm)| = t \leq |Av(x^\pm)|).$$

□

In the following example, we show that the converse of Theorem 2 may not be true necessarily.

**Example 2.** Let  $G = (\Omega, \sigma^\pm, \mu^\pm)$  be the grey graph on graph  $C_3$  that is depicted in Figure 2. Computations show that  $g^\circ(a^\pm) \leq g^\circ(b^\pm)$  and  $|Av(a^\pm)| \leq |Av(b^\pm)|$ , while  $(ab)^\pm$  is not one-valued.

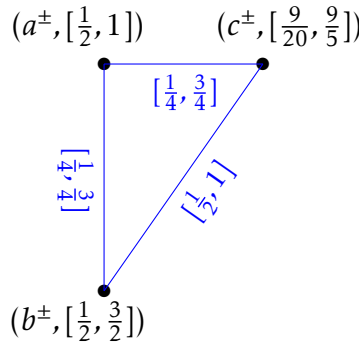


**Figure 2:** The grey graph  $G = (\Omega, \sigma^\pm, \mu^\pm)$  on  $C_3$ .

**Definition 5.** Let  $\Omega$  be a universe and  $x^\pm \subseteq \Omega$ . Then,  $x^\pm$  is called 1-polar if  $T_{pr}(x^-, x^+) \geq 0$ . Figures 3 and 4 show (non-)negative-polar and (non-)positive-polar, respectively.

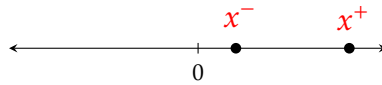


**Figure 3:** Position of the grey number  $x^\pm$  on the real line ((non-)negative-polar).

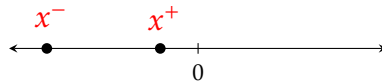


**Figure 4:** Position of the grey number  $x^\pm$  on the real line ((non-)positive-polar).

Based on Theorem 2, we need to solve the linear inequalities  $(g^\circ(x^\pm) \leq g^\circ(y^\pm) \text{ and } |Av(x^\pm)| \leq |Av(y^\pm)|)$ ,  $(g^\circ(y^\pm) \leq g^\circ(x^\pm) \text{ and } |Av(x^\pm)| \leq |Av(y^\pm)|)$ ,  $(g^\circ(x^\pm) \leq g^\circ(y^\pm) \text{ and } |Av(y^\pm)| \leq |Av(x^\pm)|)$ , and  $(g^\circ(y^\pm) \leq g^\circ(x^\pm) \text{ and } |Av(y^\pm)| \leq |Av(x^\pm)|)$ .

We consider the three cases  $\mu(\Omega) < 2$ ,  $\mu(\Omega) = 2$  and  $\mu(\Omega) > 2$ .

**Theorem 3.** If  $\mu(\Omega) = 2$  and  $\mu^\pm$  is non-zero and one-valued, then one of the following statements is true.

- (i)  $(x^+ = 0, y^- - y^+ \leq x^- \text{ and } -|y^- + y^+| \leq x^- \leq 0)$  or  $(x^- = 0, x^+ \leq y^+ - y^- \text{ and } 0 \leq x^+ \leq |y^+ + y^-|)$ .
- (ii)  $(|x^+ + x^-| \leq |y^+ + y^-| \text{ and } x^- \leq 0)$  or  $(y^+ + x^- - y^- \leq 0 \text{ and } |x^+ + x^-| \leq |y^+ + y^-|)$ .
- (iii)  $(y^- < 0 \text{ and } |y^+ + y^-| \leq |x^+ + x^-|)$  or  $(x^- - x^+ - y^- > 0 \text{ and } |y^+ + y^-| \leq |x^+ + x^-|)$ .
- (iv)  $(y^+ = 0, x^- - x^+ \leq y^- \text{ and } -|x^- + x^+| \leq y^- \leq 0)$  or  $(y^- = 0 \text{ and } y^+ \leq x^+ - x^- \text{ and } 0 \leq y^+ \leq |x^+ + x^-|)$ .

*Proof.* Let  $xy \in E$  and  $t \in \mathbb{R}$ . We use Theorem 2 in what follows.

(i) If  $g^\circ(x^\pm) \leq g^\circ(y^\pm)$  and  $|Av(x^\pm)| \leq |Av(y^\pm)|$ , then  $g^\circ(x^\pm) = |Av(x^\pm)|$ . Since  $\mu(\Omega) = 2$ ,  $x^- = 0$  or  $x^+ = 0$ . Also,  $g^\circ(x^\pm) \leq g^\circ(y^\pm)$  and  $|Av(x^\pm)| \leq |Av(y^\pm)|$  allow us to conclude that  $x^+ \leq (y^+ + x^-) - y^-$  and  $-(|y^+ + y^-| + x^-) \leq x^+ \leq (|y^+ + y^-|) - x^-$ . Thus, for  $\mu(\Omega) = 2$ ,

$$\begin{aligned} & (x^+ = 0, y^- - y^+ \leq x^- \text{ and } -|y^- + y^+| \leq x^- \leq |y^+ + y^-|) \text{ or} \\ & (x^- = 0 \text{ and } x^+ \leq y^+ - y^- \text{ and } 0 \leq x^+ \leq |y^+ + y^-|). \end{aligned}$$

(ii) If  $(g^\circ(y^\pm) \leq g^\circ(x^\pm) \text{ and } |Av(x^\pm)| \leq |Av(y^\pm)|)$ , then  $g^\circ(y^\pm) = |Av(x^\pm)|$ . Since  $\mu(\Omega) = 2$ ,  $x^+ = y^+ - (x^- + y^-)$  or  $x^+ = y^- - (x^- + y^+)$ . Also,  $g^\circ(y^\pm) \leq g^\circ(x^\pm)$  and  $|Av(x^\pm)| \leq |Av(y^\pm)|$  allow us to conclude that  $x^+ > (y^+ + x^-) - y^-$  and  $-(|y^+ + y^-| + x^-) \leq x^+ \leq (|y^+ + y^-|) - x^-$ . Thus, for  $\mu(\Omega) = 2$ ,

$$\begin{aligned} & (|x^+ + x^-| \leq |y^+ + y^-| \text{ and } x^- \leq 0) \text{ or} \\ & (y^+ + x^- - y^- \leq 0 \text{ and } |x^+ + x^-| \leq |y^+ + y^-|). \end{aligned}$$

(iii) If  $g^\circ(x^\pm) \leq g^\circ(y^\pm)$  and  $|Av(y^\pm)| \leq |Av(x^\pm)|$ , then  $g^\circ(x^\pm) = |Av(y^\pm)|$ . Since  $\mu(\Omega) = 2$ ,  $y^+ = x^+ - x^- - y^-$  or  $y^+ = x^- - x^+ - y^-$ . Also,  $g^\circ(x^\pm) \leq g^\circ(y^\pm)$  and  $|Av(y^\pm)| \leq |Av(x^\pm)|$  allow us to conclude that  $y^+ > (x^+ - x^-) + y^-$  and  $-(|x^+ + x^-| + y^-) \leq y^+ \leq (|x^+ + x^-|) - y^-$ . Thus, for  $\mu(\Omega) = 2$ ,

$$\begin{aligned} & (y^- \leq 0 \text{ and } |y^+ + y^-| \leq |x^+ + x^-|) \text{ or} \\ & (x^- - x^+ - y^- > 0 \text{ and } |y^+ + y^-| \leq |x^+ + x^-|). \end{aligned}$$

(iv) If  $g^\circ(y^\pm) \leq g^\circ(x^\pm)$  and  $|Av(y^\pm)| \leq |Av(x^\pm)|$ , then  $g^\circ(y^\pm) = |Av(y^\pm)|$ . Since  $\mu(\Omega) = 2$ ,  $y^- = 0$  or  $y^+ = 0$ . Also,  $g^\circ(y^\pm) \leq g^\circ(x^\pm)$  and  $|Av(y^\pm)| \leq |Av(x^\pm)|$  allow us to conclude that  $y^+ \leq (x^+ + y^-) - x^-$  and  $-(|x^+ + x^-| + y^-) \leq y^+ \leq (|x^+ + x^-|) - y^-$ . Thus, for  $\mu(\Omega) = 2$ ,

$$\begin{aligned} & (y^+ = 0, x^- - x^+ \leq y^- \text{ and } -|x^- + x^+| \leq y^- \leq |x^+ + x^-|) \text{ or} \\ & (y^- = 0 \text{ and } y^+ \leq x^+ - x^- \text{ and } 0 \leq y^+ \leq |x^+ + x^-|). \end{aligned}$$

□

**Example 3.** (i) Let  $\Omega = [-1, 1]$  and consider the cycle graph  $C_3$ . Then,  $G = (\Omega, \sigma^\pm, \mu^\pm)$  is a grey graph on the graph  $C_3$ , depicted in Figure 5. Clearly,  $(c^- = 0$  and  $c^+ \leq a^+ - a^-$  and  $0 \leq c^+ \leq |a^+ + a^-|)$ , and  $(ac)^\pm$  is one-valued.

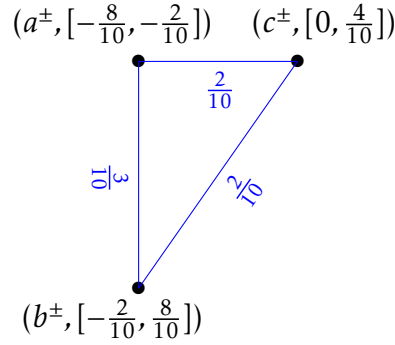


**Figure 5:** The grey graph  $G = (\Omega, \sigma^\pm, \mu^\pm)$  on  $C_3$ .

(ii) Let  $\Omega = [-2, 0]$  and consider the cycle graph  $C_3$ . Then,  $G = (\Omega, \sigma^\pm, \mu^\pm)$  is a grey graph on the graph  $C_3$ , depicted in Figure 6. Clearly,  $b^- \leq 0$  and  $a^+ - a^- \leq |a^+ + a^-|$ , while  $(ab)^\pm$  is not one-valued. This reveals that the converse of Theorem 3(iii) may not be true necessarily.

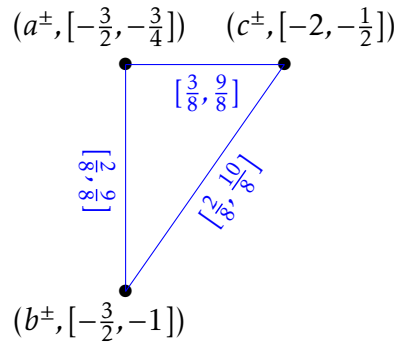


**Figure 6:** The grey graph  $G = (\Omega, \sigma^\pm, \mu^\pm)$  on  $C_3$ .

**Theorem 4.** If  $\mu(\Omega) = 2$  and one of the following statements is true, then  $\mu^\pm$  is non-zero and one-valued.

- (i)  $(x^+ = 0, y^- - y^+ \leq x^-$  and  $-|y^- + y^+| \leq x^- \leq 0)$  or  $(x^- = 0$  and  $x^+ \leq y^+ - y^-$  and  $0 \leq x^+ \leq |y^+ + y^-|)$ .
- (ii)  $(x^+ = y^+ - (x^- + y^-)$  and  $x^- \leq 0)$  or  $(x^+ = y^- - (x^- + y^+), y^+ + x^- - y^- \leq 0$  and (either  $y^\pm$  is (non) positive-polar or is (non) negative-polar)).
- (iii)  $(y^+ = 0, x^- - x^+ \leq y^-$  and  $-|x^- + x^+| \leq y^- \leq 0)$  or  $(y^- = 0$  and  $y^+ \leq x^+ - x^-$  and  $0 \leq y^+ \leq |x^+ + x^-|)$ .

*Proof.* The proof is similar to that of Theorem 3.  $\square$

**Theorem 5.** If  $0 < \mu(\Omega) < 2$  and  $\mu^\pm$  is non-zero and one-valued, then one of the following statements is true.

- (i)  $(x^+ = (\frac{p}{q})x^-, x^- \leq \frac{q\mu(y^\pm)}{2\mu(\Omega)}$  and  $\frac{-q|Av(y^\pm)|}{2} \leq x^- \leq \frac{q|Av(y^\pm)|}{2})$  or  
 $(x^+ = (\frac{q}{p})x^-, x^- \geq \frac{-p\mu(y^\pm)}{2\mu(\Omega)}$  and  $-\frac{p|Av(y^\pm)|}{2} \leq x^- \leq \frac{p|Av(y^\pm)|}{2})$ .
- (ii)  $(y^+ = (\frac{p}{q})y^-, y^- \leq \frac{q\mu(x^\pm)}{2\mu(\Omega)}$  and  $\frac{-q|Av(x^\pm)|}{2} \leq y^- \leq \frac{q|Av(x^\pm)|}{2})$  or  
 $(y^+ = (\frac{q}{p})y^-, y^- \geq \frac{(p)(-\mu(x^\pm))}{2\mu(\Omega)}$  and  $\frac{-p|Av(x^\pm)|}{2} \leq y^- \leq \frac{p|Av(x^\pm)|}{2})$ .

Here,  $p = 2 + \mu(\Omega)$  and  $q = 2 - \mu(\Omega)$ .

*Proof.* Let  $xy \in E$  and  $t \in \mathbb{R}$ . We use Theorem 2 in what follows.

(i) If  $g^\circ(x^\pm) = t \leq g^\circ(y^\pm)$  and  $|Av(x^\pm)| = t \leq |Av(y^\pm)|$ , then

$$g^\circ(x^\pm) = |Av(x^\pm)|, g^\circ(x^\pm) \leq g^\circ(y^\pm) \text{ and } |Av(x^\pm)| \leq |Av(y^\pm)|.$$

Since  $\mu(\Omega) \neq 2$ ,  $g^\circ(x^\pm) = |Av(x^\pm)|$  implies  $x^+ = (\frac{2 + \mu(\Omega)}{2 - \mu(\Omega)})x^-$  or  $x^+ = (\frac{2 - \mu(\Omega)}{2 + \mu(\Omega)})x^-$ . Also,  $g^\circ(x^\pm) \leq g^\circ(y^\pm)$  and  $|Av(x^\pm)| \leq |Av(y^\pm)|$  allow us to conclude that

$$x^+ \leq (y^+ + x^-) - y^- \text{ and } -(|y^+ + y^-| + x^-) \leq x^+ \leq (|y^+ + y^-|) - x^-.$$

Thus, for  $\mu(\Omega) < 2$ ,

$$\begin{aligned} (x^+ = (\frac{2 + \mu(\Omega)}{2 - \mu(\Omega)})x^-, x^- \leq \frac{(2 - \mu(\Omega))(y^+ - y^-)}{2\mu(\Omega)} \text{ and} \\ \frac{(2 - \mu(\Omega))(|y^+ + y^-|)}{4} \leq x^- \leq \frac{(\mu(\Omega) - 2)(|y^+ + y^-|)}{4}) \text{ or} \\ (x^+ = (\frac{2 - \mu(\Omega)}{2 + \mu(\Omega)})x^-, x^- \geq \frac{(2 + \mu(\Omega))(y^- - y^+)}{2\mu(\Omega)} \text{ and} \\ \frac{(2 + \mu(\Omega))(|y^+ + y^-|)}{-4} \leq x^- \leq \frac{(\mu(\Omega) + 2)(|y^+ + y^-|)}{4}). \end{aligned}$$

(ii) If  $g^\circ(y^\pm) \leq g^\circ(x^\pm)$  and  $|Av(y^\pm)| \leq |Av(x^\pm)|$ , then  $g^\circ(y^\pm) = |Av(y^\pm)|$ . Since  $\mu(\Omega) \neq 2$ ,  $g^\circ(y^\pm) = |Av(y^\pm)|$  implies  $y^+ = (\frac{2 + \mu(\Omega)}{2 - \mu(\Omega)})y^-$  or  $y^+ = (\frac{2 - \mu(\Omega)}{2 + \mu(\Omega)})y^-$ . In addition,  $g^\circ(y^\pm) \leq g^\circ(x^\pm)$  and  $|Av(y^\pm)| \leq |Av(x^\pm)|$  allow us to conclude that

$$y^+ \leq (x^+ + y^-) - x^- \text{ and } -(|x^+ + x^-| + y^-) \leq y^+ \leq (|x^+ + x^-|) - y^-.$$

Thus, for  $\mu(\Omega) < 2$ ,

$$(y^+ = (\frac{2 + \mu(\Omega)}{2 - \mu(\Omega)})y^-, y^- \leq \frac{(2 - \mu(\Omega))(x^+ - x^-)}{2\mu(\Omega)} \text{ and}$$

$$\begin{aligned} \frac{(2 - \mu(\Omega))(|x^+ + x^-|)}{-4} \leq y^- \leq \frac{(-\mu(\Omega) + 2)(|x^+ + x^-|)}{4} \quad \text{or} \\ \left( y^+ = \left( \frac{2 - \mu(\Omega)}{2 + \mu(\Omega)} \right) y^-, y^- \geq \frac{(2 + \mu(\Omega))(x^- - x^+)}{2\mu(\Omega)} \right) \quad \text{and} \\ \frac{(2 + \mu(\Omega))(|x^+ + x^-|)}{-4} \leq y^- \leq \frac{(\mu(\Omega) + 2)(|x^+ + x^-|)}{4}. \end{aligned}$$

□

**Theorem 6.** If  $\mu(\Omega) \neq 2$  and  $\mu^\pm$  is non-zero and one-valued, then one of the following statements is true.

- (i)  $(q\mu(y^\pm) - 2\mu(\Omega)x^- \geq 0)$  and  $-\mu(\Omega)|Av(y^\pm)| \leq (\mu(y^\pm)) \leq \mu(\Omega)|Av(y^\pm)|$  or  $(-p\mu(y^\pm) - 2\mu(\Omega)x^- \geq 0)$  and  $-\mu(\Omega)|Av(y^\pm)| \leq \mu(y^\pm) \leq \mu(\Omega)|Av(y^\pm)|$ .
- (ii)  $(y^+ = (\frac{2\mu(x^\pm) - y^- \mu(\Omega)}{\mu(\Omega)}, q\mu(x^\pm) - 2\mu(\Omega)y^- \geq 0)$  and  $-\mu(\Omega)|Av(x^\pm)| \leq \mu(x^\pm) \leq \mu(\Omega)|Av(x^\pm)|$  or  $(y^+ = (\frac{-2\mu(x^\pm) - y^- \mu(\Omega)}{\mu(\Omega)}, p\mu(x^\pm) + 2\mu(\Omega)y^- \leq 0)$  and  $-\mu(\Omega)|Av(x^\pm)| \leq \mu(x^\pm) \leq \mu(\Omega)|Av(x^\pm)|$ .

Here,  $q = 2 - \mu(\Omega)$  and  $p = 2 + \mu(\Omega)$ .

*Proof.* The proof is similar to that of Theorem 5. □

In the following example, we observe that the converse of Theorem 6 may not be true necessarily.

**Example 4.** Let  $\Omega = [-2, 3]$  and consider the cycle graph  $C_3$ . Then,  $G = (\Omega, \sigma^\pm, \mu^\pm)$  is a grey graph on the graph  $C_3$ , depicted in Figure 7.

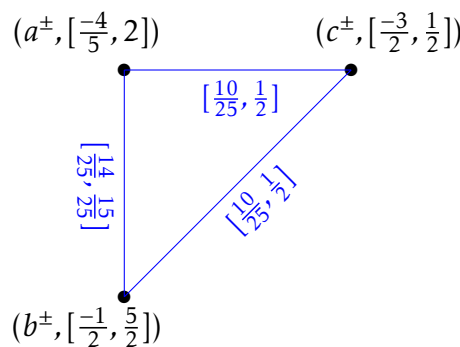


**Figure 7:** The grey graph  $G = (\Omega, \sigma^\pm, \mu^\pm)$  on  $C_3$ .

Computations show that  $(-3\mu(c^\pm) - 10a^- > 0)$  and  $-5|Av(c^\pm)| \leq \mu(c^\pm) \leq 5|Av(c^\pm)|$ , while  $(ca)^\pm$  is not one-valued.



**Theorem 7.** Let  $\Omega$  be a universe. Consider a graph  $G^\pm = (V, E)$ . Also, let  $xy \in E$  and  $G = (\Omega, \sigma^\pm, \mu^\pm)$  be a grey graph with  $\mu(\Omega) > 2$ . Then,  $\mu^\pm$  is non-zero and one-valued if and only if one of the following statements is true.

$$(i) \left( x^+ = \left(\frac{p}{q}\right)x^-, x^- \geq \frac{q\mu(y^\pm)}{2\mu(\Omega)} \text{ and } \frac{q|Av(y^\pm)|}{2} \leq x^- \leq \frac{-q|Av(y^\pm)|}{2} \right) \text{ or}$$

$$\left( x^+ = \left(\frac{q}{p}\right)x^-, x^- \geq \frac{(p)(-\mu(y^\pm))}{2\mu(\Omega)} \text{ and } \frac{p|Av(y^\pm)|}{-2} \leq x^- \leq \frac{p|Av(y^\pm)|}{2} \right).$$

$$(ii) \left( y^+ = \left(\frac{p}{q}\right)y^-, y^- \geq \frac{q\mu(x^\pm)}{2\mu(\Omega)} \text{ and } \frac{q|Av(x^\pm)|}{2} \leq y^- \leq \frac{-q|Av(x^\pm)|}{2} \right) \text{ or}$$

$$\left( y^+ = \left(\frac{q}{p}\right)y^-, y^- \geq \frac{(p)(-\mu(x^\pm))}{2\mu(\Omega)} \text{ and } \frac{p|Av(x^\pm)|}{-2} \leq y^- \leq \frac{p|Av(x^\pm)|}{2} \right).$$

Here,  $q = 2 - \mu(\Omega)$  and  $p = 2 + \mu(\Omega)$ .

*Proof.* The proof is similar to that of Theorem 5. □

**Example 5.** Let  $\Omega = [0, 3]$  and consider the cycle graph  $C_3$ . Then  $G = (\Omega, \sigma^\pm, \mu^\pm)$  is a grey graph on the graph  $C_3$ , depicted in Figure 8. This example shows that, if one part of the conditions of Theorem 7 is not satisfied, then the property of being one-valued cannot be deduced.

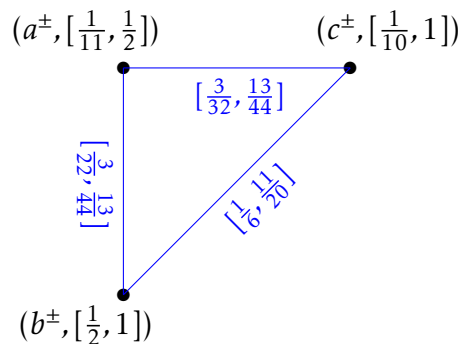


**Figure 8:** The grey graph  $G = (\Omega, \sigma^\pm, \mu^\pm)$  on  $C_3$ .

**Theorem 8.** Let  $\Omega$  be a universe. Consider a graph  $G^\pm = (V, E)$ . Also, let  $xy \in E$  and  $G = (\Omega, \sigma^\pm, \mu^\pm)$  be a grey graph. Then,  $\mu^\pm(xy)$  is zero and one-valued if and only if one of the following statements is true.

- (i)  $\{(x^\pm, [0, 0]), (y^\pm, [\alpha, \beta]) : \alpha, \beta \in \mathbb{R}\} \subseteq \sigma^\pm$ .
- (ii)  $\{(x^\pm, [\alpha, \alpha]), (y^\pm, [-\beta, \beta]) : \alpha, \beta \in \mathbb{R}\} \subseteq \sigma^\pm$ .
- (iii)  $\{(x^\pm, [-\alpha, \alpha]), (y^\pm, [\beta, \beta]) : \alpha, \beta \in \mathbb{R}\} \subseteq \sigma^\pm$ .
- (iii)  $\{(y^\pm, [0, 0]), (x^\pm, [\alpha, \beta]) : \alpha, \beta \in \mathbb{R}\} \subseteq \sigma^\pm$ .

*Proof.* Let  $xy \in E$ . Since  $[\mu^-(xy), \mu^+(xy)] = 0$ ,  $\mu^-(xy) = 0 = \mu^+(xy)$ . Now,  $\mu^-(xy) = 0$  implies  $T_{\min}(g^\circ(x^\pm), g^\circ(y^\pm)) = 0$ . Also, since  $\mu^-(xy) \geq 0$ ,  $g^\circ(x^\pm) = 0$  or  $g^\circ(y^\pm) = 0$ . In addition,  $\mu^+(xy) = 0$  implies  $T_{\min}(|Av(x^\pm)|, |Av(y^\pm)|) = 0$ , and since  $\mu^+(xy) \geq 0$ , we get  $|Av(x^\pm)| = 0$  or  $|Av(y^\pm)| = 0$ . Thus,  $(g^\circ(x^\pm) = 0 \text{ and } |Av(x^\pm)| = 0)$ ,  $(g^\circ(x^\pm) = 0 \text{ and } |Av(y^\pm)| = 0)$ ,  $(g^\circ(y^\pm) = 0 \text{ and } |Av(x^\pm)| = 0)$  or  $(g^\circ(y^\pm) = 0 \text{ and } |Av(y^\pm)| = 0)$ . Hence, by solving the above equations we get  $(x^+ = x^- \text{ and } x^+ = -x^-)$ ,  $(x^+ = x^- \text{ and } y^+ = -y^-)$ ,  $(y^+ = y^- \text{ and } x^+ = -x^-)$  or  $(y^+ = y^- \text{ and } y^+ = -y^-)$ .  $\square$

#### 4 Discrete Grey Vertices in Grey Graphs

In this section, we prove some results on discrete grey vertices in grey graphs.

**Definition 6.** Let  $\Omega$  be a universe and  $x^\pm \subseteq \Omega$ . Then,  $x^\pm$  is called *2-polar*, if  $T_{pr}(x^-, x^+) < 0$ , as shown in Figure 9.

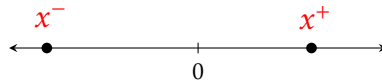


**Figure 9:** Position of the grey number  $x^\pm$  on the real line (2-polar).

**Proposition 1.** *The following statements are true.*

- (i) If  $\mu(\Omega) = 2$  and,  $x^\pm$  and  $y^\pm$  are 2-polar, then  $(xy)^\pm \notin \mu^\pm$ .
- (ii) If  $\mu(\Omega) < 2$ ,  $x^+ > (\frac{2 + \mu(\Omega)}{2 - \mu(\Omega)})x^-$  and  $y^+ > (\frac{2 + \mu(\Omega)}{2 - \mu(\Omega)})y^-$ , then  $(xy)^\pm \notin \mu^\pm$ .
- (iii) If  $Av(x^\pm) = 0$ , then for all  $xy \in E$ ,  $(xy)^\pm \notin \mu^\pm$ .
- (iv) If  $Av(x^\pm) \neq 0$  and  $g^\circ(x^\pm) \leq Av(x^\pm)$ , then for all  $xy \in E$ ,  $(xy)^\pm \in \mu^\pm$ .
- (v) If  $x^\pm$  is a non-zero and one-valued vertex, and  $y^\pm$  is a grey vertex, then for all  $xy \in E$ ,  
 $(xy)^\pm \in [0, T_{\min}(|x|, |Av(y^\pm)|)]$ .
- (vi) If  $y^\pm$  is a non-zero and one-valued vertex, and  $x^\pm$  is a grey vertex, then for all  $xy \in E$ ,  
 $(xy)^\pm \in [0, T_{\min}(|y|, |Av(x^\pm)|)]$ .
- (vii) If  $x^\pm, y^\pm$  are non-zero and one-valued vertices, then for all  $xy \in E$ ,  $(xy)^\pm \in [0, T_{\min}(|x|, |y|)]$ .

*Proof.* (i) Let  $xy \in E$ . Since  $x^\pm$  and  $y^\pm$  are 2-polar,

$$x^- - x^+ < x^- + x^+ < x^+ - x^- \text{ and } y^- - y^+ < y^- + y^+ < y^+ - y^-.$$

Then  $|x^- + x^+| < x^+ - x^-$ ,  $|y^- + y^+| < y^+ - y^-$  and using  $\mu(\Omega) = 2$ , we get

$$g^\circ(x^\pm) > |Av(x^\pm)|$$

and

$$g^\circ(y^\pm) > |Av(y^\pm)|.$$

Thus,  $T_{min}(g^\circ(x^\pm), g^\circ(y^\pm)) > T_{min}(|Av(x^\pm)|, |Av(y^\pm)|)$ , and so  $\mu^-(xy) > \mu^+(xy)$ , which means  $(xy)^\pm \notin \mu^\pm$ .

(ii) Let  $xy \in E$ . Since  $x^+ > (\frac{2+\mu(\Omega)}{2-\mu(\Omega)})x^-$  and  $y^+ > (\frac{2+\mu(\Omega)}{2-\mu(\Omega)})y^-$ , using  $\mu(\Omega) < 2$  we get

$$\frac{2(x^- - x^+)}{\mu(\Omega)} < x^- + x^+ < \frac{2(x^+ - x^-)}{\mu(\Omega)} \text{ and } \frac{2(y^- - y^+)}{\mu(\Omega)} < y^- + y^+ < \frac{2(y^+ - y^-)}{\mu(\Omega)}.$$

Then,

$$\frac{|x^- + x^+|}{2} < \frac{x^+ - x^-}{\mu(\Omega)}, \frac{|y^- + y^+|}{2} < \frac{y^+ - y^-}{\mu(\Omega)}.$$

So,  $g^\circ(x^\pm) > |Av(x^\pm)|$  and  $g^\circ(y^\pm) > |Av(y^\pm)|$ . Therefore,

$$T_{min}(g^\circ(x^\pm), g^\circ(y^\pm)) > T_{min}(|Av(x^\pm)|, |Av(y^\pm)|).$$

Thus,  $\mu^-(xy) > \mu^+(xy)$ , which means  $(xy)^\pm \notin \mu^\pm$ .

(iii) Let  $xy \in E$ . If  $x^\pm = 0$  is a one-valued number, then  $[\mu^-, \mu^+] = 0$  and so,  $(xy)^\pm \notin \mu^\pm$ . Let  $x^\pm \neq 0$ . Then  $Av(x^\pm) = 0$  implies  $x^+ = -x^- \neq 0$ . Using  $g^\circ(x^\pm) > 0$ , we conclude that  $[\mu^-, \mu^+] = \emptyset$ . So,  $(xy)^\pm \notin \mu^\pm$ .

(iv) Let  $xy \in E$ . Since  $g^\circ(x^\pm) \leq Av(x^\pm)$ , we get

$$T_{min}(g^\circ(x^\pm), g^\circ(y^\pm)) \leq T_{min}(|Av(x^\pm)|, |Av(y^\pm)|).$$

Thus,  $(xy)^\pm \in \mu^\pm$ .

(v) Let  $xy \in E$ . Since  $x^\pm$  is a non-zero and one-valued vertex, and  $y^\pm$  is a grey vertex, we get  $g^\circ(x^\pm) = 0$  and  $Av(x^\pm) = x$ . It follows that  $(xy)^\pm \in [0, T_{min}(|x|, |Av(y^\pm)|)]$ .

(vii) This immediately follows from (v) and (vi).  $\square$

**Theorem 9.** Let  $\Omega$  be a universe,  $\mu(\Omega) \leq 1$ , consider a graph  $G^\pm = (V, E)$ , and let  $xy \in E$ . If  $x^\pm$  and  $y^\pm$  are 2-polar, then  $(xy)^\pm \notin \mu^\pm$ .

*Proof.* Let  $xy \in E$ . Since  $x^- < 0 < x^+$ ,  $|x^+ - x^-| > |x^- + x^+|$ . Using  $\mu(\Omega) \leq 1$ , we get

$$g^\circ(x^\pm) = \frac{x^+ - x^-}{\mu(\Omega)} \geq (x^+ - x^-) > |x^- + x^+| > \left| \frac{x^- + x^+}{2} \right|.$$

Then,  $g^\circ(x^\pm) > |Av(x^\pm)|$ .

Similarly,  $g^\circ(y^\pm) > |Av(y^\pm)|$ , since  $y^\pm$  is 2-polar. Thus,  $\mu^-(xy) > \mu^+(xy)$  and so,  $(xy)^\pm \notin \mu^\pm$ .  $\square$

**Example 6.** Let  $G^\pm = (V, E)$  be the path graph  $P_2$ ,  $\Omega = [-0.5, 0.5]$ ,  $x^\pm \in [-0.3, 0.3]$  and  $y^\pm \in [-0.5, 0.4]$ . Then  $(xy)^\pm \notin \mu^\pm$ .

In the following theorem, we describe a system  $G = (\Omega, \sigma^\pm, \mu^\pm)$  that cannot be a grey graph, and a fuzzy graph at the same time, because grey graphs and fuzzy graphs are based on non-null graphs.

**Theorem 10.** Let  $\Omega$  be a universe,  $G^\pm = (V, E)$  be a graph, and  $G = (\Omega, \sigma^\pm, \mu^\pm)$  be a grey graph on  $G^\pm$ . Then,  $G = (\Omega, \sigma^\pm, \mu^\pm)$  cannot be a fuzzy graph.

*Proof.* Let  $xy \in E$  be an arbitrary edge. If  $G = (\Omega, \sigma^\pm, \mu^\pm)$  is a fuzzy graph on  $G^\pm$ , then there are  $a, b, c \in \Omega$  such that  $x^\pm = [a, a]$ ,  $y^\pm = [b, b]$  and  $(xy)^\pm = [c, c]$ , where  $c \leq T_{min}(a, b)$ . In this case, since  $G = (\Omega, \sigma^\pm, \mu^\pm)$  is a grey number-based graph on  $G^\pm$ , we get  $\mu^\pm = 0$ . Applying Proposition 1(iii), for any  $x, y \in V$  we conclude  $(xy)^\pm = 0$ . So, there is  $n \in \mathbb{N}$  such that  $G \cong N_n$ .  $\square$

## 5 Some Applications of Grey Graphs

The goal of this section is to present some applications of grey graphs in the real world.

### Complex Computer Networks

Let  $V = \{Pc1, Pc2, Pc3, Pc4\}$  be a set of computer systems, which have performance errors as in Table 1 (which are unknown to us), and changes based on various factors, including the passage of time and energy fluctuations, which we denote by a grey number  $[a, b] \subseteq [0, 100] = \Omega$ . For instance,  $(Pc2)^\pm \in [10, 30]$  means that the performance error of system Pc2 changes from 10% to 30%. We want to construct a complex network via these computer systems and check their performance in the link of this network via various factors, including the passage of time, energy fluctuations, and the relative measure of the processing power of systems, as shown in Figure 10. In conclusion, with the link of systems Pc4 and Pc1, we get  $(Pc1Pc4)^\pm \in [\frac{3}{10}, 15]$ , which means that the performance error is reduced from 1% to 0.3%. On the other hand, system Pc2 is a weak system, because its performance error changes from 25% to 75%. Thus, as shown in Figure 10, this complex network is optimized by linking the computer systems.

**Table 1:** A complex computer network based on grey numbers

Computer System	Pc1	Pc2	Pc3	Pc4
Performance Error	[0, 30]	[10, 30]	[25, 50]	[25, 75]

### Complex Economic Networks

Let  $V = \{M1, M2, M3, M4\}$  be a set of industrial factories in an industrial area, which have (Dollar-based) economic outcomes in each hour as shown in Table 2, and change

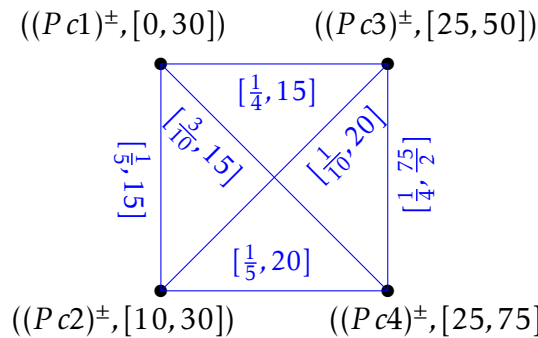


**Figure 10:** The grey graph  $G = (\Omega, \sigma^\pm, \mu^\pm)$  on  $C_4$ .

due to the fluctuations of the production and consumption market, energy price fluctuations, and fluctuations in the quality of raw materials, which we denote by a grey number  $[a, b] \subseteq [-0.4, 1.5] = \Omega$ . For instance,  $(M1)^\pm \in [-0.2, 1.2]$  means that the industrial factory M1 can lose 0.2 Dollars and benefit 1.2 Dollars at most each hour. Also,  $(M3)^\pm \in [0.4, 0.6]$  means that the industrial factory M3 can benefit from 0.4 Dollars to 0.6 Dollars in each hour. We want to optimize the resulting losses of an industrial area for the link of these industrial factories in a complex network, and the relative measure of the economic outcome of these factories in each hour, as depicted in Figure 11.

**Table 2:** A complex economic network based on grey numbers

Industrial Factory	M1	M2	M3	M4
Economic Outcome	$[-0.2, 1.2]$	$[-0.1, 0.4]$	$[0.4, 0.6]$	$[0.5, 0.7]$

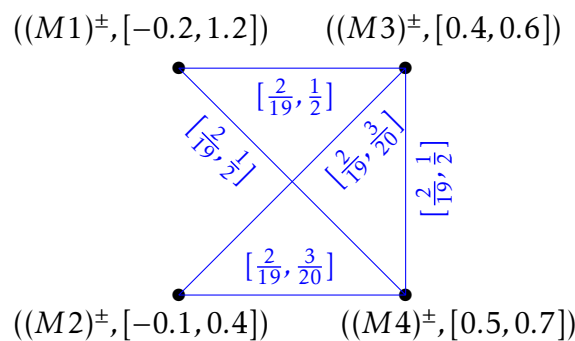


**Figure 11:** The grey graph  $G = (\Omega, \sigma^\pm, \mu^\pm)$  on  $C_4$ .

As can be seen from Figure 11, the industrial factories M1 and M2 cannot be linked, and  $(M1M3)^\pm \in [\frac{2}{19}, \frac{1}{2}]$  means that the industrial factories M1 and M3 are profitable in this complex network, while out of the network, M1 and M3 can lose at most 0.2 Dollars and 0.1 Dollars in each hour, respectively.

### Critical Complex Networks in Nature

In practice, by a grey number, we mean an indeterminate number whose possible value can be taken within a broad set of numbers or an interval. The theory of grey systems provides effective models for systems with both known and unknown data. Complex networks such as weighted graphs play a fundamental role in some problems in the real world, including social, economic, cultural, and natural issues. Primarily, grey graphs cover the weaknesses of ordinary networks, complex networks, and weighted networks. Hence, we can apply grey graphs in the design of different networks based on graphs and fuzzy graphs, which have weaknesses in facing critical situations in nature.

Suppose that we want to check a transportation network between two cities,  $A$  and  $B$ , a path,  $A, C, D, E, B$  of cities. Usually, the distance-time between these cities is  $n$  hours. However, with a natural disaster, the distance-time between these two cities is more than  $n$  hours. So, we cannot use a fuzzy graph in this way, because with changes in the conditions, the transportation graph cannot be changed. However, we can design the same network based on a grey graph.

## 6 Conclusion and Ideas for Further Work

This research analyzed and optimized some real problems on the novel notion of grey graph based on a given graph. Indeed, we proposed a new extension of graphs supported by grey numbers. Also, we found some properties by solving linear inequalities based on the averages and relative measures of grey numbers. We observed the difference between the concepts of a fuzzy graph and grey graph, which was based on a fundamental difference between grey numbers and fuzzy subsets. Moreover, we proved that the weaknesses of fuzzy graphs could be covered by grey graphs. Finally, we presented some optimization techniques and their application and some usages of grey graphs in the real world.

In future studies, we try to establish different results on hypergraphs based on grey numbers, as a generalization of graphs based on grey numbers. Also, we try to obtain some results on complete grey graphs, traceable grey graphs, Hamiltonian grey graphs, Eulerian grey graphs, and their usages.

### References

- [1] Chen N., Xie N. (2020). "Uncertainty representation and information measurement of grey numbers", *Grey Systems: Theory and Applications*, 10(4), 495-512.
- [2] Cui J., Tan Q., Zhang C., Yang B. (2021). "A novel framework of graph Bayesian optimization and its applications to real-world network analysis", *Expert Systems with Applications*, 170(15), 114524.

- [3] Darvishi Salookolaei D., Forrest J., Liu S. (2019). "A comparative analysis of grey ranking approaches", *Grey Systems: Theory and Applications*, 9(4), 472-487.
- [4] Darvishi Salookolaei D., Forrest J., Liu S. (2021). "Grey linear programming: a survey on solving approaches and applications", *Grey Systems: Theory and Applications*, 11(1), 110-135.
- [5] Darvishi Salookolaei D., Liu S., Babaei P. (2017). "Application of grey system theory in rainfall estimation", *Control and Optimization in Applied Mathematics*, 2(2), 15-31.
- [6] Deng J. (1989). "Introduction to grey system theory", *Journal of Grey Systems*, 1(1), 1-24.
- [7] Jalving J., Cao Y., Zavala V.M. (2019). "Graph-based modeling and simulation of complex systems", *Computers & Chemical Engineering*, 125(9), 134-154.
- [8] Khatamov N.M. (2020). "Translation-invariant extreme Gibbs measures for the Blume-Capel model with wand on a Cayley tree", *Ukrainian Mathematical Journal*, 72, 623-641.
- [9] Liab L., Wang P., Yan J., Wang Y., Lib S., Jiang J., Sun Z., Tang B., Chang T.H., Wang S., Liu Y. (2020). "Real-world data medical knowledge graph: construction and applications", *Artificial Intelligence in Medicine*, 103, 101817.
- [10] Lin Y., Chen M.Y., Liu S.F. (2004). "Theory of grey systems: capturing uncertainties of grey information", *Kybernetes*, 33(2), 196-218.
- [11] Liu S., Lin Y. (2006). "Grey Information, theory and practical applications", Springer-Verlag, London.
- [12] Luo D., Huihui Z. (2020). "Grey clustering model based on Kernel and information field", *Grey Systems: Theory and Applications*, 10(1), 56-67.
- [13] Mierzwiak R., Nowak M., Xie N. (2020). "A new approach to the degree of greyness", *Grey Systems: Theory and Applications*, 11(2), 241-252.
- [14] Mordeson J.N., Nair P.S. (2000). "Fuzzy graph and fuzzy hypergraph", Physica-Verlag, Heidelberg, New York.
- [15] Pourofoghi F., Darvishi Salookolaei D. (2020). "Applying Duality Results to Solve the Linear Programming Problems with Grey Parameters", *Control and Optimization in Applied Mathematics*, 5(1), 15-28.
- [16] Tavakolli M. (2019). "Global Forcing Number for Maximal Matchings under Graph Operations", *Control and Optimization in Applied Mathematics*, 4(1), 53-63.
- [17] Ward J.P., Narcowich F.J., Ward J.D. (2020). "Interpolating splines on graphs for data science applications", *Applied and Computational Harmonic Analysis*, 49(2), 540-557.
- [18] Yang Y., John R. (2012). "Grey sets and greyness", *Information Sciences*, 185(1), 249-264.
- [19] Yin K., Xu J., Li X. (2019). "A new grey comprehensive relational model based on weighted mean distance and induced intensity and its application", *Grey Systems: Theory and Applications*, 9(3), 374-384.
- [20] Yin K., Xu T., Li X., Cao Y. (2021). "A study of the grey relational model of interval numbers for panel data", *Grey Systems: Theory and Applications*, 11(1), 200-211.
- [21] Zadeh L. (1965). "Fuzzy sets", *Information and Control*, 8(3), 338-353.

**How to Cite this Article:**

Hamidi, M., Norouzi, K., Rezaei, A. (2022). "On grey graphs and their applications in optimization", *Control and Optimization in Applied Mathematics*, 6(2): 79-95. doi: 10.30473/COAM.2022.61195.1181

**COPYRIGHTS**

© 2021 by the authors. Licensee PNU, Tehran, Iran. This article is an open access article distributed under the terms and conditions of the Creative Commons Attribution 4.0 International (CC BY4.0) (<http://creativecommons.org/licenses/by/4.0>)





Payame Noor University



Control and Optimization in Applied Mathematics (COAM)

Vol. 6, No. 2, Summer-Autumn 2021 (97-115), ©2016 Payame Noor University, Iran

DOI. [10.30473/coam.2022.62442.1189](https://doi.org/10.30473/coam.2022.62442.1189) (Cited this article)

## Research Article

# Optimization of Stakeholders' Interaction in the Lean Management Process via a Dynamic Game Theory Approach: A Case Study of the National Southern Oilfields Company

Aziz Zobeidi<sup>1</sup>, Abdolhossein Neysi<sup>2,\*</sup>, Tahmoures Sohrabi<sup>3</sup>

<sup>1</sup> Industrial Management, Faculty of Management, Central Tehran Branch, Islamic Azad University, Tehran, Iran,

<sup>2</sup> Faculty of Economics and Social Sciences, Department of Management, Shahid Chamran University of Ahvaz, Ahvaz, Iran,

<sup>3</sup> Faculty of Management, Central Tehran Branch, Islamic Azad University, Tehran, Iran.

Received: January 24, 2022; Accepted: May 04, 2022.

**Abstract.** The aim of this paper is to assess and optimize the interaction of stakeholders in the lean management process via a dynamic game theory approach within the National Southern Oilfields Company. The present research is applied in terms of the purpose, and qualitative in terms of the data. Also, in terms of its nature and the implementation method, it is based on foundational data. To form the framework of the optimal stakeholder interaction management strategy and measure its effects on lean management (including the dimensions of components and indicators, etc.), scientific and legal documents were studied, experts who utilized the Delphi technique were interviewed, relevant data were summarized and, focus groups and brainstorming were held based on the data foundation method. The findings revealed that the organization in charge of the game selected Stackelberg's game instead of Nash's game, since compared to the latter, the former could produce more than twice when it came to total profit, production of suppliers and manufacturers, etc., thus showing a 100% improvement compared to the cooperative games. In fact, in this study, the manufacturer under consideration preferred Stackelberg's game with the manufacturer acting as the leader and making decisions independent of the suppliers, gaining more profit and consequently more acceptance among people because of optimal production. In this model, three types of parameters played a key role in obtaining the outputs, the first of which was the cost of production. The rise in this parameter indicated the level of competition in profit and production. The second effective parameter was the coefficient of sensitivity to the level of demand for goods. An increase in this parameter caused a decrease in the profit and production of all members of the supply chain. Finally, the last effective parameter was the share of the base goods.

**Keywords.** Optimization, Stakeholders' interaction, Lean management, Dynamic game theory, Southern Oilfields company

**MSC.** 26A33; 92B20; 34H10.

---

\* Corresponding author

zobeidi.a@gmail.com, aneyasi@scu.ac.ir, tah.sohrabi@iauctb.ac.ir

<http://mathco.journals.pnu.ac.ir>

## 1 Introduction

In the third millennium, the methods and procedures used for the management and administration of production organizations have substantially changed compared to the past [1]. In the contemporary arena, an organization is a set of processes aiming to create value for stakeholders, which entirely depends on value creation within the organization itself. Lean production is among the new perspectives on production that has emerged pursuant to mass production [9]. The fundamental concept of “pure thinking” lies in the eradication of waste and creation of value in the organization. Pure thinking is an attitude with the objectives of boosting productivity, continuous value creation and, minimizing expenditures and losses. The term lean was first coined in 1980. It is based on the utilization of less (raw materials, labor, time, etc.) compared to mass production [19].

Within this approach, customer satisfaction, the fruit of continuous improvement of production quality and services, is the primary foundation of the organization's function, and it is only through this approach that the organization can focus on the maximization of earnings [16]. At the heart of lean management is all-encompassing engagement. Participants can manage their success only via engaging. They are inclusive of the entire workforce of the company as well as the participation of third-party teams. The participants' partial mission [13] and the impact on the way participants behave have various effects on them [4, 14]. This system has two main goals. The first one is to eliminate waste from processes, and the second is to create value for the customer. In fact, the main focus of this management system is on the elimination of any activity that consumes resources and adds to costs, without adding value to the customer [10].

Game theory, on the other hand, seeks to achieve mathematical behavior in strategic or game situations, where one's success in selection depends on the choices of the others. Dependency means that each player is influenced by what the others do in the game, and a player's behavior also affects that of the others. The outcome of the game depends on everyone's decisions, and no one has full control over what happens. Individuals recognize these interdependencies and incorporate them into their decisions [12].

Businesses are affected by several stakeholders in the lean management process. Compliant with dynamic game theory, by constructing a three-stage game model, this research analyzed the mechanism of interaction between internal and external stakeholders affecting the implementation of lean management by an organization.

Nowadays, the phenomenon of lean thinking has been considered as a new strategy by all developed countries of the world. But our country is still in the early stages of considering this phenomenon. To be able to maintain themselves in the prevailing global competition and respond to the customer demands, organizations must adopt a system of lean thinking. Therefore, the use of lean thinking in the game theory of Iran's national petroleum industry is also a necessity. For this reason, the aim of the present study is to assess the interaction of stakeholders in the lean management process via a dynamic game theory approach in the National Southern Oilfields Company.

## 2 Theoretical Foundations of the Research

Due to increasing complexity, business management systems are required to use new decision-making procedures for their activities. The top executives of each company need to formulate a long-term strategy and policy in accordance with the internal logic of the organization and its specific characteristics. Decision-making has been studied in various situations by many researchers of the scientific and business communities. Hence, utilizing various decision-making techniques to evaluate the criteria that affect decision-making can lead to superior decisions. Therefore, choosing the right decision criteria is quite important [3].

Lean production is among the new perspectives on production emerging pursuant to mass production [9] It is also known as “smooth production” and “timely production”. Its underlying philosophies are to minimize the waste, enhance the product quality, and improve continuously. Lean production is not only concerned with the product, but also concerns customer satisfaction, the maximization of revenue and profit, and improvement of the workplace environment.

Lean management induces the acquisition and multiplication of customers, job satisfaction for both executives and personnel concerning their performance, enhanced productivity in materials, time, human resources and capital, extended life expectancy of organizations, significant improvement of the products, quality of services, significant reduction of organizational costs, and the increment of competitiveness in the current business world [16].

Game theory uses mathematics to assess behavior in strategic situations or games in which one’s success in making choices is based on the choices of the others. Dependency means that each player is influenced by what the others do in the game, and the player’s behavior also affects that of the others. The outcome of the game depends on everyone’s decisions, and no one has full control over what happens. Individuals recognize these interdependencies and incorporate them into their decisions [12].

A game consists of a set of players, a set of moves or strategies, and a specific outcome for each combination of the strategies. Winning a game is not just a matter of luck, rather, it has its own principles and rules, and each player tries to get closer to victory by using those principles during the game.

Based on dynamic game theory, by constructing a three-stage game model, this research investigated the mechanism of interaction between internal and external stakeholders that affect the implementation of the firm’s lean management.

Lean philosophy is a business approach focusing on the minimization of waste by increasing benefit utilization and reducing latency [21], and creates more value for customers by eliminating non-value-added activities [2]. Several academics have examined the effects of lean methods on performance. They believe that lean systems improve sustainability [20]. Lean systems have been considered as a determining factor in the improvement of overall sustainability [5]. Dos Santos and Gerson in 2018 examined the relationship between lean production and operating performance, in the four dimensions of cost, quality, delivery, and flexibility. They found a positive relationship between the purity of a production system and the operating performance [6].

Fullerton et al. in 2013 found the existence of a direct, positive relationship between lean manufacturing performance and simplified strategic reporting system, value-based costing, visual performance measurement information, and employee empowerment [8].

By examining the relationship between the philosophy of lean production and management accounting, [15] revealed the endeavor of the lean production method to minimize waste and maximize the efficiency of human resources, capital and capabilities. Also, by examining the management and accounting methods of lean manufacturing environment management, Khodami-Pour et al. in 2014 concluded the wide applicability of the lean strategy as the dominant paradigm in manufacturing companies [11]. According to Pouya and Soltani (2015), industries that pay more attention to timely production, suppliers and customers, have a higher performance in lean manufacturing [18]. In 2017, Faghhi-Farahmand and Poppendick used a combination of confirmatory factor analysis, clustering and LINMAP techniques to offer a model for the evaluation of lean manufacturing in small- and medium-sized industries [7, 17]. The research findings provided a model with eight structures for lean manufacturing, namely, *timely production, total quality management, repairs and maintenance, supplier relationships, customer relations, human resource management, process management, and factory-level improvement programs*.

Achieving optimal production is among topics worthy of serious consideration in all Iranian industries, and in particular, in the petroleum industry. Lean manufacturing provides a set of data and tools for senior and middle-ranked managers as well as employees that, if utilized properly, can reduce waste, minimize production time, cut down on costs, maximize employee participation, increase the lifespan of devices, standardize the production methods, etc. Although for some time, we have seen the use of lean management in some industrial projects, in this study, using a newer approach called lean thinking, we provide an optimal model in lean processes via a dynamic game theory approach within the National Iranian Oil Company.

### 3 Research Methodology

The present research is applied in terms of the purpose, and qualitative in terms of the data. Also, in terms of its nature and the implementation method, it is based on foundational data. In this paper, with the help of investigating scientific and legal documents, interviewing experts who utilized the Delphi technique, summarizing the relevant data, and holding focus groups and brainstorming based on the data method, the framework of stakeholder interaction management strategy, including the dimensions of components and indicators that have built the blueprint, is formed and its impact on lean management is measured.

Assessing the internal validity of the findings, comparing the results with theoretical foundations, confirming experts' opinions, verifying the accuracy of the data by the research members, and examining the validity of the interview form were conducted through content validity. In terms of data collection, the research can be considered as field research. The statistical population of this research consisted of twenty-five

key experts in the field, including all senior managers, middle-ranked managers, and employees of the National Iranian Oil Company. Collection was made through a purposeful sampling method in three stages of developing a data theory model (structured interview), the Delphi method, panel of experts, brainstorming, required data from expert thinkers, etc.

Books, related articles, the internet, library resources, and the archives of the National Iranian Oil Company were utilized to collect the research data as well to inform the National Iranian Oil Company and its customers concerning advanced options and hypotheses based on each party's preferences and the ranking of those preferences as well as to evaluate the optimal interaction. In the process of implementing lean management, interviews were performed via a dynamic game theory approach.

### 3.1 Modeling

In this section, various issues on the relationship between the two levels of lean supply chain management, including the manufacturer and several non-suppliers, are presented. The offered supply rate is greater than the demand rate; hence, the sum of the demand rate ratio to the supply rate must be less than 1. Meanwhile, the demand for each product depends on its cost.

First, the assumptions governing the problem, variables and parameters utilized in the supplier and manufacturer models are analyzed as follows. Thereafter, the mathematical model of each chain member, including the objective function (service level), and its constraints are separately presented. In this paper, the interaction between suppliers and producers in the two modes of play (with and without cooperation) has been studied.

Uncooperative play is assessed in two different scenarios. (i) Simultaneous decision-making (ii) Stackelberg. In the first scenario, the weights of suppliers and manufacturers are the same in the chain, and they make decisions simultaneously. In the second one, which is a more common scenario, suppliers have more power in the chain and make decisions first, and then the producer makes his own decisions. In the game mode, with the cooperation of suppliers and manufacturers, they make their decisions in cooperation with each other and in a coordinated manner.

#### 3.1.1 Assumptions

The proposed mathematical model considers several suppliers and one manufacturer, where production occurs in all categories of chain management. The planning horizon is unlimited. This means that the mathematical model is presented for one course only. The parameters, except demand, are definite and predetermined, and no uncertainties are considered. Also, the game is played with complete information, so that the members of the chain are aware of the parameters of each other. The demand for each commodity depends on the cost; whereas the cost increases, demand decreases. Here again, in order to make the model more practical, this relationship is considered

nonlinear. There is no shortage because the production rate of petroleum products is higher than the demand rate, due to international sanctions imposed on the country. Of course, the supplier is dealing with budget constraints to offer the product. Since the producer market is in full competition, there must be at least two suppliers for each product to compete with each other. In addition, a supplier can supply more than one type of goods.

### 3.1.2 Producer's mathematical model

The producer's goal is to determine the optimal level of accumulated items needed ( $Q$ ) the optimal cost of supplying petroleum products to exporting countries ( $\psi$ ), and the optimal joint production cycle ( $T$ ) enabling the maximization of production levels and earnings. Here, the model is considered in the form of several types of goods and with a limit on the amount of production. Hence, even if there is a demand for traction, the manufacturer cannot supply any product of any size. In other words, the producer has a limited supply capacity. The mathematical model of the producer entails a function of the variables of the producer's decision, referred to as the *net profit function*, described as follows. Moreover, the variable ( $F_{js}$ ) is the cost of providing the products, determined by the suppliers, and the variable ( $v_{js}$ ) is the level of products provided by the suppliers.

$$\begin{aligned} \max \quad \pi_M(\psi, T, Q_j) = & \sum_{i=1}^n \left[ \psi_i \sum_{r=1}^R D_{ir} \right] - \sum_{i=1}^n \left[ Cm_i \sum_{r=1}^R D_{ir} \right] \\ & - \sum_{j=1}^J \sum_{i=1}^S F_{js} V_{js} \frac{\sum_{i=1}^n AS_i}{T} \\ & - \frac{T}{2} \sum_{i=1}^n \left[ hm_i \sum_{r=1}^R D_{ir} \left( 1 + \frac{1}{K_{ir}} - \frac{\sum_{r=1}^R D_{ir}}{P_i} \right) \right] \end{aligned} \quad (1)$$

s.t.

$$\begin{aligned} T \sum_{i=1}^n \left[ Cm_i \sum_{r=1}^R D_{ir} \right] & \leq B_m \\ Q_j = u_{ji} \left( \sum_{r=1}^R D_{ir} \right) & \quad j = 1, 2, 3, \dots, J \end{aligned}$$

The first constraint is the production budget, and the second is the level of required materials and equipment.

It must also generate the demand of the applicants, considering that the period of collecting  $T$  items is considered and all the products must be presented in this period. It is worth mentioning that the production time of the products is considered. Hence, the following constraints remain.

$$\begin{aligned} \sum_{i=1}^n \frac{T \sum_{r=1}^R D_r}{P_i} & \leq T, \\ \sum_{i=1}^n \frac{T \sum_{r=1}^R D_r}{P_i} & \leq 1. \end{aligned} \quad (2)$$

Consequently, the producer's model should be as follows.

$$\begin{aligned}
 \max \quad & \pi_M(\psi_i, T, Q_{ij}) = \sum_{i=1}^n \left[ \psi_i \sum_{r=1}^R D_{ir} \right] - \sum_{i=1}^n \left[ C m_i \sum_{r=1}^R D_{ir} \right] \\
 & - \sum_{j=1}^J \sum_{i=1}^S F_{js} V_{js} \frac{\sum_{i=1}^n A S_i}{T} \\
 & - \frac{T}{2} \sum_{i=1}^n \left[ h m_i \sum_{r=1}^R D_{ir} \left( \frac{\sum_{r=1}^R D_{ir}}{P_i} \right) \right] \\
 \text{s.t.} \quad & \\
 & T \sum_{i=1}^n \left[ C m_i \sum_{r=1}^R D_{ir} \right] \leq B_m \\
 & Q_{ij} = u_{ji} \left( \sum_{r=1}^R D_{ir} \right) \quad j = 1, 2, 3, \dots, J \\
 & \sum_{j=1}^J Q_{ij} \leq P_i \\
 & \min_{ij} \{Q_{ij}\} < Q_{ij'} < \max_{ij} \{Q_{ij}\} \quad \forall j' \in \{1, \dots, j\}
 \end{aligned} \tag{3}$$

### 3.1.3 The mathematical model of suppliers

The objective of suppliers is to determine the optimal product size of the manufacturer ( $v_{js}$ ) and the optimal supply per unit of product ( $F_{js}$ ) to maximize the profit level of each supplier. Mathematically, this model includes a function of the suppliers' decision variables, presented as the production function and profit of the suppliers, as follows.

$$\begin{aligned}
 \max \quad & \pi_{S_s}(F_{ijs}, v_{ijs}) = \sum_{j=1}^J \sum_{i=1}^I F_{ijs} v_{ijs} - \sum_{j=1}^J \sum_{i=1}^I C S_{ijs} v_{ijs} \\
 \text{s.t.} \quad & \\
 & v_{ijs} = Q_{ij} - \eta_{ijs} F_{ijs} + \sum^S \theta_{ijs} F_{ijs} \\
 & \sum_{s=1}^S v_{ijs} = Q_{ij} \quad j = 1, 2, \dots, J \\
 & v_{ijs} \leq C a_{js} \quad j = 1, 2, \dots, J
 \end{aligned} \tag{4}$$

The first constraint is the limitation of competition on prices offered by the suppliers toward procuring materials. The second constraint guarantees the amounts of materials ordered, obtained from the total demand of applicants, that the suppliers are obliged to provide. Finally, the third constraint represents the production capacity of each producer (the ability to provide products).

### 3.1.4 Playing without simultaneous cooperation (The fair mode)

When suppliers and producers have the same decision-making power, they make decisions simultaneously and without cooperation. In this event, a Nash game takes place between the supplier and the manufacturer, and the solution to such a structure is to obtain the Nash equilibrium point of the game. The Nash Equilibrium Problem can be written as follows.

$$\begin{aligned} \max \quad \pi_M(\psi_i, T, Q_{ij}) = & \sum_{i=1}^n \left[ \psi_i \sum_{r=1}^R D_{ir} \right] \\ & - \sum_{i=1}^n \left[ Cm_i \sum_{r=1}^R D_{ir} - \sum_{j=1}^J \sum_{s=1}^S F_{ijs} V_{ijs} \frac{-\sum_{i=1}^n AS_i}{T} \right] \\ & - \frac{T}{2} \sum_{i=1}^n \left[ hm_i \sum_{r=1}^R D_{ir} \left( \frac{\sum_{r=1}^R D_{ir}}{P_i} \right) \right] \end{aligned} \quad (5)$$

s.t.

$$\begin{aligned} T \sum_{i=1}^n \left[ Cm_i \sum_{r=1}^R D_{ir} \right] & \leq B_m \\ Q_i = u_{ji} \left( \sum_{r=1}^R D_{ir} \right) & \quad j = 1, 2, 3, \dots, J. \end{aligned}$$

$$\max \quad \pi_{S_s}(F_{js}, v_{js}) = \sum_{j=1}^J F_{js} v_{js} - \sum_{j=1}^J Cs_{js} v_{js}$$

s.t.

$$\begin{aligned} v_{js} &= Q_j - \eta_{js} F_{js} + \sum_{s=1}^S \theta_{js} F_{js} \\ \sum_{s=1}^S v_{js} &= Q_j \quad j = 1, 2, \dots, J \\ v_{js} &\leq Ca_{js} \quad j = 1, 2, \dots, J. \end{aligned}$$

### 3.1.5 Playing without sequential cooperation

In this section, the confrontation between suppliers and producers is considered in the form of the Stackelberg game, where one of the players (members of the chain) plays the role of the leader and can impose his desired strategy on the other players (followers).

$$\begin{aligned} \max \quad \pi_M(\psi_i, T, Q_{ij}) = & \sum_{i=1}^n \left[ \psi_i \sum_{r=1}^R D_{ir} \right] \\ & - \sum_{i=1}^n \left[ Cm_i \sum_{r=1}^R D_{ir} - \sum_{j=1}^J \sum_{s=1}^S F_{ijs} V_{ijs} \frac{-\sum_{i=1}^n AS_i}{T} \right] \\ & - \frac{T}{2} \sum_{i=1}^n \left[ hm_i \sum_{r=1}^R D_{ir} \left( \frac{\sum_{r=1}^R D_{ir}}{P_i} \right) \right] \end{aligned} \quad (6)$$

s.t.

$$\begin{aligned} T \sum_{i=1}^n \left[ Cm_i \sum_{r=1}^R D_{ir} \right] & \leq B_m \\ Q_{ij} = u_{ji} \left( \sum_{r=1}^R D_{ir} \right) & \quad j = 1, 2, 3, \dots, J \quad , i = 1, 2, \dots, I \\ (F_{ijs}, v_{ijs}) \in \arg \max \pi_{S_s}(F_{ijs}, v_{ijs}) &= \sum_{j=1}^J F_{ijs} v_{ijs} - \sum_{j=1}^J Cs_{ijs} v_{ijs} \\ v_{ijs} &= Q_{ij} - \eta_{ijs} F_{ijs} + \sum_{s=1}^S \theta_{ijs} F_{ijs} \\ \sum_{s=1}^S v_{ijs} &= Q_{ij} \quad j = 1, 2, \dots, J \quad , i = 1, 2, \dots, I \\ v_{ijs} &\leq Ca_{ijs} \quad j = 1, 2, \dots, J \quad , i = 1, 2, \dots, I. \end{aligned}$$

To use the game without sequential cooperation (the Stackelberg game) in pure supply chain management with this model, we first try to solve the profit and production function of the suppliers, which are considered as followers in this model, and then



determine the outputs. To do so, we enter the result obtained from the manufacturer model into the manufacturer (leader) model, execute the manufacturer's service function, and finally present the profit and decision variables obtained for each member of the supply chain.

### 3.1.6 The collaborative game

In this section, the collaborative game approach toward assisting the supply chain (involving suppliers and producers) is evaluated. Taking into account the constraints of suppliers and producers (meaning that, all suppliers are considered as one member), the mathematical model (with performed calculations) will be as follows.

$$\begin{aligned}
 \max \quad & \pi_M(\psi_i, T, Q_{ij}) = \sum_{i=1}^n \left[ \psi_i \sum_{r=1}^R D_{ir} \right] \\
 & - \sum_{i=1}^n \left[ Cm_i \sum_{r=1}^R D_{ir} \right] - \frac{\sum_{i=1}^n AS_i}{T} \\
 & - \frac{T}{2} \sum_{i=1}^n \left[ hm_i \sum_{r=1}^R D_{ir} \left( \frac{\sum_{r=1}^R D_{ir}}{P_i} \right) \right] \\
 \text{s.t.} \quad & \\
 & T \sum_{i=1}^n \left[ Cm_i \sum_{r=1}^R D_{ir} \right] \leq B_m \\
 & Q_{ij} = u_{ji} \left( \sum_{r=1}^R D_{ir} \right) \quad j = 1, 2, 3, \dots, J \\
 & v_{ijs} = Q_{ij} - \eta_{ijs} F_{ijs} + \sum_{s=1}^S \theta_{ijs} F_{ijs} \\
 & \sum_{s=1}^S v_{ijs} = Q_{ij} \quad j = 1, 2, \dots, J, \quad i = 1, 2, \dots, I \\
 & v_{ijs} \leq Ca_{js} \quad j = 1, 2, \dots, J, \quad i = 1, 2, \dots, I.
 \end{aligned} \tag{7}$$

## 4 The Findings

Initially, the most important criteria and key sub-criteria affecting the supply chain were localized utilizing the Delphi hourly method. Next, using the fuzzy Dematel method and by the aid of experts in this field, the relationships between these factors were determined. The members of the decision-making team were three managers from the supply chain departments, and in all the stages alluded to in this paper, the experts were the members of this team.

In order to localize the variables, the criteria affecting production and profit were provided to the experts, and they were requested to comment on the primary factors under consideration. Based on the range from 1 to 10 (from insignificant to very important), each of the main numerical factors was assigned, and other effective factors and criteria consistent with the research objective were introduced, if necessary. Only those factors and criteria that had an average of more than 7 were considered. Thereafter,

the questionnaire related to sub-factors (sub-criteria) was provided to the experts in order to be reviewed and completed as the previous questionnaire.

The criteria and sub-criteria extracted from the literature review (after localization) are shown in Table 1.

**Table 1:** The utilized criteria and sub-criteria and their abbreviations

Criterion	Financial Capability (FC)	Logistics Capability (LC)	Experience (HE)	Production Capacity (HC)
Sub-Criteria	Up-To-Date and Efficient Equipment (FC2)	Suitable Location (LC1)	Expert Human-Resources (HE2)	New Production Goods (HC2)
	Aviation Equipment (FC1)	Land Transportation (LC2)	Construction (HE3)	Production Staff (HC2)
		Production Speed (LC3)		

In order to assess the factors affecting the supply chain, four main criteria and nine sub-criteria were used. See Table 1 for more details. The following steps were undertaken to perform the fuzzy Dematel technique.

The first step was to calculate the average matrix of expert opinions. Each expert was asked to express their opinions on the effects of factor  $i$  on factor  $j$ , specifically, whether they were *ineffective*, *less effective*, *of medium effect*, *highly effective* and *of a very high effect*.

Their opinions as well as the corresponding triangular fuzzy numbers are shown in Table 2.

**Table 2:** The sub-criteria direct correlation matrix (Average of the three experts' opinions)

	FC <sub>1</sub>			...	HC <sub>2</sub>			HC <sub>3</sub>			Σ ui
	l	m	u	...	l	m	u	l	m	u	
FC <sub>1</sub>	0	0	1	...	1	3	4	2	3	4	36
FC <sub>2</sub>	3	3	4	...	1.6667	2.6667	3.6667	2	3	4	31.3333
LC <sub>1</sub>	0	1	2	...	2	3	4	2	3	4	33.6667
LC <sub>2</sub>	2	3	4	...	2	3	4	2	3	4	37
LC <sub>3</sub>	1	2	3	...	3	3	4	2	3	4	33
HE <sub>1</sub>	2	3	4	...	2.6667	3	4	2	3	4	38.6667
HE <sub>2</sub>	2.6667	3	4	...	2	3	4	2	3	4	40
HE <sub>3</sub>	3	3	4	...	2	3	4	2	3	4	38
HC <sub>1</sub>	1	2	3	...	2	3	4	1	2	3	34
HC <sub>2</sub>	2	3	4	...	0	0	1	3	3	4	40
HC <sub>3</sub>	2.6667	3	4	...	2.3333	2.6667	3.6667	0	0	1	37.6667
Σ uj		37		...		40.3333			40		

First, we acquired the opinions (average) of all the experts, and then we got the average of the experts' opinions by deleting the  $i_M$  expert. For the third, second and first expert questionnaires, the values obtained for reliability were 96.72, and 95.23 and 96.24, respectively. The second step was the normalization of the matrix as a direct fuzzy connection of the sub-criteria. The third step was to calculate the complete fuzzy correlation matrix of the sub-criteria and criteria. The fourth step was to obtain the

intensity and direction of the impact of factors and draw a causal diagram. To draw and analyze the graph, we required two indicators of impact intensity and, effectiveness and direction of impact, calculated using the above two indicators for each  $i = j$  and in the form of Table 3.

**Table 3:** Calculation of the intensity index and the direction of impact of each sub-criterion (Fuzzy)

	$d'i$			$r'j$			$d'i + d'j$			$d'i - d'j$		
	$I$	$m$	$u$	$I$	$m$	$u$	$I$	$m$	$u$	$I$	$m$	$u$
FC1	0.7022	1.6925	9.2766	0.8585	1.7762	9.5921	1.5607	3.4687	18.8687	-8.8899	-0.0836	8.4181
FC2	0.6025	1.4072	8.1897	0.7244	1.6522	9.1205	1.3296	3.0594	17.3102	-8.5180	-0.2450	7.4653
LC1	0.5782	1.5708	8.7271	0.2753	1.0501	6.8247	0.8535	2.6209	15.5519	-6.2465	-0.5207	8.4519
LC2	0.7010	1.7533	9.5058	0.6705	1.6439	9.0274	1.3715	3.3972	18.5359	-8.3264	-0.1093	8.8380
LC3	0.5946	1.5017	8.5481	0.7190	1.6680	9.1795	1.3135	3.1697	17.7276	-8.5849	-0.1664	7.8292
HE	0.9037	1.8496	9.8743	0.8868	1.8462	9.8594	1.7905	3.6959	19.7337	-8.9557	-0.0034	8.9875
HE2	0.8926	1.9359	10.2036	0.6876	1.7139	9.3558	1.5802	3.6498	19.5594	-8.4632	0.2221	9.5160
HE3	0.8812	1.8130	9.7345	0.8710	1.8602	9.9128	1.7523	3.6732	19.6473	-9.0316	-0.0472	8.8635
HC1	0.5824	1.5724	9.8181	0.6775	1.7247	9.3958	1.2599	3.2971	18.2139	-8.8134	-0.1523	8.1406
HC2	0.9309	1.9359	10.2036	0.9276	1.9523	9.2641	1.8605	3.8882	20.4677	-8.3332	-0.0164	9.2740
HC3	0.7947	1.7878	9.6362	0.8641	1.9324	10.1881	1.6588	3.7201	19.8243	-8.3934	-0.1446	8.7721

**Table 4:** Calculation of the intensity index and the direction of impact of each criterion (Fuzzy)

	$D'i$			$R'j$			$D'I + R'j$			$D'I - R'j$		
	$I$	$m$	$u$	$I$	$m$	$u$	$I$	$m$	$u$	$I$	$m$	$u$
FC	0.2400	0.5598	3.1723	0.2864	0.6146	3.3800	0.5264	1.1743	6.5523	-3.1400	-0.0548	2.8859
LC	0.2234	0.5820	3.2441	0.1953	0.5211	3.0145	0.4186	1.1032	6.2585	-2.7911	-0.0609	3.0488
HE	0.3297	0.6820	3.6175	0.2968	0.6559	3.5156	0.6265	1.3379	7.1331	-3.1860	0.0261	3.3207
HC	0.2821	0.6444	3.4765	0.2966	0.6766	3.6003	0.5787	1.3209	7.0768	-3.3182	-0.0322	3.1799

**Table 5:** The definitive matrix of complete correlation of the sub-criteria (Ts)

	FC1	FC2	LC1	LC2	LC3	HE1	HE2	HE3	HC1	HC2	HC3
PC1	0.2655	0.3203	0.1985	0.2942	0.2990	0.3196	0.3196	0.3371	0.2970	0.3463	0.3441
PC2	0.3027	0.2217	0.1605	0.2336	0.2381	0.2779	0.2892	0.3090	0.2570	0.3032	0.3088
LC1	0.2653	0.2516	0.1704	0.2789	0.2847	0.3183	0.2872	0.3036	0.2975	0.3286	0.3257
LC2	0.3349	0.2979	0.2031	0.2528	0.3210	0.3417	0.3031	0.3433	0.3263	0.3540	0.3509
LC3	0.2829	0.2545	0.1840	0.2899	0.2299	0.3135	0.2521	0.2908	0.2913	0.3280	0.3196
HE1	0.3474	0.3240	0.2332	0.3336	0.3367	0.2915	0.3155	0.3623	0.3385	0.3718	0.3649
HE2	0.3610	0.3408	0.2397	0.3370	0.3418	0.3705	0.2831	0.3669	0.3478	0.3783	0.3750
HE3	0.3494	0.3309	0.2308	0.3017	0.3284	0.3559	0.3354	0.2891	0.3120	0.3632	0.3607
HC1	0.2915	0.2776	0.1889	0.2897	0.2790	0.3199	0.3045	0.3066	0.2422	0.3306	0.3060
HC2	0.3576	0.3409	0.24000	0.3373	0.3478	0.3691	0.3471	0.3672	0.3483	0.3152	0.3811
HC3	0.3425	0.3242	0.2510	0.2976	0.3024	0.3319	0.3309	0.3503	0.3229	0.3554	0.2925

**Table 6:** The definitive matrix of complete correlation of the criteria (Tc)

	FC	LC	HE	HC
FC	0.2776	0.2373	0.3087	0.3094
LC	0.2812	0.2461	0.3059	0.3247
HE	0.34227	0.2981	0.3300	0.3569
HC	0.3224	0.2815	0.3364	0.3216

**Table 7:** Calculation of the definite indicators of intensity and direction of impact

Criterion Type	(D-R) <sup>def</sup>	(D + R) <sup>def</sup>	Sub-Criteria	Criterion Type	(D-R)	(D + R)	
Impact (Causal)	-0.1598	6.8417	FC1	Impact (Effect)	-0.0909	2.3568	FC
Impact (Effect) (Causal)	-0.3857	6.1890	FC2				
Impact (Effect)	0.8117	5.4118	LC1	Impact (Causal)	0.0949	2.2209	LC
Impact (Effect)	0.1826	6.6755	LC2				
Impact (Causal)	-0.2721	6.3451	LC3				
Impact (Effect)	0.009	7.2290	HE1	Impact (Causal)	0.0467	2.6088	HE
Impact (Effect)	0.3742	7.1098	HE2				
Impact (Causal)	0.0656	7.1865	HE3				
Impact (Causal)	-0.2276	7.2308	HC1	Impact (Effect)	-0.0507	2.5744	HC
Impact (Causal)	-0.0230	7.5261	HC2				
Impact (Causal)	-0.2444	6.5170	HC3				

To draw a relationship map, the threshold value should be calculated. The value of the criteria threshold, the average of all the numbers in Table 6, is equal to

$$\text{Criteria Threshold Value} = \frac{0.2776 + 0.2373 + 0.3087 + \dots + 0.3216}{16} = 0.3050.$$

**Table 8:** Impact or non-impact of the criteria

	FC	LC	HE	HC
FC		0	1	1
LC	0		1	1
HE	1	0		1
HC	1	0	1	

To map the internal relations of the criteria, we first calculate the value of the threshold. The value of this threshold can be obtained from the arithmetic mean of all the components listed in Table 5 (the Ts matrix):

$$\text{Sub-Criteria Threshold Value} = \frac{0.2655 + 0.3203 + 0.1985 + \dots + 0.2925}{121} = 0.3069.$$

**Table 9:** Impact or non-impact of the sub-criteria

	FC <sub>1</sub>	FC <sub>2</sub>	LC <sub>1</sub>	LC <sub>2</sub>	LC <sub>3</sub>	HE <sub>1</sub>	HE <sub>2</sub>	HE <sub>3</sub>	HC <sub>1</sub>	HC <sub>2</sub>	HC <sub>3</sub>
FC <sub>1</sub>	0	0	1	0	0	1	1	1	0	1	1
FC <sub>2</sub>	0	0	0	0	0	0	0	1	0	0	1
LC <sub>1</sub>	0	0	0	0	0	1	0	1	0	1	1
LC <sub>2</sub>	1	0	0	0	1	1	0	1	1	1	1
LC <sub>3</sub>	0	0	0	0	0	1	0	1	1	1	1
HE <sub>1</sub>	1	1	0	1	1	0	1	1	1	1	1
HE <sub>2</sub>	1	1	0	1	1	1	0	1	1	1	1
HE <sub>3</sub>	1	1	0	1	1	1	1	0	1	1	1
HC <sub>1</sub>	0	0	0	0	1	0	0	0	0	1	0
HC <sub>2</sub>	1	1	0	1	1	1	1	1	1	0	1
HC <sub>3</sub>	1	1	0	0	0	1	1	1	1	1	0

Thereafter, the findings of the proposed algorithm in solving non-cooperative models of simultaneous and combined types and with cooperation in sample problems were

discussed. The proposed algorithm provided the exact solution of each of the proposed models for different levels of the supply chain. First, the problem was modeled in a real state and then, it was compared in three scenarios: the Nash, Stackelberg and cooperative games.

#### 4.1 Assessment in the event of a hypothetical case study

In this research, the provided services were, respectively, in two categories of services as well as supply and production of products. The first product was M2, and the other one was M3. The number of equipment and basic materials required to provide the both categories of services were both equal to 8. The equipment was procured from three different suppliers.

Table 10 presents the input parameters of the manufacturer. In this case, it is assumed that the manufacturer produces two different categories of services, primarily composed of eight raw materials. The unit considered in this research is *one thousand Rials* (for parameters  $cm_i$ ,  $AS_i$ ,  $\psi_i$  and  $hm_i$ ). In addition, the unit of  $P_i$  is *number per second*,  $u_{ij}$  and  $Q_j$  are expressed in *numbers*, and finally, the unit of  $T$  is assumed to be *per second*.

**Table 10:** Government supplier’s input parameters

$U_{8i}$	$U_{7i}$	$U_{6i}$	$U_{5i}$	$U_{4i}$	$U_{3i}$	$U_{2i}$	$U_{1i}$	$p_i$	$hm_i$	$AS_i$	$Cm_1$	Parameter Product
3	2	4	6	3	2	5	3	300	3	100	60	1
3	1	4	2	1	5	4	4	250	4	150	70	1

Table 11 displays the input parameters of raw material suppliers. In this instance, three suppliers are considered for each raw material. The number of raw materials required to produce the two categories of services was 8, provided by the suppliers. In this section, the measurement unit of  $F_{js}$  and  $Cs_{js}$  is *one thousand Rials*, and the unit of  $V_{js}$  is *number per second*. Finally,  $\eta_{js}$  and  $\theta_{js}$  do not have any measurement unit.

**Table 12:** General input parameters

$\gamma_i$	Base share of $i$ in the market (materials and equipment required to be purchased by the supplier)
$\alpha_i$	Base share of commodity $i$
$\beta_i$	Coefficient of sensitivity to the offered product $i$

$$\beta_2 = 2, \beta_1 = 3, \alpha_2 = 170000, \alpha_1 = 150000$$

#### 4.2 A case study of the outputs of the Nash game model

Table 13 shows the decision variables of the suppliers, namely, the costs of production services and the amount of raw material produced by the suppliers.

**Table 11:** The suppliers' input parameters

Supplier Parameter	Raw Material	1	2	3	Supplier Parameter	Raw Material	1	2	3
$\eta_{js}$	1	4	5	4	$\theta_{js}$	1	2	2	1.5
$\eta_{js}$	2	5	6	6	$\theta_{js}$	2	2.5	2	2.5
$\eta_{js}$	3	3	2	5	$\theta_{js}$	3	1	1.5	2
$\eta_{js}$	4	6	5	2	$\theta_{js}$	4	1.5	2	0.5
$\eta_{js}$	5	5	6	5	$\theta_{js}$	5	1	2	1.5
$\eta_{js}$	6	7	5	6	$\theta_{js}$	6	0.5	2.5	1
$\eta_{js}$	7	4	2	4	$\theta_{js}$	7	1.5	2	1.5
$\eta_{js}$	8	3	1	4	$\theta_{js}$	8	1.5	1.5	0.5
$Cs_{js}$	1	5	5	6	-	-	-	-	-
$Cs_{js}$	2	4	3	3	-	-	-	-	-
$Cs_{js}$	3	5	5	6	-	-	-	-	-
$Cs_{js}$	4	5	3	6	-	-	-	-	-
$Cs_{js}$	5	4	5	6	-	-	-	-	-
$Cs_{js}$	6	2	3	1	-	-	-	-	-
$Cs_{js}$	7	5	3	4	-	-	-	-	-
$Cs_{js}$	8	2	3	2	-	-	-	-	-

**Table 13:** Nash game model decision variables of suppliers

Supplier Parameter	Raw Material	1	2	3	Supplier Parameter	Raw Material	1	2	3
$F_{js}$	1	27075.9	27075.9	23691.8	$V_{js}$	1	41292.3	28066.7	20717.9
$F_{js}$	2	23014.4	23011	22014	$V_{js}$	2	11381.5	15171.6	11378.5
$F_{js}$	3	35975.5	35857.5	35960	$V_{js}$	3	10739.9	2334.7	10741.6
$F_{js}$	4	3199.68	3198.79	2300.12	$V_{js}$	4	28685.2	35040.3	28688.5
$F_{js}$	5	7193.85	7194.3	7194.5	$V_{js}$	5	59751.2	72477.5	59756.6
$F_{js}$	6	8851.44	8852	8850.96	$V_{js}$	6	55207.8	55911.1	55204.2
$F_{js}$	7	5757.42	5756.58	5757	$V_{js}$	7	15567.4	18828.2	15562.1
$F_{js}$	8	28767	2866	2580	$V_{js}$	8	77066.2	10273.2	77066.2

The decision variables of the manufacturers, namely, the wholesale price of each product, the joint production cycle of the products, and the required quantity of raw materials, are as follows.

$$\begin{aligned}
 \psi_1^* &= 60311.5, & \psi_2^* &= 70407.4, & T^* &= 0.015, \\
 Q_1^* &= 23937.5, & Q_2^* &= 37931.6, & Q_3^* &= 85057.2, & Q_4^* &= 63618.3, \\
 Q_5^* &= 127236.6, & Q_6^* &= 6997.1, & Q_7^* &= 32683.8, & Q_8^* &= 25686.7, \\
 D_1^* &= 0, & D_2^* &= 29185.2.
 \end{aligned}$$

The profit and production quantities of each chain member can be written as follows.

$$\begin{aligned}
 \pi_{s1}^* &= 1.0349 * 10^9, \pi_{s2}^* = 1.11284 * 10^9, \pi_{s3}^* = 1.514492 * 10^9, \\
 \pi_M^* &= 4.03798 * 10^9, \pi_T^* = 7.75735 * 10^9.
 \end{aligned}$$

Based on the obtained outputs, the cycle time in this game was 0.0015 seconds, and the costs of preparing each product were 6031.5 and 70407.4 thousand Rials, respectively. Next, the monetary figures for raw materials (required for each type of material) were 23937.5, 37931.6, 85057.3, 63618.3, 127236.6, 6997.1, 32683.8 and 25686.7. Finally, we obtained the demand for each of the final products, which were 0 and 29185.2, respectively. In this game, pursuant to the calculations and obtaining the decision variables of each member of the chain, we tried to separately obtain the level of service of each member (plus the service of the entire game), which were equal to 103490, 1112840, 1514492, 403798 and 775735 thousand Rials, respectively.

### 4.3 The outputs of the Stackelberg game model

Table 14 presents the decision variables of the suppliers, namely, the production costs and the amount of raw material produced by the suppliers.

**Table 14:** The decision variables of the suppliers in the Stackelberg model

3	2	1	Raw Material	Supplier Parameter	3	2	1	Raw Material	Supplier Parameter
8027.7	255952.4	202117.4	1	$V_{js}$	31812.6	23855.2	23546	1	$F_{js}$
231062.1	441416.9	331069.6	2		46507.4	45582.7	23906	2	
330308.4	330307	330308	3		40813.2	33030.3	23253	3	
85000.6	850866	850868.6	4		28362.3	28362.3	19994.5	4	
170173.7	430173.6	160173.6	5		64872.4	53465.6	59983.8	5	
17904.4	21904.4	27904.4	6		51616.2	44877.8	23955.7	6	
99943.95	18994.02	19994.4	7		24178.5	19994.6	15810.7	7	
16955.9	226081.5	169558.9	8		38579.1	22327.8	32546.3	8	

$$\begin{aligned} \psi_1^* &= 71694.1, & \psi_2^* &= 557926.1, & T^* &= 0.03, \\ Q_1^* &= 538350, & Q_2^* &= 110355, & Q_3^* &= 653613, & Q_4^* &= 538350, \\ Q_5^* &= 107670, & Q_6^* &= 121881, & Q_7^* &= 688328, & Q_8^* &= 565199, \\ D_1^* &= 149978, & D_2^* &= 888350. \end{aligned}$$

The profit level of each member of the chain can be obtained as follows.

$$\begin{aligned} \pi_{s1}^* &= 2.65324 * 10^{22}, & \pi_{s2}^* &= 2.54436 * 10^{22}, \\ \pi_{s3}^* &= 2.65347 * 10^{22}, & \pi_M^* &= 7.96040 * 10^{22}, \\ \pi_T^* &= \pi_M^* + \pi_{s1}^* + \pi_{s2}^* + \pi_{s3}^* = 1.09105 * 10^{21}. \end{aligned}$$

In line with the outputs obtained in this game, our cycle time was 0.03 seconds, and the cost of services and goods provided were 71694.1 and 557926.1 thousand Rials, respectively. Next, the amounts of raw materials required for each type of material were 538350, 110355, 653613, 538350, 107670, 121881, 688328 and 565199, respectively. The demands for the item were also determined to be 149978 and 888350, respectively. In this game, after calculations and obtaining the decision variables of

each chain member, we tried to separately obtain the profit and production level of each member (as well as the total level of service in the game), which were equal to 265340000, 254436000, 265347000, 796040000 and 10910500 thousand Rials, respectively.

**4.4 A case study of the outputs in the collaboration game model**

Table 15 reports the decision variables of the suppliers, namely, production costs and level of raw materials produced by the suppliers, respectively.

**Table 15:** The decision variables of the collaboration model

3	2	1	Raw Material	Supplier Parameter	3	2	1	Raw Material	Supplier Parameter
187863	224022	202509	1	$V_{js}$	27752.2	30465.6	25311	1	$F_{js}$
271809	371514	319061	2		34760.7	34298.3	28460.4	2	
94368	1584410	129488	3		34760.7	34493.9	29605.6	3	
107281	160920	138661	4		15781.2	15780.6	11597.1	4	
205554	347043	220223	5		36033.6	30329.9	23588.8	5	
50506,7	155120	116741	6		30333.5	26864.9	21403.6	6	
85851.4	134063	108832	7		14967.7	12875.6	10784.1	7	
111100	190270	124675	8		33723	25547.6	30656.6	8	

$$\begin{aligned} \psi_1^* &= 60334.8, & \psi_2^* &= 70324, & T^* &= 0.001, \\ Q_1^* &= 624394, & Q_2^* &= 962385, & Q_3^* &= 484751, & Q_4^* &= 536338, \\ Q_5^* &= 107268, & Q_6^* &= 793390, & Q_7^* &= 367343, & Q_8^* &= 426047, \\ D_1^* &= 168996, & D_2^* &= 29351.9. \end{aligned}$$

The profit and production levels of each chain member can be obtained as follows.

$$\begin{aligned} \pi_{s1}^* &= 5.53741 * 10^6, \pi_{s2}^* = 7.1111 * 10^6, \pi_{s3}^* = 5.00183 * 10^6, \\ \pi_M^* &= 1.22475 * 10^{10}, \\ \pi_T^* &= \pi_M^* + \pi_{s1}^* + \pi_{s2}^* + \pi_{s3}^* = 1.22298 * 10^{10}. \end{aligned}$$

Based on the outputs obtained in this game, our cycle time was 0.001 seconds, and moreover, the production costs were 60334.8 and 70324 thousand Rials, respectively. Additionally, the levels of basic equipment required for the various types of materials were 624394, 962385, 484751, 536338, 107268, 793390, 367343 and 426047, respectively. Finally, we obtained the demand for each of the final products (168996 and 29351.9, respectively). In this game, pursuant to calculations and acquiring the decision variables of each member of the chain, an effort was made to obtain the levels of production and earning profit for each member separately, as well as the earning profit level of the entire game, which were equal to 5537.41, 71111.1, 50018.3, 12247.5 and 12229.8 thousand Rials, respectively.



## 5 Summary and Conclusion

The aim of this paper was to optimize the interaction of stakeholders in the lean management process via a dynamic game theory approach in the National Company of Southern Oilfields. According to the investigation conducted in this research, if the desired chain vertically increases its type of coordination, that is, so that the manufacturer plays the role of the leader and imposes all its policies on the following members (suppliers), then the horizontal coordination and other types of coordination will be more profitable, which is the same as what happens in the Stackelberg game. After studying the sensitivity of important and key parameters of the problem and analyzing the final results of each of the games, we found the important role played by the manufacturer among the supply chain members in this industry and case study. According to the outputs obtained by the Stackelberg game for this case, studies with production optimization will be most beneficial. So, the organizations in question must first examine their existing policies if these are based on the Stackelberg game policies. In order to further increase the profit with more efficient production, it is necessary to change the important parameters of the model. But, if the policy governing the policy organization is different from the policies proposed in the Stackelberg game, the relevant organization must first create the necessary infrastructure to implement the new policy and then try to change the important parameters.

## References

- [1] Abtahi Froushani Z. S. (2012). "Familiarity with the process of analysis of key stakeholders in oil and gas projects in Iran", *Scientific Monthly of Oil & Gas Exploration & Production*, 131.
- [2] Caldera H. T. S., Desha C., Dawes L. (2017). "Exploring the role of lean thinking in sustainable business practice: A systematic literature review", *Journal of Cleaner Production*, 167, 1546-1565.
- [3] Chang C. H., Lin S. J. (2011). "The effects of national culture and behavioral pitfalls on investors' decision-making: Herding behavior in international stock markets", *International Review of Economics & Finance*, Elsevier, 37(C), 380-392.
- [4] Chavez R., Yu W., Jacobs M., Fynes B., Wiengarten F., Lecuna A. (2014). "Internal lean practices and performance: the role of technological turbulence", *International Journal of Production Economics*, 160, 157-171.
- [5] Das K. (2018). "Integrating lean systems in the design of a sustainable supply chain model", *International Journal of Production Economics*, 198, 177-190.
- [6] Dos Santos G., Géron T. (2018). "Developing an instrument to measure lean Manufacturing maturity and its relationship with operational performance", *Journal Total Quality Management & Business Excellence*, 29, Issue 9-10.
- [7] Feghhi-Farahmand N. (2017). "A Model for evaluating lean manufacturing in small and medium industries utilizing a combination of confirmatory factor analysis methods, clustering and LINMAP Technique (Study of Small and Medium Industries of Basic Metals and Factories)", *Productivity Management*, 11, 221-258.

- [8] Fullerton R., Kennedy F., Widener S. (2013). "Management accounting and control practices in a lean manufacturing environment", *Accounting Organizations & Society*, 38 , 50-71.
- [9] Ghavidel A. (2015). "Lean management and its application in the world of education", *Journal of Inclusive Management*, 11, 52-61.
- [10] Grove A., Meredith J., Macintyre M., Angelis J., Neailey K. (2010). "Lean implementation in primary care health visiting services in national health service UK", *Quality & Safety in Health Care*, 19, Pages e43.
- [11] Khodami-Pour A., Birjandi H, Haakemi B. (2014). "Accounting methods of management in the production environment", *International Conference on Business Development and Excellence*, Tehran.
- [12] Mac Milan J. (1996). "Games, Strategies and Manager: How managers can use game theory to make better business decision", Oxford University Press, USA, page 246.
- [13] Marin-Garcia A., Bonavia T. (2015). "Relationship between employee involvement and lean manufacturing and its effect on performance in a rigid continuous process industry", *International Journal of Production Research*, 53(11), 3260-3275.
- [14] Martins A. F., Costa Affonso R., Tamayo S., Lamouri S., Baldy Ngayo C. (2015). "Relationships between national culture and lean management: A literature review", *International Conference on Industrial Engineering and Systems Management (IESM)*, 352-361.
- [15] Mohammadi-Zarchi S. M. H., Babaei-Khalili J. (2012). "The relationship between lean production philosophy and management accounting", *The First Regional Conference on New Approaches to Accounting & Auditing*, Bandar-Gaz.
- [16] Niaz-Azari K., Taghvayyi-Yazdi M., Niaz-Azari M. (2015). "Theories of organization and management in the third millennium", Ghaemshahr Publishing: Mehralanbi.
- [17] Poppendieck M. (2002). "Principles of lean thinking", Eden Prairie, MN 55346 USA.
- [18] Pouya A., Soltani-Fasghandis Gh. (2015). "A model for evaluating net production in small and medium industries utilizing a combination of confirmatory factor analysis methods, clustering and promotee technique", *Journal of Industrial Management Studies*, 13(37), 90-97.
- [19] Radnor Z., Bucci G. (2011). "Analysis of lean implementation in UK business schools and universities. London", UK: Association of Business Schools Lean Report.
- [20] Ruiz-Benitez R., López C., Real J. C. (2019). "Achieving sustainability through the lean and resilient management of the supply chain", *International Journal of Physical Distribution & Logistics Management*, 49(2), 122-155.
- [21] Thanki S., Thakkar J. (2018). "A quantitative framework for lean and green assessment of supply chain performance", *International Journal of Productivity and Performance Management*, 67(2), 366-400.

**How to Cite this Article:**

Zobeidi, A., Neysi, A., Sohrabi, T. (2022).“Optimization of stakeholders’ interaction in the lean management process via a dynamic game theory approach: A case study of the national Southern Oilfields Company”, Control and Optimization in Applied Mathematics, 6(2): 97-114. doi: 10.30473/coam.2022.62442.1189

**COPYRIGHTS**



© 2021 by the authors. Lisensee PNU, Tehran, Iran. This article is an open access article distributed under the terms and conditions of the Creative Commons Attribution 4.0 International (CC BY4.0) (<http://creativecommons.org/licenses/by/4.0>)